University of São Paulo

The Institute of Astronomy, Geophysics and Atmospheric Sciences

Department of Atmospheric Sciences

Diego Fernando Rodríguez Zimmermann

# SUBTROPICAL JET CLIMATOLOGY OVER SOUTH AMERICA

(Climatologia do Jato Subtropical na América do Sul)

São Paulo

2017

Diego Fernando Rodríguez Zimmermann

# SUBTROPICAL JET CLIMATOLOGY OVER SOUTH AMERICA

(Climatologia do Jato Subtropical na América do Sul)

Dissertation presented at the Institute of Astronomy, Geophysics and Atmospheric Sciences at the University of São Paulo as a partial requirement for obtaining the title of Master of Sciences.

Area of Concentration: Meteorology

Advisor: PhD. Rita Yuri Ynoue

**"Corrected version. The original is available at the Unity."**

São Paulo

2017

*To my grandparents that still watch over me from the skies*

Acknowledgments to

• Conselho Nacional de Desenvolvimento Científico e Tecnológico (CNPq),

• The postgraduate program in meteorology of Institute of Astronomy, Geophysics and Atmospheric Sciences (IAG)

• My advisor PhD Rita Yuri Ynoue

• To my family, specially mi parents

• To the professors Rosmeri Porfirio da Rocha and Ricardo Hallak

• Vannia, for her company and support.

• My friends here, Mario, Ana Maria, Yuugo, Daniela, Juan Pablo, Marcos, Franky and many others.

• To Dona Claudia.

• To Cristina and Eleazar, for their support at the beginning of my magister science.

**RESUMO**

O jato subtropical (JS) é analisado durante um período de 30 anos (1979-2008) para o hemisfério sul na vizinhança da América do Sul, entre 100° e 30°W e 10° e 40°S, utilizando dados de reanálise do ERA-INTERIM com uma resolução de 0,5º de longitude x 0,5º de latitude. Para estabelecer critérios para a posição do JS, comparações manuais diárias (12 UTC) foram feitas para janeiro e julho de 2014. O JS é identificado em serviços operacionais usando a carta de 250 hPa onde a velocidade do vento é de pelo menos 30 $ms^{-1}$ e a temperatura potencial entre 330 e 340 K. Usando esses limites, os resultados objetivos foram muito semelhantes aos JS identificados pelos meteorologistas do Centro de Previsão de Tempo e Estudos Climáticos (CPTEC). No entanto, quando sobrepostas sobre imagens de satélite de vapor de água estes critérios não conseguiram distinguir o JS do jato polar (JP) quando ambos estavam acoplados. Finalmente, o método adotado para este estudo consistiu em uma inspeção visual diária (12 UTC) do perfil vertical da velocidade do vento horizontal e temperatura potencial entre 100 e 400 hPa. Para identificar adequadamente o núcleo do JS, foram consideradas a altitude, localização, temperatura e forma, resultando na identificação da latitude JS para cada 10° de longitude na área de estudo. O JS obtido por este método não só mostrou ser consistente quando comparado com imagens de satélite de vapor de água, mas também mostrou um fluxo adequado ao longo dos dias de cada mês, reproduzindo a variação sazonal de intensidade e movimento em direção ao Equador. Após a obtenção da posição diária de JS no período de 30 anos estudado, obtivemos uma climatologia mensal. O JS varia de 16 °- 35 °S, 330 K e 40 $ms^{-1}$, durante o verão, a 18° - 29 °S, 340 K e 60 $ms^{-1}$, durante o inverno. Por fim, verificou-se que durante os eventos ENSO o comportamento do JS foi diferente em meses específicos, mas, em geral, eventos de "La Niña" (LN) enfraquecem o JS, mais pronunciadamente durante o inverno, e eventos "El Niño" intensificam o JS, especialmente durante o verão.

**ABSTRACT**

The Subtropical Jetstream (SJ) is analyzed over a period of 30 years (1979-2008) for the Southern Hemisphere in the vicinity of South America, between 100° and 30°W and 10° and 40°S, using ERA-INTERIM reanalysis data with a resolution of 0.5º of longitude x 0.5º of latitude. In order to stablish criteria for the SJ position, 12UTC daily manual comparisons were made for January and July of 2014. SJ is identified in operational services using the 250 hPa level chart where wind velocity is at least 30ms$^{-1}$ and potential temperature between 330 and 340 K. Using these limits, objective results were very similar to the SJ identified by meteorologists at the Centro de Previsão de Tempo e Estudos Climáticos (CPTEC). However when overlaid over water vapor satellite images these criteria failed to distinguish the SJ from the Polar Jet (PJ) when both were merged. At last, the adopted method for this study consisted in a daily (12 UTC) visual inspection of the vertical profile of the horizontal wind speed and potential temperature between 100 and 400 hPa. In order to properly identify the subtropical jet core, the altitude, location, temperature and shape were considered, resulting in the identification of the SJ latitude for each 10° of longitude in the area of study. The SJ obtained by this method not only proved to be consistent when compared to water vapor satellite images but also showed a proper flow over the days of each month, reproducing the seasonal variation of intensity and movement towards the Equator. After obtaining the daily SJ position over the 30-year period studied, we obtained a monthly climatology. The SJ varies from 16°-35°S, 330K and 40 ms$^{-1}$, during the summer to 18°-29°S, 340K and 60 ms$^{-1}$, during the winter. Finally, we found that during ENSO events the SJ behavior was different in specific months, but, overall, “La Niña” (LN) weakens the SJ, more pronouncedly during the winter, and “El Niño” (EN) intensifies the SJ, especially during the summer.

**CONTENTS**

LIST OF FIGURES ..... iii
LIST OF TABLES ..... viii
1. CHAPTER 1: INTRODUCTION ..... 1
1.1. Initial considerations ..... 1
1.2. Motivations ..... 1
1.3. Objectives ..... 2
2. CHAPTER 2: THEORETICAL BACKGROUND ..... 3
2.1. The Subtropical Jet (SJ) ..... 3
2.2. The El Niño Southern Oscillation (ENSO) ..... 11
2.3. The El Niño Phenomenon and the SOI INDEX ..... 13
3. CHAPTER 3: DATA AND METHODOLOGY ..... 15
3.1. Data ..... 15
3.2. Methodology ..... 16
4. CHAPTER 4: RESULTS AND DISCUSSIONS ..... 17
4.1. Subtropical jet identification ..... 17
4.2. Subtropical Jet Climatology ..... 37
4.2.1. Monthly climatology of the SJ latitude ..... 38
4.2.2. Subtropical Jet Wind Speed ..... 47
4.2.3. Subtropical Jet Pressure Level ..... 52
4.2.4. Subtropical Jet Potential Temperature ..... 55
4.2.5. Subtropical Jet Summary ..... 57
4.3. The Subtropical jet and the ENSO ..... 58
4.3.1.a The Subtropical jet behavior during “El Niño events” (position) ..... 58
4.3.1.b The Subtropical jet behavior during “El Niño events” (wind speed) ..... 67
4.3.2.a The Subtropical jet behavior during “La Niña events” (position) ..... 70
4.3.2.b The Subtropical jet behavior during “La Niña events” (wind speed) ..... 79
4.4. Comparison between normal, El Niño and La Niña conditions ..... 81
5. CHAPTER 5: CONCLUSIONS ..... 84
6. CHAPTER 6: SUGESTIONS FOR FUTURE STUDIES ..... 84
7. CHAPTER 7: REFERENCES ..... 87

## LIST OF FIGURES

Figure 2.1 - Vertical longitudinal cut of the three cell circulation in the Southern Hemisphere (Source: National Weather System, http://www.srh.noaa.gov/jetstream/global/jet.htm, 2016). ..... 5

Figure 2.2 - CPTEC 250 hPa analysis. Subtropical jet identified by red, northern Polar Jet branch by orange and southern Polar Jet by white dashed lines. ..... 9

Figure 2.3 - Water vapor image superimposed with ARPEGE analysis of vertical velocity (10 Pa/s, orange upwards, blue downwards) at 400 hPa and wind vectors at 300 hPa (above 90 kt) for December 19, 1998: (A) band or dry latent spot; (B) deformed dry band; (C / E) dynamic band or spot. (Source: Georgiev and Kozinarova, 2009) ..... 10

Figure 2.4 - El Niño Southern Oscillation (ENSO) patterns during “El Niño” and “La Niña” events. (Source: https://www.climate.gov/enso) ..... 12

Figure 2.5 - Southern Oscillation Index Source (SOI) for all years (monthly) (Source: https://www.ncdc.noaa.gov/teleconnections/enso/indicators/soi/) ..... 13

Figure 3.1 - Map of the study area of the subtropical jet (shaded background: altitude; foreground: wind speed at 250 hPa in $ms^{-1}$). ..... 15

Figure 4.1a - (Left) ERA-Interim 250 hPa: horizontal wind (shaded, $ms^{-1}$) and **θ** (dashed lines, K). (Right) 250 hPa CPTEC chart analyses. (1st, 11th, 21st and 31st January 2014). ..... 22

Figure 4.1b - (Left) ERA-Interim 250 hPa: horizontal wind (shaded, $ms^{-1}$) and **θ** (dashed lines, K). (Right) 250 hPa CPTEC chart analyses. (1st, 11th, 21st and 31st July 2014)..... 23

Figure 4.2a - Subtropical jet position defined as the northernmost latitude at 250 hPa where wind speed ≥30$ms^{-1}$ and **θ**: 330-340K for every 10 degrees of longitude on January 2014..... 25

Figure 4.2b - Subtropical jet position defined as the northernmost latitude at 250 hPa where wind speed ≥30$ms^{-1}$ and **θ**: 330-340K for every 10 degrees of longitude on July 2014..... 26

Figure 4.3 - Background: Water vapor satellite image, Foreground: wind speed above 30 $ms^{-1}$ between 330 and 340 K potential temperature at 250 hPa (shaded), and for the first days of January, April, July and October 2014. ..... 28

Figure 4.4a - **Figure 4.4a** Vertical profiles of horizontal wind above 30 $ms^{-1}$ (shaded) and potential temperature (330 and 340K in purple), for 100°W (Left), 60°W (Center) and 30°W (Right) between 100 and 400 hPa from ERA-Interim (1st, 11th, 21st and 31st January 2014). ..... 30

Figure 4.4b - Vertical profiles of horizontal wind above 30 $ms^{-1}$ (shaded) and potential temperature (330 and 340K in purple), for 100°W (Left), 60°W (Center) and 30°W (Right) between 100 and 400 hPa from ERA-Interim (1st, 11th, 21st and 31st July 2014)……32

Figure 4.5a - Maps of the subtropical jet (SJ core position (o at every 10 degrees of longitude) for January 2014 (Days 1st, 11th, 21st and 31st) overlaid water vapor satellite imagery. .....34

Figure 4.5b - Maps of the subtropical jet (at every 10 degrees of longitude) for July 2014 (Days 1st, 11th, 21st and 31st) overlaid water vapor satellite imagery……..35

Figure 4.6 - Average Percentage (%) when the Subtropical Jet could not be identified between 100° and 30°W in the period 1979-2008 by **(a)** longitude, and **(b)** month…38

Figure 4.7a - Boxplots corresponding to January, considering the period 1979-2008. .....41

Figure 4.7b - Boxplots corresponding to February, considering the period 1979-2008……41

Figure 4.7c - Boxplots corresponding to March, considering the period 1979-2008……42

Figure 4.7d - Boxplots corresponding to April, considering the period 1979-2008. …….....42

Figure 4.7e - Boxplots corresponding to May, considering the period 1979-2008. . …….....43

Figure 4.7f - Boxplots corresponding to June, considering the period 1979-2008. . …….....43

Figure 4.7g - Boxplots corresponding to July, considering the period 1979-2008. . …….....44

Figure 4.7h - Boxplots corresponding to August, considering the period 1979-2008. . …….....44

Figure 4.7i - Boxplots corresponding to September, considering the period 1979-2008..…….....45

Figure 4.7j - Boxplots corresponding to October, considering the period 1979-2008. . …….....45

Figure 4.7k - Boxplots corresponding to November, considering the period 1979-2008. . …….....46

Figure 4.7l - Boxplots corresponding to December, considering the period 1979-2008. . …….....46

Figure 4.8a - Bar graphics expressing the percentage (%) the SJ core is within wind speed limits (1) January, (2) February and (3) March. .....48

Figure 4.8b - Bar graphics expressing the percentage (%) the SJ core is within wind speed limits (1) April, (2) May and (3) June……..49

Figure 4.8c - Figure 4.8c Bar graphics expressing the percentage (%) the SJ core is within wind speed limits (1) July, (2) August and (3) September……..50

Figure 4.8d - Bar graphics expressing the percentage (%) the SJ core is within wind speed limits (1) October, (2) November and (3) December……...51

Figure 4.9a - Bar graphics expressing the percentage (%) of the SJ core vertical level (1) January, (2) February, (3) March, (4) April, (5) May and (6) June.....53

Figure 4.9b - Bar graphics expressing the percentage (%) of the SJ core vertical level (1) July, (2) August, (3) September, (4) October, (5) November and (6) December.54

Figure 4.10 - Bar graphics expressing the percentage (%) when SJ core has a certain potential temperature (1) January, (2) February, (3) March, (4) April, (5) May, (6) June, (7) July, (8) August, (9) September, (10) October, (11) November and (12) December.....56

Figure 4.11a - Boxplots corresponding to January, considering the period of El Niño events.....61

Figure 4.11b - Boxplots corresponding to February, considering the period of El Niño events…….....61

Figure 4.11c - Boxplots corresponding to March, considering the period of El Niño events. …….....62

Figure 4.11d - Boxplots corresponding to April, considering the period of El Niño events. …….....62

Figure 4.11e - Boxplots corresponding to May, considering the period of El Niño events. …….....63

Figure 4.11f - Boxplots corresponding to June, considering the period of El Niño events. …….....63

Figure 4.11g - Boxplots corresponding to July, considering the period of El Niño events. …….....64

Figure 4.11h - Boxplots corresponding to August, considering the period of El Niño events. …….....64

Figure 4.11i - Boxplots corresponding to September, considering the period of El Niño events. …….....65

Figure 4.11j - Boxplots corresponding to October, considering the period of El Niño events. ……..……..…….....65

Figure 4.11k - Boxplots corresponding to November, considering the period of El Niño events. ……..…….....66

Figure 4.11l - Boxplots corresponding to December, considering the period of El Niño events. ……..…….....66

Figure 4.12a - Bar graphics expressing the SJ wind speed anomaly in “El Niño” events: (1) January, (2) February, (3) March, (4) April, (5) May and (6) June. .....68

Figure 4.12b - Bar graphics expressing the SJ wind speed anomaly in “El Niño” events: June, (7) July, (8) August, (9) September, (10) October, (11) November and (12) December. ……..…….....69

Figure 4.13a - Boxplots corresponding to January, considering the period of La Niña events.....73

Figure 4.13b - Boxplots corresponding to February, considering the period of La Niña events. ……..…….....73

Figure 4.13c - Boxplots corresponding to March, considering the period of La Niña events. ……..…….....74

Figure 4.13d - Boxplots corresponding to April, considering the period of La Niña events. ……..…….....74

Figure 4.13e - Boxplots corresponding to May, considering the period of La Niña events. ……..…….....75

Figure 4.13f - Boxplots corresponding to June, considering the period of La Niña events. ……..…….....75

Figure 4.13g - Boxplots corresponding to July, considering the period of La Niña events. ……..…….....76

Figure 4.13h - Boxplots corresponding to August, considering the period of La Niña events. ……..…….....76

Figure 4.13i - Boxplots corresponding to September, considering the period of La Niña events. ……..…….....77

Figure 4.13j - Boxplots corresponding to October, considering the period of La Niña events. ……..…….....77

Figure 4.13k - Boxplots corresponding to November, considering the period of La Niña events. ……..…….....78

Figure 4.13l - Boxplots corresponding to December, considering the period of La Niña events. ……..……..…….....78

Figure 4.14a - Bar graphics expressing the SJ wind speed anomaly in “La Niña” events: (1) January, (2) February, (3) March, (4) April, (5) May and (6) June. .....80

Figure 4.14b - Bar graphics expressing the SJ wind speed anomaly in “El Niño” events: June, (7) July, (8) August, (9) September, (10) October, (11) November and (12) December. ……..……..…….....81

Figure 4.15a - Subtropical jet climatology (black marks), El Niño JS (red marks) and La Niña (blue Marks). (1) January, (2) February, (3) March, (4) April, (5) May and (6) June. .....82

Figure 4.15b - Subtropical jet climatology (black marks), El Niño JS (red marks) and La Niña (blue Marks). (7) July, (8) August, (9) September, (10) October, (11) November and (12) December. ……..……..…….....83

## LIST OF TABLES

Table 4.1 - Latitudinal position identified for the subtropical jet according to the CPTEC analysis at the level of 250 hPa for January 2014. .....18

Table 4.2 - Latitudinal position identified for the subtropical jet in ERA-Interim reanalysis at the 250 hPa level for January 2014 using only wind speed above 30 $ms^{-1}$ between 20 and 45$^{o}$S. .....19

Table 4.3 - Latitudinal position identified for the subtropical jet in ERA-Interim reanalysis at the 250 hPa level for January 2014 using wind speed above 30 $ms^{-1}$, potential temperature between 330 and 340K and between 18 and 46$^{o}$S. .....20

Table 4.4 - Latitudinal position identified for the subtropical jet according to the longitudinal vertical profiles for January 2014. .....33

Table 4.5 - Percentage (%) of times the Subtropical Jet could not be found between 100° and 30°W in the period of 1979-2008. .....37

Table 4.6a - Months affected by “El Niño” events according to the Southern Oscillation Index during the period of study (1979-2008) .....58

Table 4.6b - Months affected by “La Niña” events according to the Southern Oscillation Index during the period of study (1979-2008)……...70

# 1. CHAPTER I: INTRODUCTION

## 1.1. Initial considerations

The Subtropical Jet (SJ) is a very important atmospheric system for South America. According to Ramaswamy (1956) as long as there is humid air with a high degree of latent instability on the equatorial side of the SJ it plays an important role in promoting large scale convection in the subtropical region. This influence can even get stronger during ENSO.

There are several investigations about the SJ in the northern hemisphere, however in the southern hemisphere it has not been studied with the same level of detail. At the same time an atmospheric system such as the SJ tends to have symmetrical characteristics in both hemispheres, and thus these studies for the northern hemisphere may be used as reference for the SJ over South America.

In the present work we analyze the SJ in the southern hemisphere, especially over South America, and take different approaches to identify, locate and describe it in a daily basis and its behavior in a monthly basis in order to create a liable SJ climatology and to examine ENSO influence in SJ behavior and intensity.

## 1.2. Motivation

Identifying the Subtropical jet position is a complicated task, especially during summer, when it is weaker, with some authors even saying the SJ disappears during this season. Also, when merged with the Polar Jet (PJ) the SJ cannot be differentiated by normal means as its characteristics get mixed with those of the PJ. However, since the SJ position and intensity affect the local weather over an extensive region of South America, it is very important to have an extensive analysis over the different seasons in order to know what to expect of it during the year.

In this sense, the knowledge and characterization of the SJ over South America will be applied to pinpoint its position and behavior during each month and also how it changes during ENSO events.

### 1.3. Objective

The main objective of this project is to establish monthly subtropical jet climatology in the vicinity of South America between the longitudes of 100° and 30°W.

The specific objectives are:

I. Establish criteria for daily identification of the subtropical jet position
II. Obtain the climatology of the subtropical jet for each month of the year, and
III. Compare the pattern and position of the subtropical jet between years with the presence of the phenomenon El Niño and years with presence of the phenomenon La Niña.

# 2. CHAPTER II: THEORETICAL BACKGROUND

## 2.1. The Subtropical Jet (SJ)

At high levels of the atmosphere, near the tropopause, there is a region where the zonal wind component, from the west, reaches maximum values. This component increases with height due to the existence of meridional temperature gradients, being a few kilometers thick, tens of kilometers wide and thousands of kilometers long. This flow is called Jet Stream or simply Jet.

The subtropical jet stream in particular is a narrow band of intense west wind, often observed near 200 hPa level on both sides of the equator (Krishnamurti, 1961). The intensities of zonal winds and temperature fields are related through the relation of the thermal wind and, therefore, the intensity and the latitudinal position of the subtropical jet suffer great seasonal variability. In each hemisphere, the subtropical jet is more intense and closer to the equator during the winter, when compared to the summer (Galvin, 2007).

On average the subtropical jet can have the appearance of being continuous around the world within the subtropical regions. Consequently, the subtropical jet can be seen as almost permanent in the climatology of the winter season. On a daily basis, however, the subtropical jet can merge with and become indistinct from the polar jet (PJ), particularly when the latter is near the equator, which makes it harder to differentiate one from the other.

The subtropical jet is present at relatively low latitudes; where - despite a relatively weak horizontal temperature gradient - is accompanied by a relatively large vertical wind shear. This is explained, in the context of the thermal wind approach (**Equation 1.1**), due to the inverse relationship between the magnitude of the thermal wind (and therefore the vertical wind shear) and the Coriolis parameter, which is smaller in lower latitudes.

$$V_T = V_g(P_1) - V_g(P_0) = -\frac{R_d}{f}\int_{P_0}^{P_1}(k \wedge \nabla T)\, d\ln P \qquad (1.1)$$

$$u_T = -\frac{R_d}{f}\left(\frac{\partial \bar{T}}{\partial y}\right)_P \ln\left(\frac{P_0}{P_1}\right) \qquad (1.2)$$

$$v_T = \frac{R_d}{f}\left(\frac{\partial \bar{T}}{\partial x}\right)_P \ln\left(\frac{P_0}{P_1}\right) \qquad (1.3)$$

Where $\mathbf{V_T}$ is the thermal wind, $\mathbf{V_g}$ is the geostrophic wind, $\mathbf{P_0}$ and $\mathbf{P_1}$ are the base and top level pressures, $\mathbf{R_d}$ is the dry air constant and **f** is the Coriolis parameter.

The subtropical jet can be related to both Hadley and Ferrel circulations, as shown in **Figure 2.1.** Hadley's tropical circulation allows heat transfer and momentum from low to high latitudes (Webster, 2004). Through this circulation, the angular momentum is transferred westward toward the poles in the subtropical regions (Mitas and Clement, 2005), which contributes to the strong west winds associated with the subtropical jet.

The Ferrell cell is associated with the flow to the tropics in the upper troposphere and the flow towards the middle latitudes in the lower troposphere. This promotes high level convergence and surface divergence in subtropics, acting to intensify the southern meridional temperature gradient above and weaken it at the surface. From the thermal wind balance, this temperature gradient at high levels, with warmer air to the equator and colder air towards the poles, gives rise to the western subtropical jet (Mesoscale Research Group, Jet and Jet streaks, 2014).

The jet stream plays a very important role in promoting large-scale convection in subtropical regions around the world, wherever there is humid air with a high degree of latent instability on the equatorial side of the subtropical jet (Ramaswamy, 1956). This author also studied the relationship between subtropical jet and large-scale convection and determined that its influence occurs in all subtropical regions of the world.

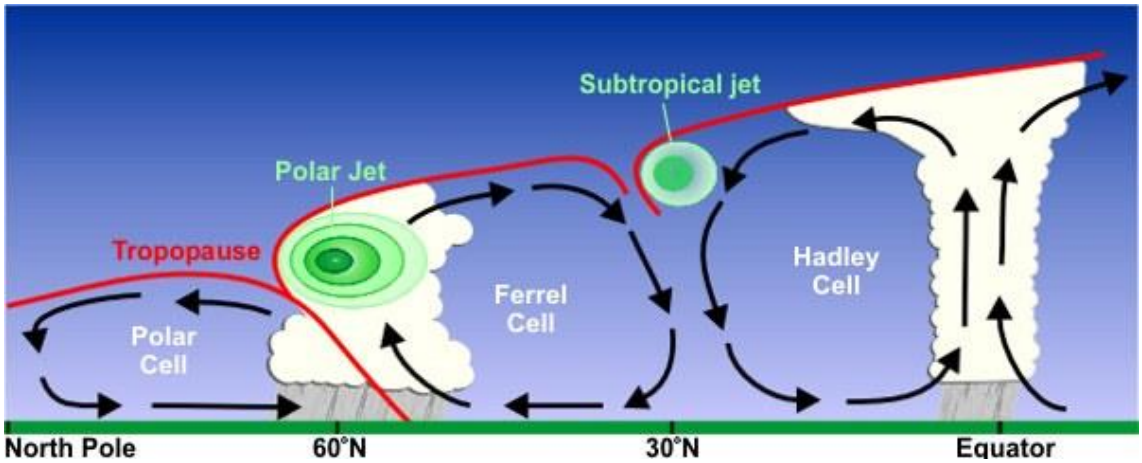


Figure 2.1 – Idealized longitudinal cut of the three cell circulation in the Northern Hemisphere (Source: National Weather System, http://www.srh.noaa.gov/jetstream/global/jet.htm, 2016).

Still, according to CPTEC:

[…]*Several researches have already been carried out, where directly or indirectly the Jet Stream has been studied. Historical reviews of the Jet Stream were made by Riehl (1969) and Reiter (1969). The importance of the Jet Stream is emphasized in Browning (1985) who associates some cases of precipitation with the Jet Stream. Also, Kousky and Cavalcanti (1984) connected the flow pattern at high levels to a blocking event that occurred in South America during the 1983 ENSO event*. […][1]

However, from a climatological point of view, in the upper air, little has been done. This is mainly due to its great spatial and temporal variability along its entire length, especially in the southern hemisphere, and the difficulty of distinguishing it from the northern branch of the polar jet, especially during winter when the latter moves north.

There are also studies that have analyzed jets in the northern hemisphere or across the globe. Barton and Ellis (2009) studied the jet analyzing maximum wind speeds at 300 hPa, but due to their methodology they failed to ensure that the jet they identified could be classified either as the subtropical jet or the polar jet. Reiter (1963) observed that when using long periods of time averages the latitudinal variability of the zonal flow was considerably large. This made it unlikely to be able to differentiate one jet from another from time to time. Also, Reiter was one of the first to note that the contrast in the horizontal and vertical dimensions of jet streams, the

[1] http://climanalise.cptec.inpe.br/~rclimanl/boletim/cliesp10a/jatclim.html, 2016

former exceeding the latter by nearly two orders of magnitude, with much larger vertical than horizontal gradients of temperature and wind speed.

Manney (2013) developed a global climatology of the jets in the upper troposphere and studied their relation with stratospheric sub vortexes and multiple tropopauses using MERRA (Modern Era Retrospective-Analysis for Research and Applications). His analysis revealed a Northern Hemisphere (NH) upper tropospheric jet that stretches nearly zonally from the mid-Atlantic across Africa and Asia. Manney (2013) also found that multiple tropopauses associated with the primary tropopause "break" commonly extend poleward from the subtropical upper tropospheric jet.

Koch (2006) elaborated a climatology based on individual events and their frequency, obtaining a data set for jet events subdivided into a two-class typology, shallow (SL) and deep (DL), that constitutes an alternative to the customary split into SJ and PJ. The associated climatology possesses major inter-hemispheric differences in the spatial distribution, frequency, and seasonal cycle of both jets. The results for the Southern hemisphere can be summed up in following paragraph:

[…]*In the SH, the frequency of both jet events possesses a quasi-annular structure, and both exhibit comparatively little latitudinal variation with season except for the DL events over the South Pacific. Both SL and DL events favor the sector between 60° and 190 °E that extends from the central western Pacific to the central eastern Pacific. The quasi-annular SL frequency distribution is located between 20° and 35°S. It is strongest in winter (JJA) with a longitudinally extended maximum in excess of 60%. It is weakest in summer (DJF) when it breaks up into two, with gaps centered in the southern and eastern Pacific Ocean, each portion with a frequency of less than 30%. The DL annulus is located between 40° and 60 °S, but in winter it acquires an equatorward arm that extends outward from the central eastern Pacific over central Australia and on into the mid-western Pacific.*[…]

Eichelberger and Hartmann (2007) studied the zonal structure of the jet through EOFs and observed significant differences in the subtropical jet between the Pacific and Atlantic sectors in the northern hemisphere, with model results indicating that the leading mode of variability depended on the distance between eddy-driven and subtropical jets. Their study revealed that eddy zonal flow feedback strength was stronger for the zonal wind distribution over the Atlantic sector than for that over the

Pacific sector, as the jet structure over the latter inhibited the necessary wave propagation to produce such feedback and therefore lead to the differences in the strength of the leading mode in the NH over the two regions.

Lachmy and Harnick (2014) showed the existence of two flow regimes in the atmosphere. One, referred as the “subtropical jet regime” where the maximum of the upper-tropospheric zonal mean wind is located at the subtropical edge of the Hadley cell and a second, called “merged jet regime” where the maximum of the wind lies inside the Ferrel cell and was created by the merging of the subtropical and eddy-driven jets. The former is dominated by thermal driving, while in the latter convergence of eddy momentum flux also plays a major role. The subtropical regime maintenance, which we are interested in, is mainly provided by a balance between the advection of momentum by the mean meridional circulation and the Coriolis force.

Lee and Kim (2003) have established, in an idealized model experiment, that the existence of an eddy-driven jet is dictated by the strength and latitude of the subtropical jet. If the SJ is sufficiently strong, the primary region of baroclinic wave growth coincides with the SJ region and therefore a polar jet front does not form at higher latitudes than the SJ. On the other hand, when the SJ is weak, baroclinic wave growth takes place in the mid-latitude baroclinic zone, establishing the polar front jet at this latitude.

Seagar (2005) observed that during the El Niño events the jets were strengthened in each hemisphere and move to the equator. Also, changes in the subtropical jet influenced the transient-eddy momentum fluxes and the eddy-driven mean meridional circulation. Thus, during El Niño events, eddy-driven ascent in the mid-latitudes of each hemisphere is accompanied by low-level convergence and brings increased precipitation.

Abish (2015) analyzed the climate change impact in the subtropical jet and found that it has been strengthened in the northern hemisphere and weakened in the southern hemisphere.

Assuming that the jet has symmetrical characteristics in both hemispheres, many of the results of the studies of the subtropical jet or jets in general obtained for the NH can be used or considered for this study in the southern hemisphere.

The CPTEC weather forecast office uses the following criteria for daily identification of the Subtropical Jet at 250 hPa (Escobar, 2012)[2]; exemplified in **Figure 2.2**:

- Wind speed, along the jet stream, with a value equal to or greater than 130kmh$^{-1}$ (36 ms$^{-1}$ or 70 kt)
- Latitudes between 20° to 40°S
- Geopotential height above 10440 gpm, typically 10680 gpm, and
- The average potential temperature associated with the jet is 340 K.

The subtropical jet is also observed in satellite images in the vapor channel, this is possible because the dry (dark) and wet (bright) areas and the boundaries between them are normally related to significant characteristics of upper level flow such as troughs, dynamic anomalies of the tropopause, but especially, in the context of this work, the jets. In these systems the boundaries of dry and wet areas has become oriented towards the upper flow of the atmospheric circulation. In addition, usually dark regions in the images tend to be associated with mid-troposphere troughs and light tones with thermal ridges (Santurette and Gergiev, 2009).

[2] http://cursos.cptec.inpe.br/~rcursos/pratico_analise_previsao_tempo/pdf/Apostila_112012.pdf

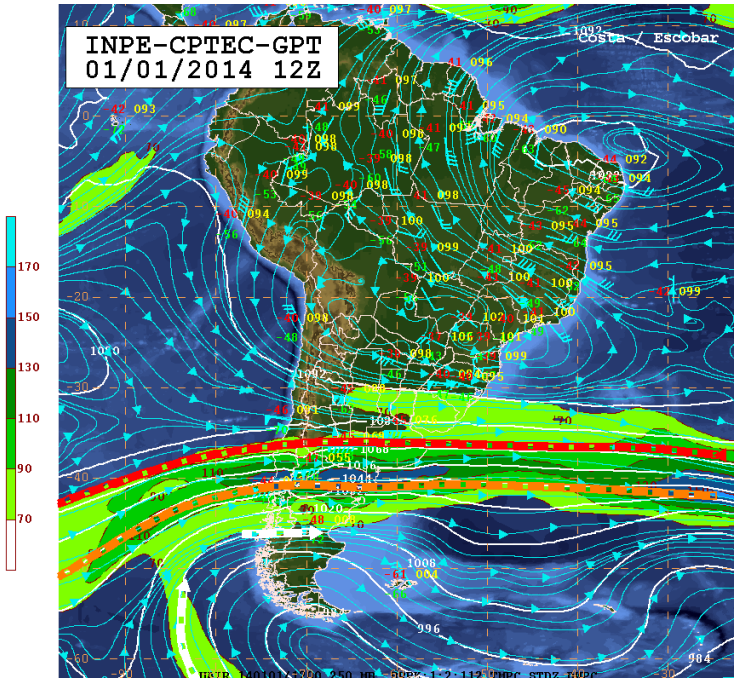


Figure 2.2 - CPTEC 250 hPa analysis. Subtropical jet identified by red, northern Polar Jet branch by orange and southern Polar Jet by white dashed lines.

In water vapor images, bands or dry spots (dark) ranging from medium gray to dark gray and which have the shape of a band or a semicircular spot that is not closed or surrounded by significant areas of significant synoptic cloudiness (almost white to shades of light grey) can be found. Georgiev and Kozinarova (2009) classified these bands in three types, of which the third type is of interest to this study:

1. Latent dry bands or spots (A in **Figure 2.3**): Medium gray (rarely dark gray) tones are associated with weak descending movements (or their absence) and a latent anomaly of the tropopause (a weak anomaly of potential vorticity – PV), but in this case there is no jet. These patterns may move according to the upper-level wind field but are not associated with further development of significant disturbances as long as they do not interact with the jet.

2. Deformed dry bands (B in **Figure 2.3**): These may be associated with subsidence but are not bounded with jets or PV anomalies. They are associated with upper-level flow deformation zones. In a specific situation, dry air at high levels, associated with such dark bands, may be favorable for the development of convection, generating instability.

3. Dynamic Dry Bands or spots: These are associated with strong subsidence, jet streams, and PV anomalies. Such a dynamically significant dry band is labeled as C in **Figure 2.3**, and is a precursor to further development of a dry intrusion. A dynamic dry spot also appears in the E position associated with significant subsidence and an anomaly of the dynamic tropopause at the base of a trough.

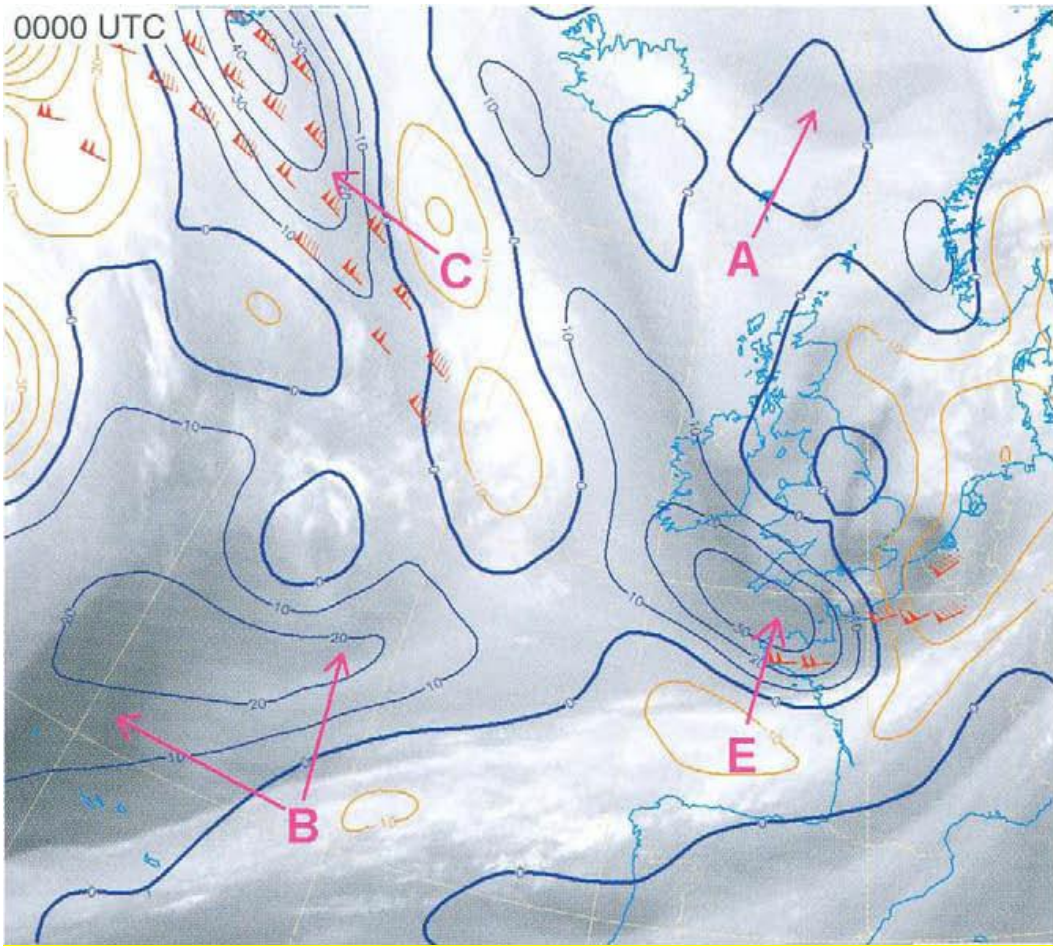


Figure 2.3 - Water vapor image superimposed with ARPEGE analysis of vertical velocity (10 $Pa.s^{-1}$, orange upwards, blue downwards) at 400 hPa and wind vectors at 300 hPa (above 90 kt) for December 19, 1998: (A) dry latent band or spot; (B) deformed dry band; (C / E) dynamic band or spot. (Source: Santurette and Gergiev, 2009)

## 2.2. The El Niño Southern Oscillation (ENSO)

As described by the World Meteorological organization (WMO) in 2014:

[…]*The El Niño/Southern Oscillation (ENSO) is a naturally occurring phenomenon involving fluctuating ocean temperatures in the central and eastern equatorial Pacific, coupled with changes in the atmosphere. This phenomenon has a major influence on climate patterns in various parts of the world.* […] *El Niño and La Niña are the oceanic components while the Southern Oscillation is the atmospheric counterpart, thus giving rise to the term El Niño/Southern Oscillation.* […]

[…]*The El Niño/Southern Oscillation comprises three phases: El Niño, La Niña and neutral. El Niño, meaning "boy child" in Spanish, was first used in the nineteenth century by fishermen in Peru and Ecuador to refer to the unusually warm waters that reduced their catch just before Christmas. El Niño events often begin in the middle of the year with large-scale warming of surface water in the central and eastern equatorial Pacific Ocean and changes in the tropical atmospheric circulation (i.e. winds, pressure and rainfall).* […]

[…] *In general, El Niño reaches a peak during November–January and then decays over the first half of the following year. It occurs every two to seven years and can last up to 18 months. Strong and moderate El Niño events have a warming effect on average global surface temperatures. The opposite of El Niño within the ENSO cycle is known as La Niña, which means "little girl" and refers to the large-scale cooling of the ocean surface temperatures in the same region in the equatorial Pacific, coupled with a reversal of the overlying atmospheric conditions. In many locations, especially in the tropics, La Niña (or cold episodes) produces the opposite climate variations to El Niño. During ENSO-neutral phases, atmospheric patterns are controlled more by other climate drivers.* […]

However in recent years the frequency of "El Niño" events has become more frequent with a variable intensity.

A scheme that shows the broad implications of the positive and negative phases of the ENSO is shown in **Figure 2.4** where we can see the difference in both the atmospheric and the sea surface temperature patterns in each event.

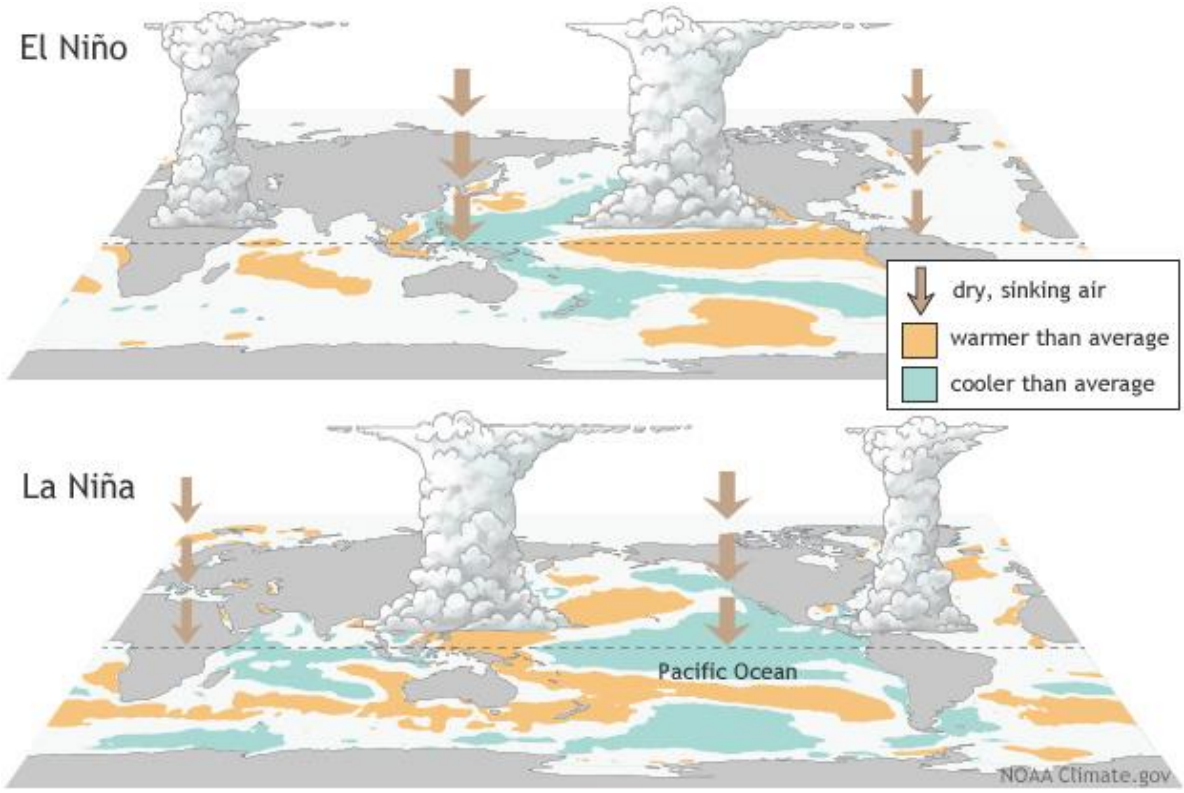


Figure 2.4 - El Niño Southern Oscillation (ENSO) patterns during “El Niño” and “La Niña” events. (Source: https://www.climate.gov/enso)

Corroborating Arkin’s (1982) earlier findings, it is known that during warm ENSO conditions the subtropical jet streams in both hemispheres tend to increase in strength and that they tend to weaken during cool “La Niña” conditions. The correlations are very high, with values of $r \geq 0.80$ for the smoothed time series (Oort and Yienger, 1996). This may be explained by the influence ENSO has in the intensity of the Hadley circulation, which as seen before has a direct relation with the subtropical jet.

## 2.3. The El Niño Phenomenon and the SOI INDEX

As described by the National Oceanic and Atmospheric Administration (NOAA):

[…] *The Southern Oscillation Index (SOI) is a standardized index based on the observed sea level pressure differences between Tahiti and Darwin, Australia. The SOI is one measure of the large-scale fluctuations in air pressure occurring between the western and eastern tropical Pacific (i.e., the state of the Southern Oscillation) during El Niño and La Niña episodes. In general, smoothed time series of the SOI correspond very well with changes in ocean temperatures across the eastern tropical Pacific. The negative phase of the SOI represents below-normal air pressure at Tahiti and above-normal air pressure at Darwin. Prolonged periods of negative (positive) SOI values coincide with abnormally warm (cold) ocean waters across the eastern tropical Pacific typical of El Niño (La Niña) episodes.* […]

The monthly results of the SOI calculations can be seen in **Figure 2.5**.

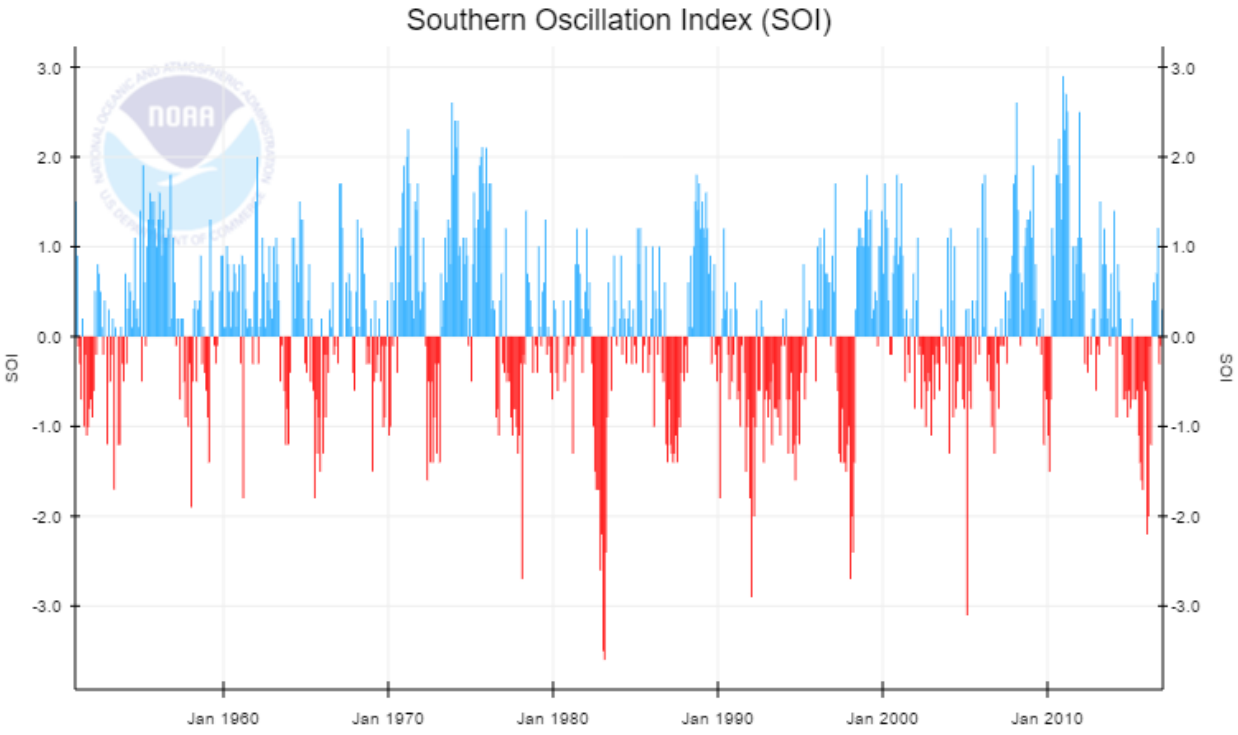


Figure 2.5 - Southern Oscillation Index Source (SOI) for all years (monthly) (Source: https://www.ncdc.noaa.gov/teleconnections/enso/indicators/soi/)

Calculation of SOI

(The anomalies are calculated as departures from the 1951-1980 base period.)

$$SOI = \frac{Standarized\ Tahiti - Standarized\ Darwin}{MSD} \qquad (\mathbf{2.1})$$

*where,*

$$Standarized\ Tahiti\ = \frac{(Actual\ Tahiti\ SLP - Mean\ Tahiti\ SLP)}{Standard\ Deviation\ Tahiti} \qquad (\mathbf{2.2}\boldsymbol{a})$$

$$Standarized\ Darwin\ = \frac{(Actual\ Darwin\ SLP - Mean\ Darwin\ SLP)}{Standard\ Deviation\ Darwin} \qquad (\mathbf{2.2}\boldsymbol{b})$$

*where,*

$$Standart\ Deviation\ = \sqrt{\sum (Actual\ SLP - Mean\ SLP)^2/N} \qquad (\mathbf{2.3})$$

*where*

$N = Number\ of\ months$

*and,*

$$MSD^* = \sqrt{\sum (Standarized\ Tahiti - Standarized\ Darwin)^2/N} \qquad (\mathbf{2.4})$$

* $Monthly\ Standard\ Deviation$

Being the limits:

EN≤-0.5

LN≥0.5

# 3. CHAPTER III: DATA AND METHODOLOGY

## 3.1. Data

The data used in this work was obtained from the ERA-Interim program with a horizontal grid resolution of 0.5° of latitude x 0.5° of longitude and a daily time resolution, using only the 12:00 UTC reanalysis for the levels between 100 and 400 hPa. The selected variables were zonal and meridional wind - used to calculate the horizontal wind speed - and temperature - used to calculate the potential temperature. To stablish the subtropical jet position climatology and analysis of the impact of the ENSO on the subtropical jet, the reanalysis data used corresponded to the period 1979-2008. However, in order to determine the best criteria of the SJ identification, the reanalysis data of January (representing a summer condition) and July (winter) 2014 were used. In addition, the synoptic charts of the CPTEC corresponding to the months of January and July 2014 and the water vapor satellite imagery of the same days were also used for validation. The studied area for January 2014 can be seen in **Figure 3.1**, however when comparing with water vapor satellite imagery the area was slightly enlarged (101° to 26°W and 14°N to 56°S) for better comparison.

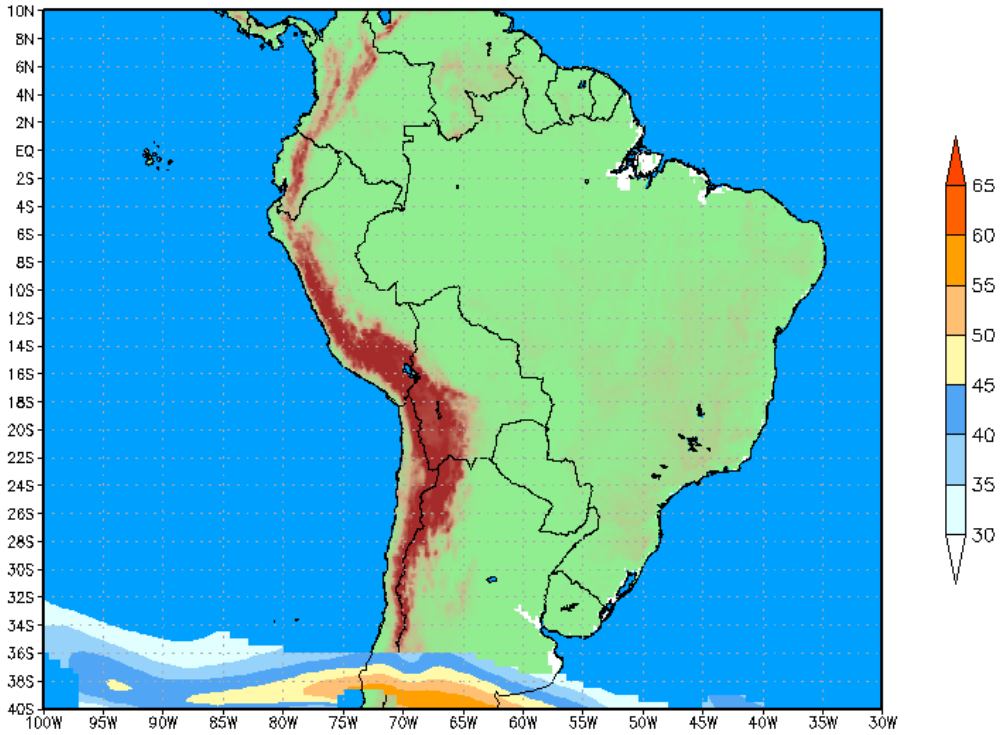


Figure 3.1 - Map of the study area of the subtropical jet (shaded background: altitude; foreground: wind speed at 250 hPa in $ms^{-1}$).

## 3.2. Methodology

The criteria considered to identify the subtropical jet had to be tested first to see if it was suited for the southern hemisphere in different seasons. We selected two months of 2014: one representative of the summer (January) and the other one of the winter (July). This period was selected for comparison and validation with CPTEC analyses. Thus, using the ERA-Interim reanalysis data of the daily 12:00 UTC of January and July 2014, the following analyses were made:

- The same CPTEC criteria: at 250 hPa level, horizontal velocity equal to or higher than 30ms$^{-1}$ and potential temperature around 340 K;

- To identify the pressure level where the SJ had its highest velocity (SJ core), vertical profile of wind speed and potential temperature were made every 10 degrees for the longitudes from 100° to 30°W, between the latitudes of 40° to 10°S and between the levels of 100 and 400 hPa.

- At the pressure level identified in the previous step, the location of the SJ was verified with thresholds of 30 ms$^{-1}$ horizontal velocity and potential temperature range between 330 and 340 K (Reiter and Whitney, 1969);

- Validation of the methodology was obtained comparing the results with the CPTEC analysis and water vapor satellite imagery to see which criteria were best suited.

The best criteria to identify the Subtropical Jet in the Southern Hemisphere turned out to be selecting the position of the jet core in a daily vertical profile with a wind speed equal or greater than 30 ms$^{-1}$. This identification was made considering all the literature characteristics and thus was done with visual inspection of each vertical profile. Since it could not be done using objective algorithms, the SJ position was visually identified for each of the 7 vertical profiles for each day (12 UTC) from January 1979 to December 2008 and this was used to elaborate the data for the monthly climatology and study the influence of ENSO episodes.

# 4. CHAPTER IV: RESULTS AND DISCUSSIONS

## 4.1. Subtropical jet identification

In order to identify the subtropical jet in the southern hemisphere, three criteria were tested for January and July of 2014 and compared to the CPTEC analyses. The results for January are shown in three Tables where the jet latitude is identified for every ten degrees of longitude, between 100° and 30°W. **Table 4.1** was taken from the CPTEC daily bulletin for the entire month of January 2014, using analyses of the 250 hPa level at 12 UTC only for the longitudes from 100° to 30°W.

In these analyses, CPTEC meteorologists identified the jets according to their experience, using mainly wind speed at 250 hPa level and geopotential height as a reference. From these charts, the latitude of the subtropical jet was identified for every 10 degrees of longitude, shown in **Table 4.1** (for the longitudes where CPTEC did not identify the subtropical jet no latitude was considered). The jet was identified in 166 of the 248 evaluated points and it was located between 27 and 47.5°S. The SJ could be seen almost all the days over the Atlantic Ocean (50° to 30°W) but only a few days over the Pacific Ocean (100° to 80W°). The jet started well defined at the beginning of the month, but then lost this continuity, especially over the Pacific where it was not observable in 15 of the 31 days analyzed.

Through visual inspection of vertical profiles, it was observed that in 100 cases of the total of 183 analyzed points the position (latitude) of the jet core coincides with the level of 250 hPa and in 54 of the 183 the jet core is either above or below the level of 250 hPa, but it is still appreciable at this level. This corroborates in fixing the 250 hPa level chart for SJ operational identification.

In **Table 4.2**, the SJ was identified in ERA-Interim reanalysis using the criteria: wind speed greater than 30 $ms^{-1}$ on 250 hPa with latitudes between 20° and 45°S. The northernmost latitude was defined as the location of the SJ. In this way the jet can be located in 167 of the evaluated 248 points. The displacement of the subtropical jet during the month is the same as in **Table 4.1**.

**Table 4.3** was obtained, considering the criteria used in **Table 4.2**, and adding potential temperature between 330 and 340K between 18° and 46°S at the level of

250 hPa. Again, the northernmost latitude of the intersection of these 3 areas was defined as the SJ position. The jet could be located in 201 of the 248 evaluated points and the spatial variation is similar to that obtained in **Table 4.1**.

Table 4.1 - Latitudinal position identified for the subtropical jet according to the CPTEC analysis at the level of 250 hPa for January 2014.

| Day/Longitude | 100°W | 90°W | 80°W | 70°W | 60°W | 50°W | 40°W | 30°W |
|---|---|---|---|---|---|---|---|---|
| **1** | -43 | -40 | -37 | -36.5 | -36.5 | -36.5 | -36.5 | -36.5 |
| **2** | -47.5 | -46 | -36 | -34 | -35 | -39 | -39 | -37.5 |
| **3** | -45 | -45 | | -29 | -33 | -36 | -40 | -43 |
| **4** | | -43 | -42 | -39.5 | -36.5 | -31 | -34 | -37 |
| **5** | | | -37 | -39 | -37 | -35.5 | -34.5 | -35 |
| **6** | | -34.5 | -37.5 | -38 | -38 | | | -33.5 |
| **7** | | -34.5 | -37.5 | -37 | -37 | | | -34 |
| **8** | | -31 | -34 | -34 | -33 | -35 | -39 | -40 |
| **9** | | -32 | -34 | -34.5 | -33 | | -36.5 | -40 |
| **10** | | | -34 | -34 | -35 | -36 | | -38 |
| **11** | | | | -30.5 | -33 | -34.5 | -37.5 | -43 |
| **12** | | | | | | -33.5 | -36.5 | -39 |
| **13** | -41 | | | | | | -36 | -36 |
| **14** | -43 | -45 | -45 | | | | -38.5 | -37 |
| **15** | | | | -44 | | | | -39 |
| **16** | -34 | -39 | | | | | | -36 |
| **17** | -31 | -36 | -42 | -43 | | | | -36.5 |
| **18** | -28 | -32 | -40 | -43 | -43 | -40.5 | | |
| **19** | | | -39 | -43 | -42.5 | -39 | | |
| **20** | | | -27 | -33 | -42 | -41 | -38 | -36.5 |
| **21** | | | -30.5 | -32 | -36 | -42 | -42 | -39 |
| **22** | | | -33.5 | -36.5 | -37 | -37 | -39 | -42 |
| **23** | | | -30.5 | -35.5 | -40 | -41 | | |
| **24** | | | | -34 | -38 | -40.5 | -41 | -40 |
| **25** | | | | | -34.5 | -37 | -38.5 | -41 |
| **26** | | -29 | | | -36 | -37 | -37.5 | -38 |
| **27** | | | -29 | -31 | -35 | -37 | -37 | -35.5 |
| **28** | | | -28 | -30 | -37 | -39.5 | -39 | -36 |
| **29** | | | | | -37 | -40 | -40.5 | -41 |
| **30** | -33 | -36.5 | | | -34.5 | -38.5 | -40 | -38.5 |
| **31** | -35.5 | -37.5 | -37 | -35.5 | -37.5 | -36 | -40 | -41 |

Table 4.2 - Latitudinal position identified for the subtropical jet in ERA-Interim reanalysis at the 250 hPa level for January 2014 using only wind speed above 30 $ms^{-1}$ between 20 and 45$^{o}$S.

| Day/Longitude | 100°W | 90°W | 80°W | 70°W | 60°W | 50°W | 40°W | 30°W |
|---|---|---|---|---|---|---|---|---|
| **1** | -42 | -38.5 | -36 | -35 | -29 | -30.5 | -32 | -31 |
| **2** | -45 | -42 | -36 | -28 | -29 | -31 | -31.5 | -30 |
| **3** | -44 | -44 | -42 | -32 | -29 | -30 | -35 | -36 |
| **4** | -41 | -41 | -40 | -38 | -34 | -28 | -31 | -34 |
| **5** | -29 | -33 | -34 | -37 | -35 | -33 | -30 | -32.5 |
| **6** | -22 | -31 | -34 | -35.5 | -35 | -34.5 | -32 | -31 |
| **7** | -20 | -26 | -32.5 | -30 | -34 | -34.5 | -37.5 | -32 |
| **8** | | -27.5 | -30.5 | -30.5 | -30 | -32 | -36.5 | -39 |
| **9** | | -29 | -30 | -30 | -29 | | -34 | -37.5 |
| **10** | | | -30 | -29.5 | -31.5 | -34 | | -36 |
| **11** | | | -32 | -29 | -32 | -32 | -34.5 | -40 |
| **12** | | -24 | -30 | -28 | -27 | -30.5 | -33.5 | -36 |
| **13** | -38.5 | -40 | -42 | | | | -36 | -34 |
| **14** | -39 | -42 | -41.5 | | | | -36.5 | -34 |
| **15** | | -40 | -42.5 | -42 | | | | -34 |
| **16** | -32 | -36.5 | -42 | -42.5 | | | | -32 |
| **17** | -30 | -31 | -39 | -41 | -40 | | | -33.5 |
| **18** | -26.5 | -29.5 | -36.5 | -40 | -39.5 | -38 | -36.5 | -33 |
| **19** | | -31.5 | -34 | -40 | -38.5 | -34.5 | -36 | -36 |
| **20** | | | -24 | -30 | -40.5 | -38.5 | -36 | -34 |
| **21** | | | -26 | -29 | -34 | -40 | -40.5 | -35.5 |
| **22** | | | -25 | -30 | -31.5 | -34.5 | -38 | -38.5 |
| **23** | | | -26 | -30 | -36 | -36 | -33 | |
| **24** | | | -28 | -30 | -33.5 | -36 | -38 | -34 |
| **25** | | | | | -31 | -32.5 | -33.5 | -36.5 |
| **26** | | | | | -31.5 | -32.5 | -33.5 | -34 |
| **27** | | -24.5 | -24.5 | -28 | -32 | -34 | -33.5 | -33 |
| **28** | | -25.5 | -25.5 | -28 | -32.5 | -34.5 | -35 | -33.5 |
| **29** | | | | | -32 | -34.5 | -36 | -36.5 |
| **30** | -31 | -34 | -30 | | -32.5 | -35.5 | -36.5 | -34.5 |
| **31** | -32 | -35 | -32 | -31.5 | | -34 | -38 | -38 |

Table 4.3 - Latitudinal position identified for the subtropical jet in ERA-Interim reanalysis at the 250 hPa level for January 2014 using wind speed above 30 $ms^{-1}$, potential temperature between 330 and 340K and between 18 and 46°S.

| Day/Longitude | 100°W | 90°W | 80°W | 70°W | 60°W | 50°W | 40°W | 30°W |
|---|---|---|---|---|---|---|---|---|
| **1** | -42 | -38.5 | -36 | -33 | -32.5 | -36 | -36.5 | -38 |
| **2** | -45 | -42 | -35.5 | -34.5 | -36.5 | -36 | -36.5 | -34.5 |
| **3** | -43.5 | -44 | -42 | -32.5 | -38 | | -46 | -44 |
| **4** | -41 | -40.5 | -40 | -38 | -34 | -36 | -42 | |
| **5** | -30 | -34 | -35 | -37 | -35 | -32.5 | -33 | -38 |
| **6** | -22.5 | -30.5 | -34 | -35 | -35.5 | -34.5 | -32 | -33.5 |
| **7** | -18.5 | -26 | -32.5 | -33 | -34.5 | -34.5 | | -32 |
| **8** | | -27 | -30.5 | -30.5 | -33.5 | -36 | -36.5 | -39 |
| **9** | | -28.5 | -30 | -30 | -29 | | -38 | -42 |
| **10** | | | -30 | -29.5 | -31 | -34 | -40 | -36 |
| **11** | | | -32 | -29 | -34 | -34 | -34.5 | -40 |
| **12** | -37.5 | -40 | -32 | -30.5 | | -32 | -36 | -39.5 |
| **13** | -38.5 | -40 | -42 | -44 | | | -35 | -34 |
| **14** | -39 | -42 | -41.5 | -45 | | | -36.5 | -33.5 |
| **15** | -38 | -39.5 | -42.5 | -41.5 | -41.5 | -43 | -34 | -34 |
| **16** | -32 | -36.5 | -42 | -42.5 | -41 | -41 | -39.5 | -32 |
| **17** | -29.5 | -32 | -39 | -41 | -39.5 | -40.5 | | -33.5 |
| **18** | -26.5 | -29.5 | -38 | -42 | -39 | -38 | -36.5 | -33 |
| **19** | | -31.5 | -30.5 | -40 | -41 | -37.5 | -36 | -36 |
| **20** | | -32 | -28.5 | -35.5 | -40.5 | -38.5 | -36 | -34 |
| **21** | | | -32 | -36 | -42 | -42 | -40.5 | -36 |
| **22** | | | -34.5 | -35 | -37.5 | -38 | -40 | -46 |
| **23** | | | -32 | -40 | -42 | -43.5 | -37.5 | -44 |
| **24** | | | -43 | | | | | -44 |
| **25** | | | | | | | | |
| **26** | -24 | -24.5 | | | -38.5 | -38 | -38 | -40 |
| **27** | | -26 | | | -36.5 | -40 | -38 | -33 |
| **28** | | | | | -38 | -39 | -37.5 | -33.5 |
| **29** | -26.5 | -36 | -40 | -44 | -38 | -42 | -42.5 | -40 |
| **30** | -31 | -34 | -34 | -34 | | -38 | -40 | -38.5 |
| **31** | -32 | -35 | -36 | -36 | -37.5 | -39 | -40 | -40.5 |

**Figures 4.1a** and **b** show the application of the last criteria (wind speed ≥ 30 $ms^{-1}$ and potential temperature between 330 and 340 K at 250 hPa) for the 1st, 11th, 21st and 31st of January (a) and July (b) of 2014, and comparing them to the CPTEC analysis. As can be seen, there is a significant similarity between the subtropical jet obtained through the methodology used with the one analyzed by the CPTEC meteorologists for both months. It is important to notice that ERA-Interim maps (left) have a length ranging from 100° to 30°W, whereas CPTEC maps have a little bit broader area, so the similarities may not be as clear at first sight.

The main difference found between these months is that the SJ is found at higher latitudes in the summer (30-45°S) and in lower latitudes in the winter (15-35°S). It is interesting to notice also that the SJ presents more discontinuity on July.

For both cases, January and July, when the SJ is merged to the northern branch of the polar jet, both are observed in the wind field bounded by the thresholds established at the beginning of the study and the SJ could be “isolated” from the PJ using the northernmost criteria.

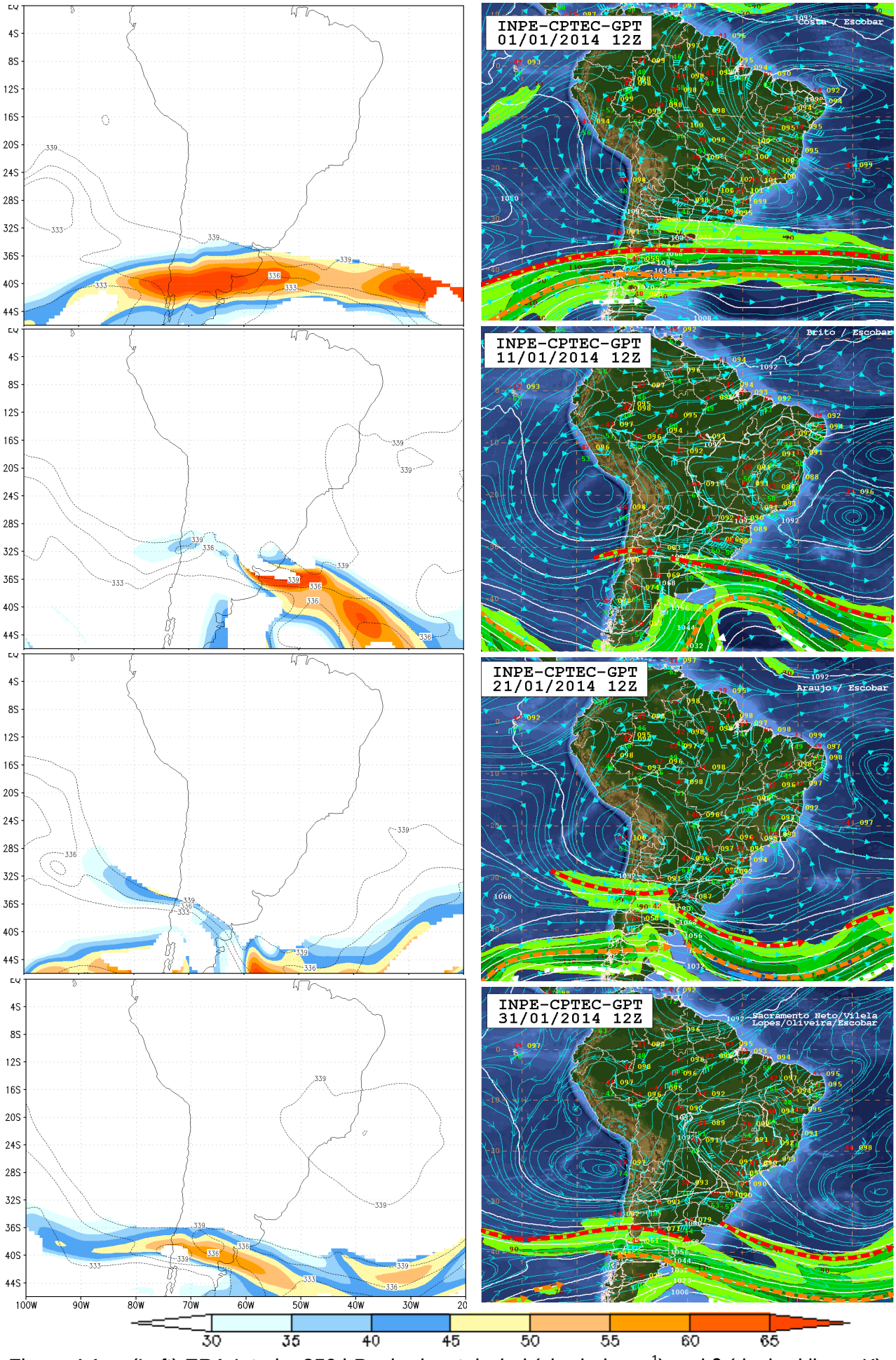


Figure 4.1a - (Left) ERA-Interim 250 hPa: horizontal wind (shaded, $ms^{-1}$) and **θ** (dashed lines, K). (Right) 250 hPa CPTEC chart analyses. SJ (red dashed lines), NPJ (orange dashed lines) and SPJ (white dashed lines);(1st, 11th, 21st and 31st January 2014).

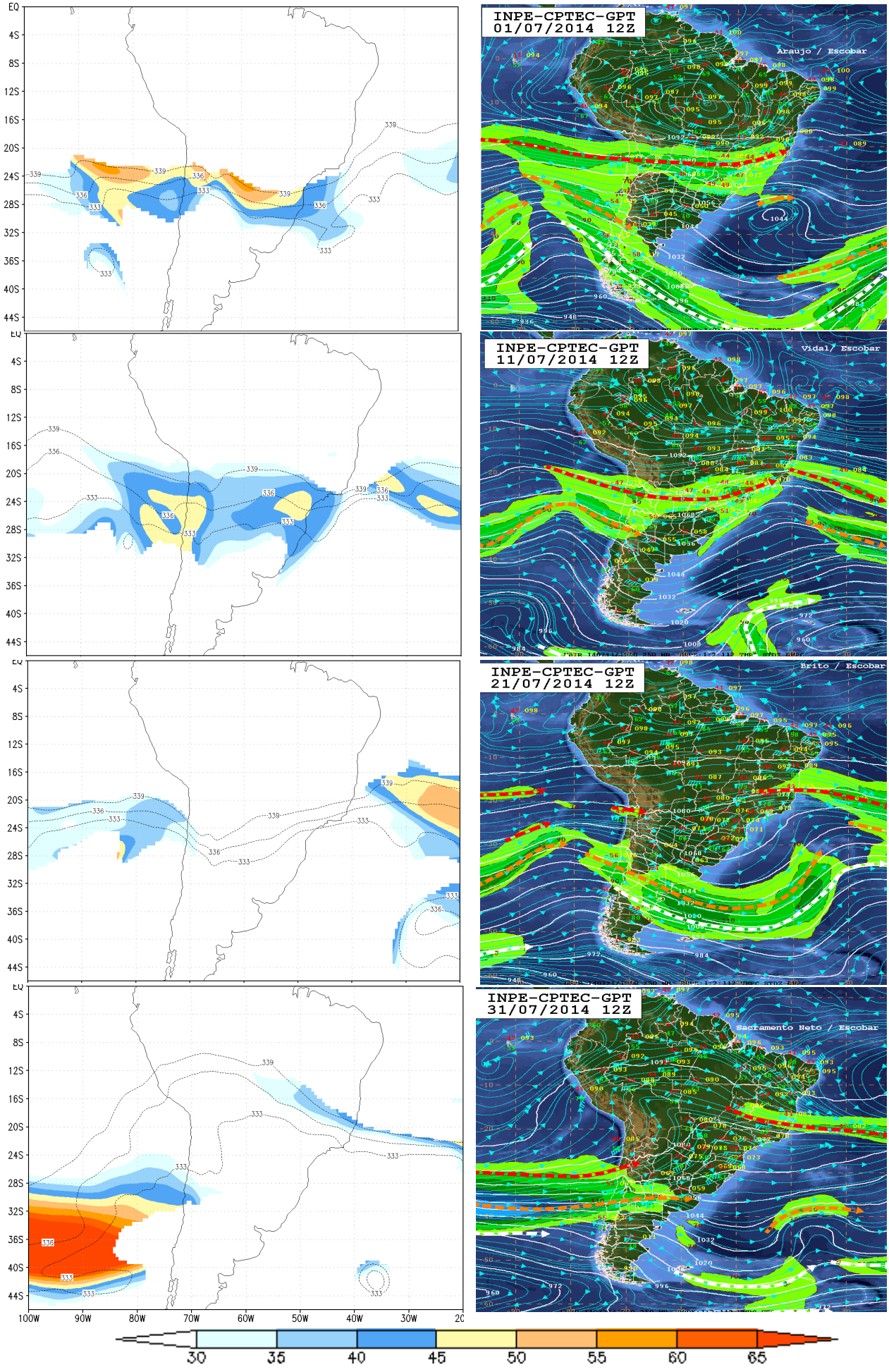


Figure 4.1b - (Left) ERA-Interim 250 hPa: horizontal wind (shaded, $ms^{-1}$) and **θ** (dashed lines, K). (Right) 250 hPa CPTEC chart analyses. SJ (red dashed lines), NPJ (orange dashed lines) and SPJ (white dashed lines);(1st, 11th, 21st and 31st July 2014).

**Figures 4.2a** and **4.2b** show the position of the subtropical jet identified for each day of the month of January and July of 2014, respectively, in groups of 5 days (6 in the last group), defined at the 250 hPa level using the wind speed and potential temperature limits stated above.

On January, the SJ could not be identified over the western part of the Pacific Ocean between the 22$^{nd}$ and 25$^{th}$. The jet had a higher variability between 100° and 70°W ranging from 20° to 45°S whereas between 60° and 30°W it varied from 30° to 46°S throughout the month (except on the 26$^{th}$).

On July (**Figure 4.2b**) the subtropical jet was less fluctuant for the first four groups, while in the last two groups it is observed that in the area over the Atlantic Ocean there are days that the subtropical jet remains at a very similar position as previous days, but there are others where the jet has a shift to the south, reaching latitudes higher than the rest of the period. In general, in comparison with January, the subtropical jet has a more northern position along the entire analyzed area with an average point position in 22°S, but with a shorter continuity, resulting in an asymmetry of the SJ over the Pacific Ocean and the Atlantic, with the jet further north over the latter. When the analysis was made in a point by point way, it can be observed occasions in which there are much displaced points from a longitude to the next. This is explained because there exists, for this month, a discontinuity in the subtropical jet that generates distinct "sections", the same that can cause an important latitudinal difference.

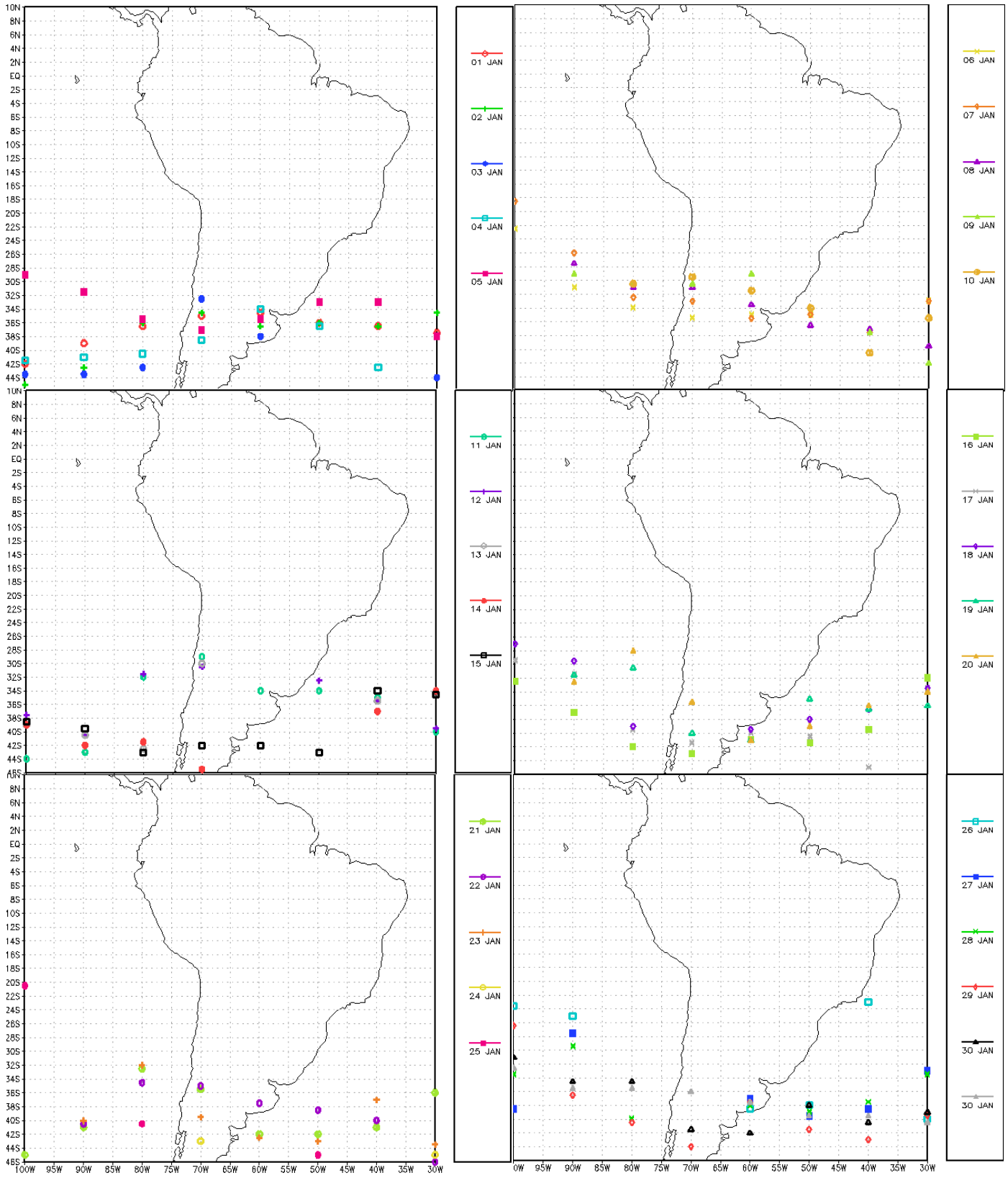


Figure 4.2a - Subtropical jet position defined as the northernmost latitude at 250 hPa where wind speed ≥30ms$^{-1}$ and **θ**: 330-340K for every 10 degrees of longitude on January 2014.

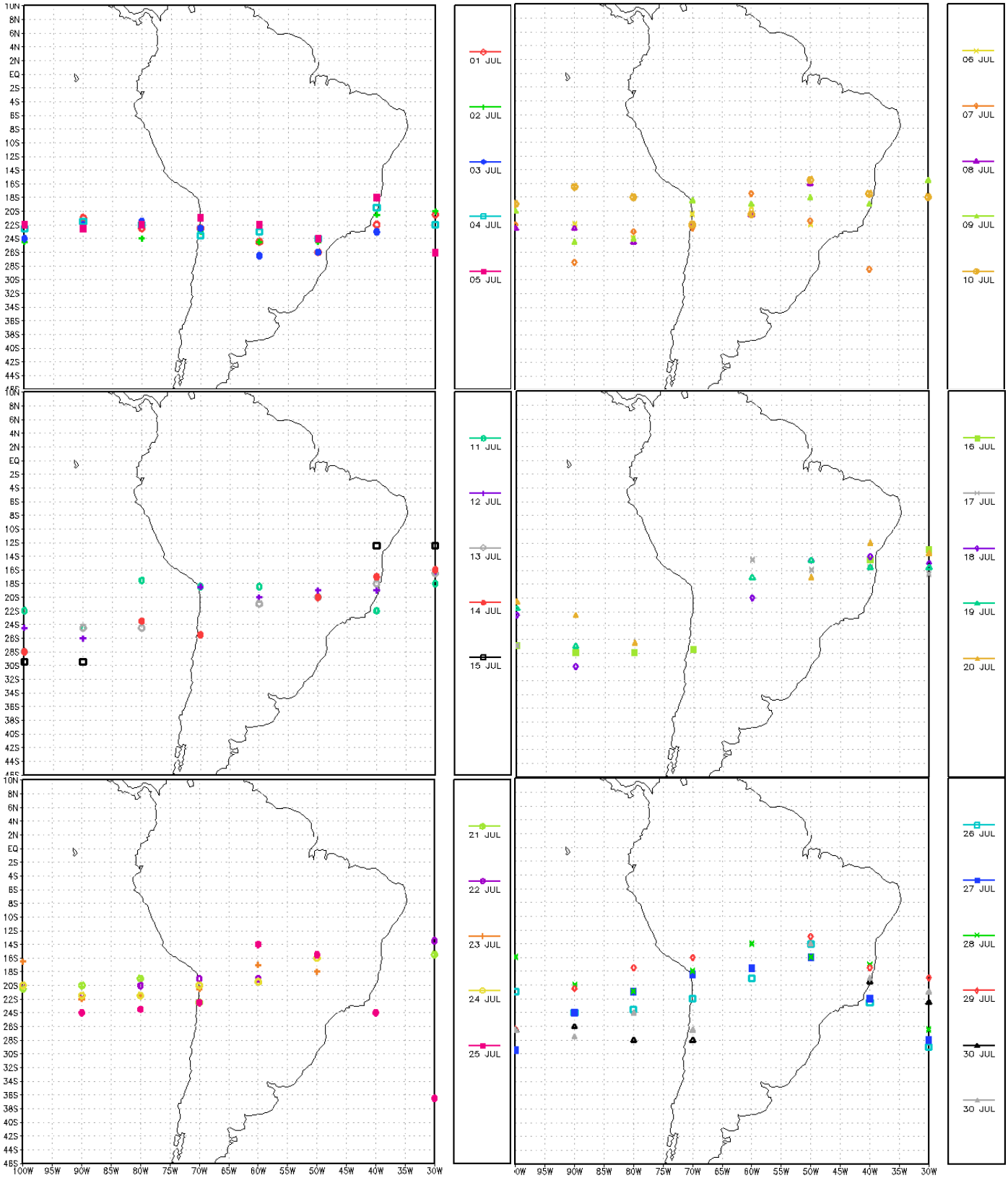


Figure 4.2b - Subtropical jet position defined as the northernmost latitude at 250 hPa where wind speed ≥30ms$^{-1}$ and **θ**: 330-340K for every 10 degrees of longitude on July 2014.

Dynamically active regions in the upper troposphere circulation are associated with several significant processes that are apparent in the water vapor images; the following two are related to the subtropical jet and allow their identification for the NH but with the appropriate considerations can be applied to the SH (Santurette and Gergiev, 2009):

1. They are associated with a dynamic tropopause anomaly (PV positive anomalies) and the strengthening of the jet that produces higher-level areas of convergence and divergence in their immediate vicinity.

2. In such a region, the jet stream is characterized by a strong light / dark gradient in the images with dry air on the polar side.

Considering this for the analysis of the water vapor images, the plots of the subtropical jet generated with the thresholds determined so far (taking as limits a horizontal wind speed of 30 $ms^{-1}$ and potential temperature between 330 and 340 K at 250 hPa) were superimposed on the water vapor channel image, both for 12 UTC, in January, April, July and October, as representative months of the seasons. Although the comparison of the CPTEC analysis and ERA-Interim plots were in very good agreement, some of the characteristics that should be identified in the water vapor images were not captured. Some examples are shown in **Figure 4.3**.

For the 1$^{st}$ of January 2014, the SJ is well identified using the 250 hPa chart for the eastern part of South America and over the Atlantic Ocean, with a good agreement between the SJ and the bands of clouds. In addition, the slope of the clouds coincides with the direction of the SJ. However, the contrast of dry/wet areas over the Pacific Ocean and west coast of South America (which is caused by the SJ) was not present. For the month of April the similarity between the images is still considerable, but there are marked regions that do not agree with the cloud pattern in the satellite image, which can be explained by the cyclone influence or because the Polar Jet is merged with the SJ. On July and October, the overall SJ pattern is observed at lower latitudes, between 15 and 30°S. The overlap between the reanalysis fields and the satellite image, considering the established thresholds, is good, but some gaps (over Rio Grande do Sul state on October, for example) could not be identified.

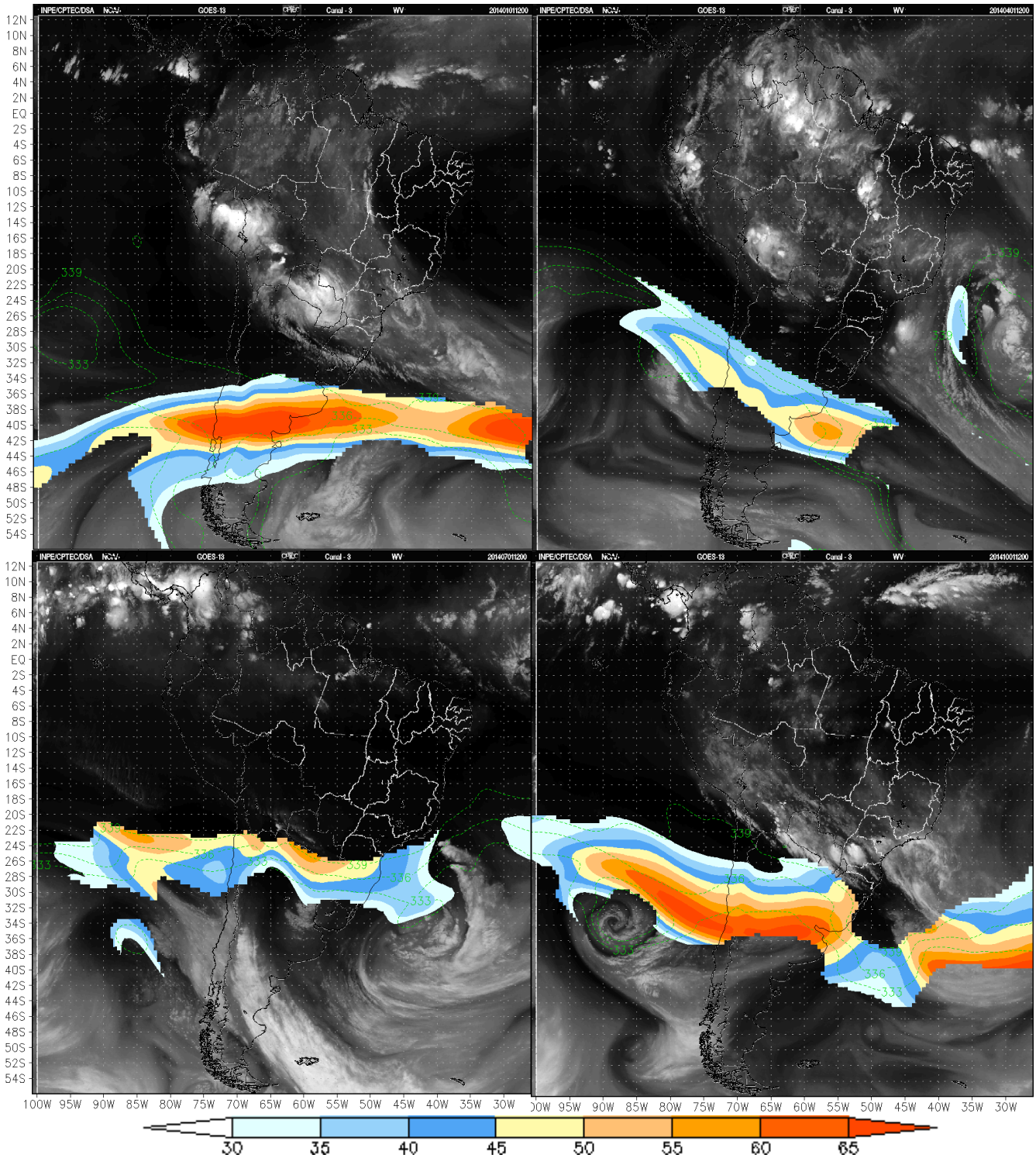


Figure 4.3 - Background: Water vapor satellite image, Foreground: wind speed above 30 $ms^{-1}$ (SJ) between 330 and 340 K potential temperature at 250 hPa (shaded), and for the first days of January, April, July and October 2014.

So, with these results in mind, we can see that obtaining a well-structured SJ position during all seasons with an objective methodology is still not possible with rigorous criteria and thus, we opted for a more subjective approach with visual analysis of the daily vertical profile to pinpoint the SJ core manually. This was done for each day at every 10° degrees of longitude of the study area taking into account all the characteristics found in the literature for the SJ and also to differentiate it from the PJ:

1. SJ core is located in mid to low latitudes and as such should be fully observable inside the area of study and have its entire core inside it (the southern wind gradient of the SJ should be observable inside the longitudinal vertical profile in **Figure 4.4**);
2. Wind speed of SJ core is lower than of PJ core (since the latter is originated from a rather intense temperature gradient);
3. SJ is a tropospheric rather than a stratospheric system.

**Figure 4.4a** shows the vertical profiles between 100 and 400 hPa for January 2014 (1$^{st}$, 11$^{th}$, 21$^{st}$ and 31$^{st}$) of the horizontal wind greater than or equal to 30 ms$^{-1}$ and the potential temperature between latitudes 10° and 40°S for three longitudes, 100°W (left panel), to observe the subtropical jet over the Pacific Ocean, 60°W (central panel), to observe the jet over South America and 30°W (right panel) to observe the jet over the Atlantic Ocean. The first criteria (that the SJ core should be fully observable inside the area of study) is only met on the 1$^{st}$ of January at 100°W and 60°W; on the 11$^{th}$ at 60°W, on the 21$^{st}$ at 100°W and 60°W and on the 31$^{st}$ at 100°W. On the 1$^{st}$ of January, at 60°W two merged cores can be seen. The core located to the south is much stronger than the northern one, considering that the PJ is many times stronger than the SJ, the SJ was pinpointed at 36°S. The other figures show only the northern wind speed gradient and thus this configuration was defined as the northern branch of the PJ.

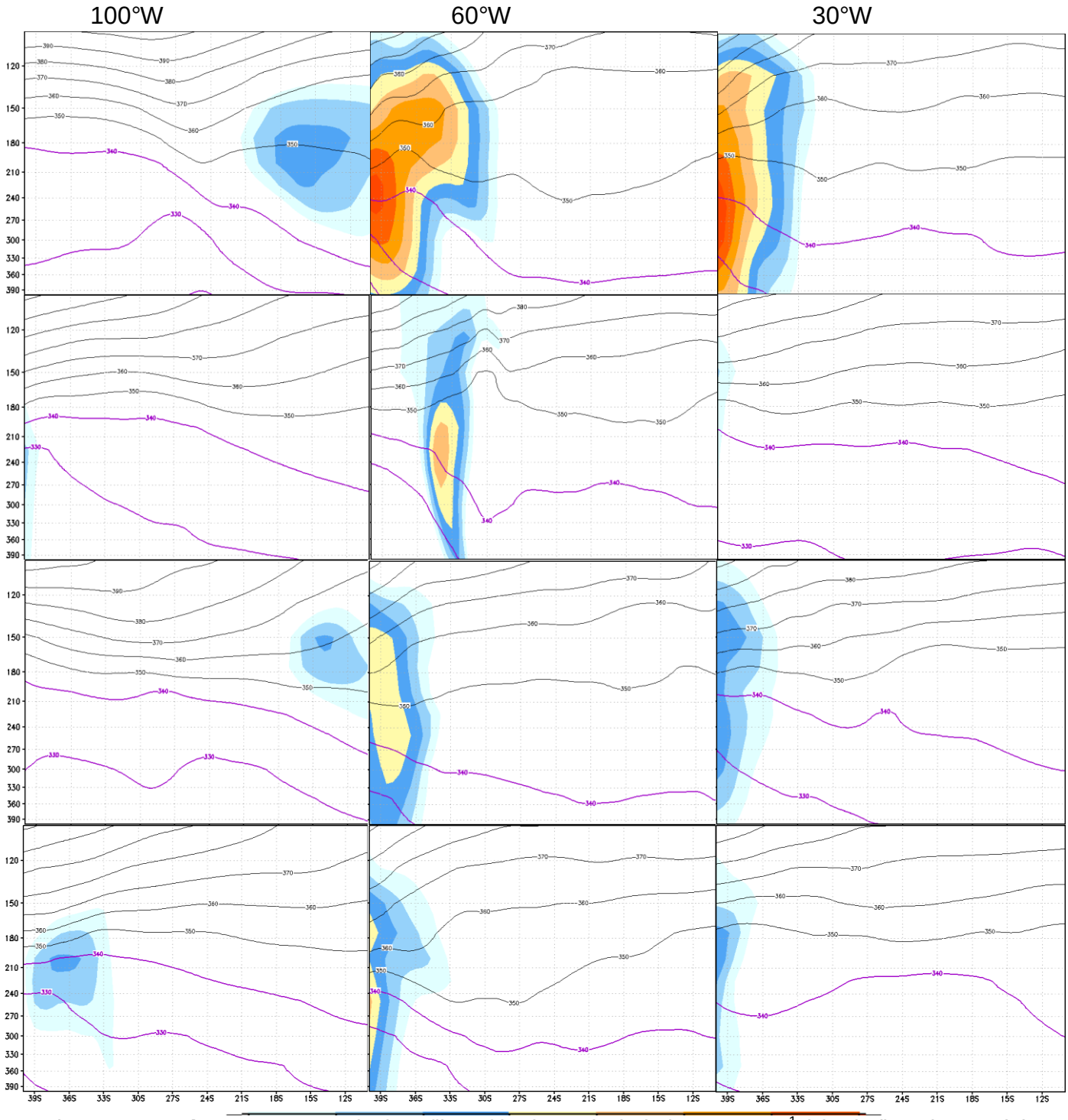


Figure 4.4a - **Figure 4.4a** - Vertical profiles of horizontal wind above 30 $ms^{-1}$ (shaded) and potential temperature (330 and 340K in purple), for 100°W (Left), 60°W (Center) and 30°W (Right) between 100 and 400 hPa from ERA-Interim (1st, 11th, 21st and 31st January 2014).

**Figure 4.4b** shows the same as **Figure 4.4a**, but for July 2014 (1st, 11th, 21st and 31st). In the vertical profiles of July we observe that the SJ is stronger in general, which coincides with the bibliography, as it is winter time and meridional temperature gradients are stronger. During July the SJ core can also be identified with the criteria explained previously, however there are some extra considerations we have to take, for example in two different latitudes, at 100°W during the first day we can observe two cores of similar intensity, one at a higher level than the other. Although SJ is an upper level system, it can be seen that the higher core extends above the troposphere and is embedded in the stratosphere (higher isentropic vertical gradient) and should not be considered as SJ. The lower one to the north (at 19°S) follows the two criteria and was identified as the SJ. The SJ location could be identified at all other profiles, with the exception of the 21st at 60°W. During the 11th, 21st and 31st at 30°W two jet cores could be seen. For all of them the northern core was identified as the SJ. On the 11th day we considered the one to the north as the SJ and the other as the PJ as the latter is known to be stronger and exist at a lower altitude, for the 21st day the northern core extends into lower levels so the one to the north was selected, and for the 31st day the southern was selected as it flows at the correct θ had a lower isentropic vertical gradient and was the continuation of the jet identified in previous days.

On the 31st, at 100°W the core had a much stronger intensity and extends bellow 400 hPa and was probably related to a very intense surface temperature gradient, corresponding to the PJ and, thus, was not considered to be the SJ.

The detailed results for January 2014 can be seen in **Table 4.4**. The latitude of the SJ varies between 13° and 39°S, and could be located in 142 of the 248 evaluated points. The jet location using this methodology for the 1st days of January, April, July and October is marked on the satellite images on **Figure 4.3**, showing good agreement with cloud patterns.

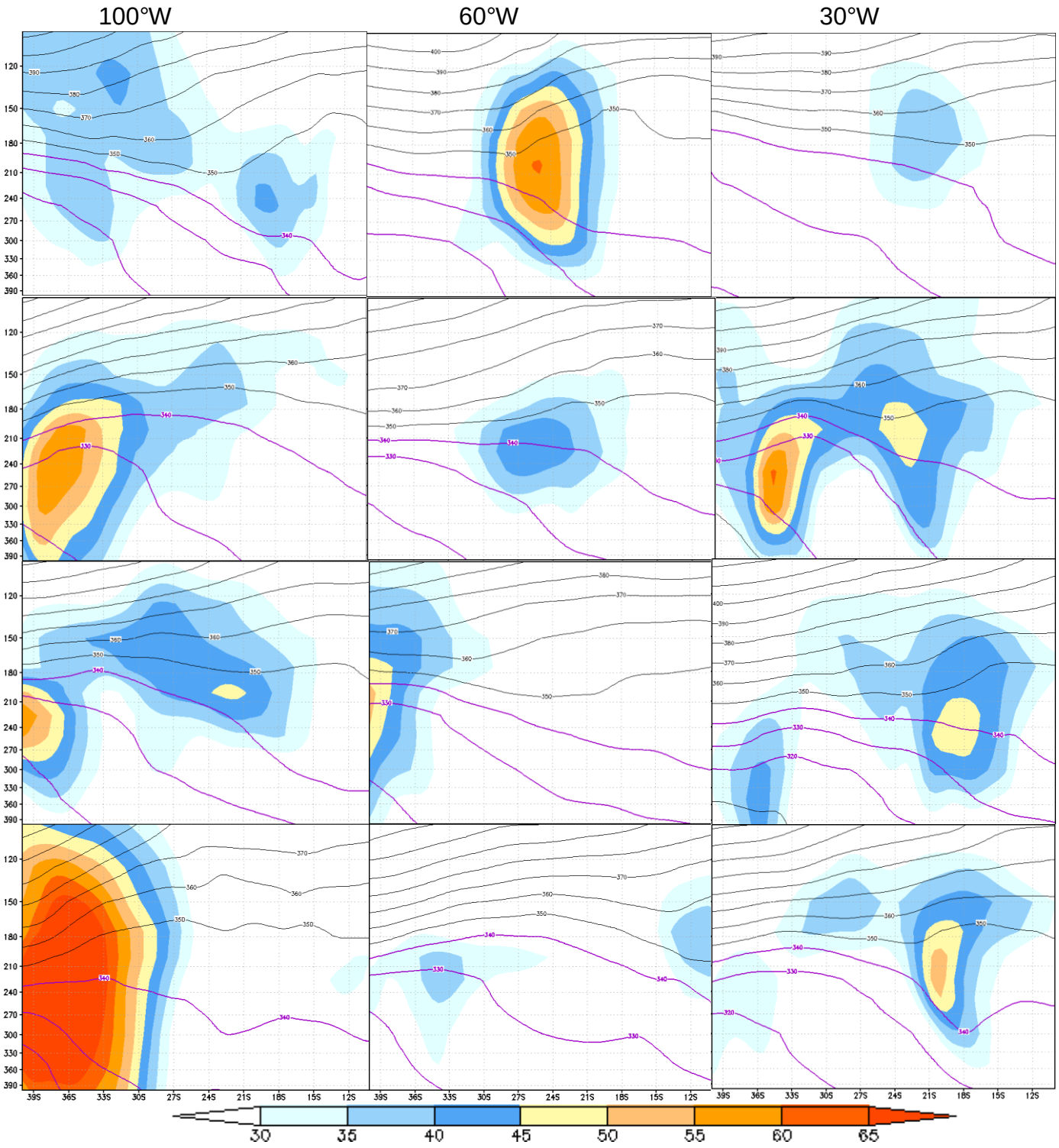


Figure 4.4b Vertical profiles of horizontal wind above 30 $ms^{-1}$ (shaded) and potential temperature (330 and 340K in purple), for 100°W (Left), 60°W (Center) and 30°W (Right) between 100 and 400 hPa from ERA-Interim (1st, 11th, 21st and 31st July 2014).

Table 4.4 - Latitudinal position identified for the subtropical jet according to the longitudinal vertical profiles for January 2014.

| Day/Longitude | 100°W | 90°W | 80°W | 70°W | 60°W | 50°W | 40°W | 30°W |
|---|---|---|---|---|---|---|---|---|
| **1** | -16 | | | -29 | -36 | -34 | -37 | |
| **2** | -18 | | -22 | -33 | -32 | -36 | -35 | |
| **3** | | | | -30 | | | | |
| **4** | | | | -30 | -30 | -32 | | |
| **5** | -32 | -38 | | | -30 | -30 | -35 | |
| **6** | -24 | -36 | -32 | -31 | | | -34 | -39 |
| **7** | -19 | -31 | -32 | -33 | | | | -34 |
| **8** | | -32 | -37 | -36 | -36 | -34 | | |
| **9** | | -32 | -35 | -36 | -34 | -36 | -37 | |
| **10** | | -29 | -32 | -33 | -34 | -38 | | |
| **11** | | -24 | -31 | -31 | -34 | -36 | | |
| **12** | | -32 | -32 | -30 | -27 | -32 | -36 | |
| **13** | | -30 | -33 | -29 | | | -36 | -36 |
| **14** | -35 | | | | | | -38 | -37 |
| **15** | | | | | | | -35 | -36 |
| **16** | -37 | | | -24 | -25 | | | -35 |
| **17** | -33 | | | | -27 | | | -36 |
| **18** | -28 | -35 | | | | | | -35 |
| **19** | | -33 | -28 | | | | | |
| **20** | | -33 | -26 | -33 | | | | |
| **21** | -14 | -28 | -33 | -34 | -38 | | | |
| **22** | -14 | | -33 | -38 | | | | |
| **23** | -13 | | -30 | -37 | | | | |
| **24** | -13 | | -28 | -35 | | -22 | -24 | -27 |
| **25** | -15 | -24 | | | -35 | -38 | | -25 |
| **26** | -17 | -26 | -28 | | -34 | -36 | -23 | -38 |
| **27** | -15 | -25 | -28 | -30 | -35 | -37 | -36 | -36 |
| **28** | -20 | -28 | -28 | -30 | -37 | | | -36 |
| **29** | -27 | -33 | -31 | -30 | -36 | | | |
| **30** | -38 | -31 | -35 | -37 | -33 | -39 | | -39 |
| **31** | -36 | -36 | -38 | -36 | | -37 | | |

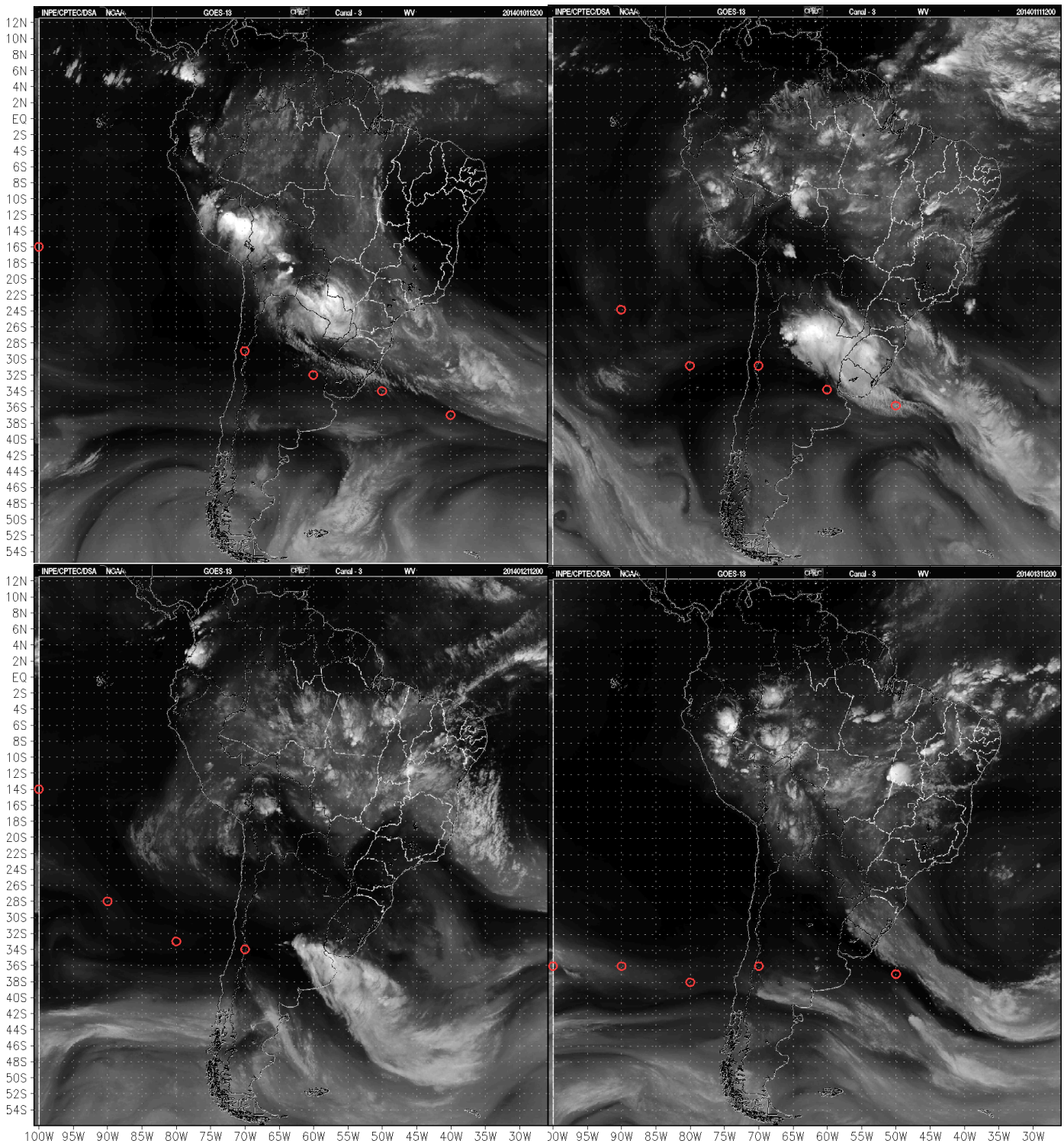


Figure 4.5a - Maps of the subtropical jet core position (o at every 10 degrees of longitude) for January 2014 (Days 1st, 11th, 21st and 31st) overlaid water vapor satellite imagery.

**Figure 4.5a** shows the subtropical jet core, identified by the o marks, overlaid over water vapor imagery on January 2014. We see that the SJ is better colocated with the one observed in the images as reflected by the cloud bands, however, because the latitude of the SJ core was rounded up it might have a slight shift in its position but of less than 0.5° degree.

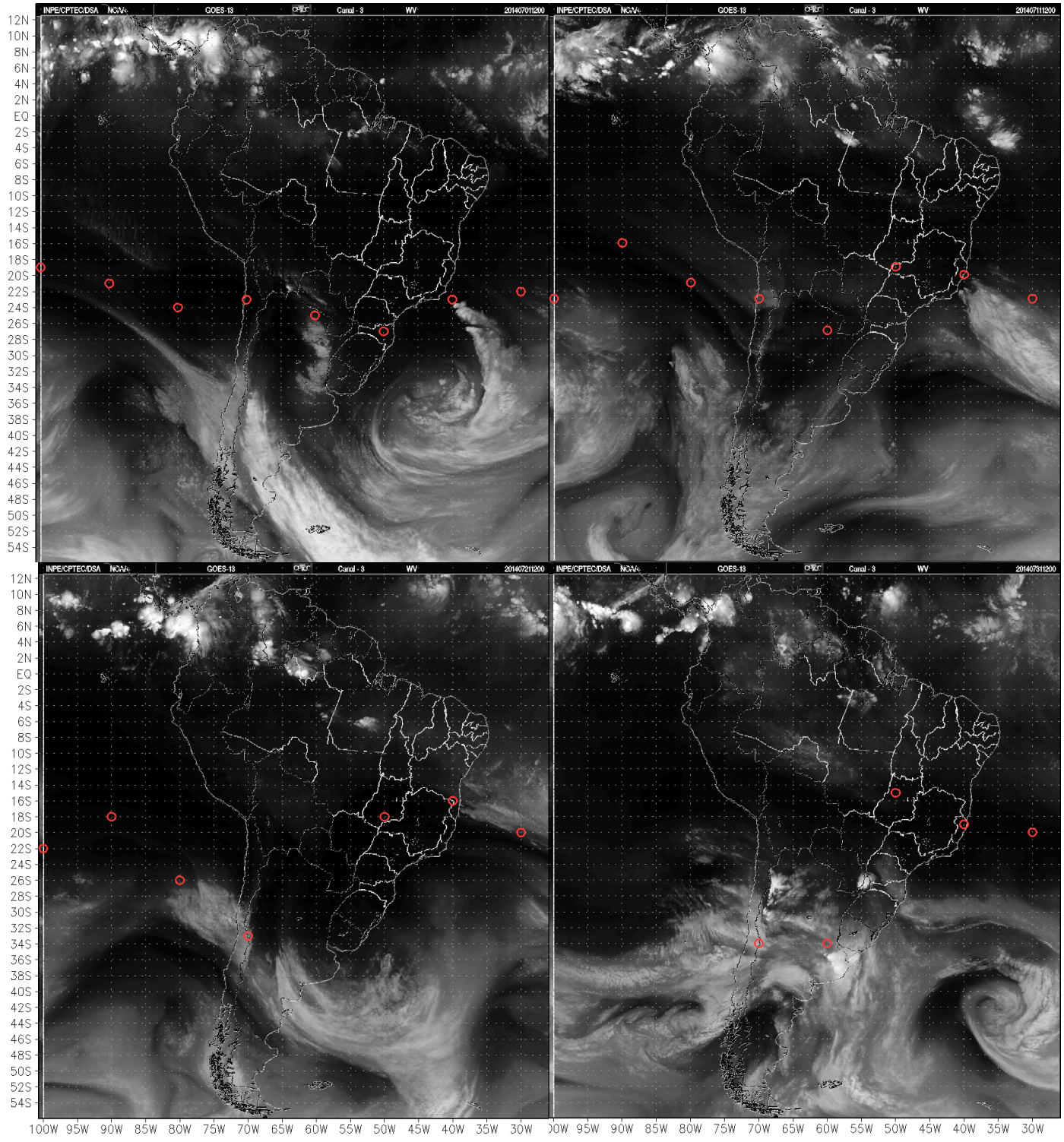


Figure 4.5b Maps of the subtropical jet core position(o at every 10 degrees of longitude) for July 2014 (Days 1st, 11th, 21st and 31st) overlaid water vapor satellite imagery.

In **Figure 4.5b** the same is done but for the month of July and it still follows well the SJ observed in the water vapor images, however it is slightly displaced to the north with respect of the cloud bands, this can be explained considering that during winter the SJ is much stronger and also wider.

## 4.2. Subtropical Jet Climatology

The same criteria for SJ core identification used in the previous section were applied for all the days of the study period (at 12 UTC, from 1st January 1979 to 31st December 2008). The SJ core latitude, vertical level, horizontal wind speed and potential temperature data were manually collected for every 10 degrees of longitude between 100 and 30°W. This data was the base for the climatological analysis.

However, there were days when the SJ was completely absent at some longitudes as presented in **Table 4.5.**

Table 4.5 - Percentage (%) of days the Subtropical Jet was absent between 100° and 30°W in the period of 1979-2008.

| Month/Longitude | 100°W | 90°W | 80°W | 70°W | 60°W | 50°W | 40°W | 30°W |
|---|---|---|---|---|---|---|---|---|
| January | 47 | 44 | 28 | 24 | 23 | 35 | 40 | 50 |
| February | 44 | 45 | 34 | 26 | 28 | 39 | 46 | 52 |
| March | 43 | 39 | 33 | 27 | 27 | 40 | 46 | 52 |
| April | 27 | 26 | 24 | 14 | 14 | 24 | 31 | 36 |
| May | 19 | 18 | 15 | 14 | 12 | 14 | 18 | 18 |
| June | 18 | 14 | 14 | 12 | 11 | 13 | 18 | 18 |
| July | 18 | 21 | 24 | 26 | 18 | 24 | 29 | 28 |
| August | 27 | 29 | 29 | 31 | 26 | 33 | 37 | 33 |
| September | 19 | 17 | 19 | 14 | 14 | 21 | 30 | 32 |
| October | 16 | 16 | 16 | 14 | 16 | 28 | 35 | 39 |
| November | 22 | 21 | 14 | 9 | 10 | 15 | 20 | 29 |
| December | 32 | 34 | 30 | 20 | 18 | 28 | 31 | 44 |

On the annual average, the SJ was less present over the Atlantic Ocean (east of 50°W) and then over the Pacific Ocean (west of 80°W), but was more present over South America, as seen in **Figure 4.6a.** It could also be more frequently identified during fall to spring, but during the summer, it could not be found in more than 30% of the period. This behavior corresponds well with what we know by literature about the SJ for most of the year, being most prominent during winter and autumn and absent a greater period of time during summer.

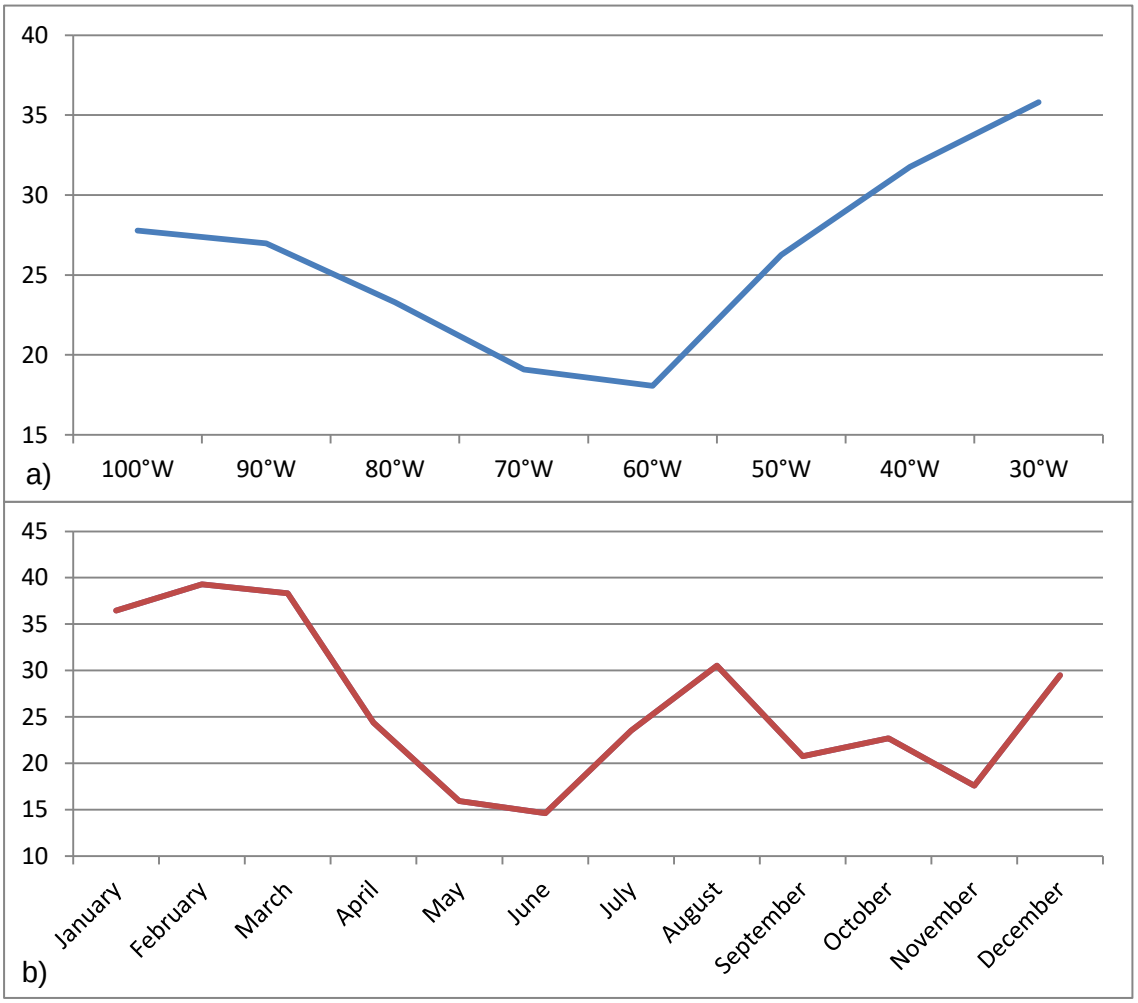


Figure 4.6 - Average Percentage (%) when the Subtropical Jet could not be identified between 100° and 30°W in the period 1979-2008 by **(a)** longitude, and **(b)** month.

### 4.2.1. Monthly climatology of the SJ latitude

**Figure 4.7a** to **Figure 4.7l** show the boxplot distribution of the SJ latitudes for each month, from January to December. The boxplot shows the minimum, 1st quartile, median, 3rd quartile and maximum latitude values. The minimum and maximum give know the extreme latitudes where the SJ has been pinpointed. The 1st quartile, median and 3rd quartile divide the data in four equal groups in relation the times a latitude class is observed, the first one comprises the lowest 25% of the data from the other 75%, the second divides the data in half and the last one comprises the highest 25% of the data. The boxplots show where the latitude of the SJ is concentrated as it varies around the median, for each month and each longitude selected.

On January, it can be seen a low fluctuation around the average latitude, for all considered longitudes except 100°W. SJ is found at lower latitudes over the Pacific and progressively moves to higher latitudes over the Atlantic. Over South America, specifically between 80° and 50°W, the SJ is almost fixed in mid latitudes (near 32° on average), while over the sea (both Pacific and Atlantic), its position (latitude) shifts more abruptly between longitudes.

February (**Figure 4.7b**) shows a behavior similar to the previous month. Since February is still a summer month in the southern hemisphere (SH) it is expected that the SJ behaves just as in January, with each boxplot position relative to the other being similar in both months, but there is little less fluctuation in the SJ latitude, especially at 100°W (compared to January) and the SJ has moved to the north over the Pacific Ocean, and to the south over South America and the Atlantic ocean in general.

In the third graphic, (**Figure 4.7c**) there is a small change in the pattern of the SJ probably because March is a transitory month between summer and autumn in the southern hemisphere. This small change is mostly noticeable over the Pacific Ocean with a mid-latitude at 100°W of 21°S, five degrees to the north than in the previous month. The position of the SJ is less fluctuant over the continent and the Atlantic and maintains itself near the same latitude on average over South America as the other months.

In the fourth graphic (**Figure 4.7d**) being fully in autumn we see a different pattern over the area analyzed with a more fluctuant jet compared to the previous months and generally placed more to the north at all longitudes. While on the first three graphics we could clearly see a gradual displacement of the SJ to the south from west to east, with a break over the continent, in the month of April we see another behavior, with the position of the SJ at lower latitudes over the Pacific, gradually moving to the south over South America and finally beginning to return to a northern position over the Atlantic, while maintaining latitudes further north than previous months, a behavior expected from the SJ during the beginning of the winter when the SJ reaches its more equatorial position due to the greater temperature gradients.

May (**Figure 4.7e**) presents the SJ further to the north and the latitudinal fluctuation of the jet is smaller at all longitudes. The distribution of the data at each longitude is more similar to a normal one than the previous months.

The SJ gets more stable, with less latitudinal variance of the median, 1$^{st}$ and 3$^{rd}$ quartiles than in previous months, and a difference of ± 1° of latitude between each interval of 10° of longitude (considering both the median and the first and third quartiles).

We continue to see the same behavior of the SJ in the following months from June through September, as seen in the next graphs (**Figure 4.7f, Figure 4.7g, Figure 4.7h and Figure 4.7i)** and the same tendency in general with the SJ, moving further to the north and maintaining itself near the same latitudes over both the Pacific and Atlantic ocean and South America, but being nearest to the equator during the winter, specifically in July, and receding to the south in the beginning of the spring (September-October), as the strong temperature gradients begin to fade.

During this period the behavior of the SJ correspond to that observed by Galvin (2007) with the shifting to the north. On the other hand results here show less fluctuation than those initially obtained by Barton and Ellis (2009) as the averaged SJ latitudinal position over a long period of time has a much bigger variability, which is the reason for their change in approach.

For the next two months, October and November, the pattern of the SJ begins to shift again, as seen in the next graphics (**Figure 4.7j, Figure 4.7k)** with a little increase in the fluctuation of the SJ latitude and a major displacement to the south for South America longitudes and to a less extent over the Atlantic. However over the Pacific the SJ remains at lower latitudes. In general the difference in latitude increases in relation to previous months varying from around 23°S, at 100°W to 29°S, at 60°W, and then the behavior of the SJ gets similar to that of the first months of the year.

For the last graph (**Figure 4.7l**), correspondent to the month of December and the beginning of the summer, we can observe a much greater fluctuation in latitude of the SJ and average positions similar to January and February.

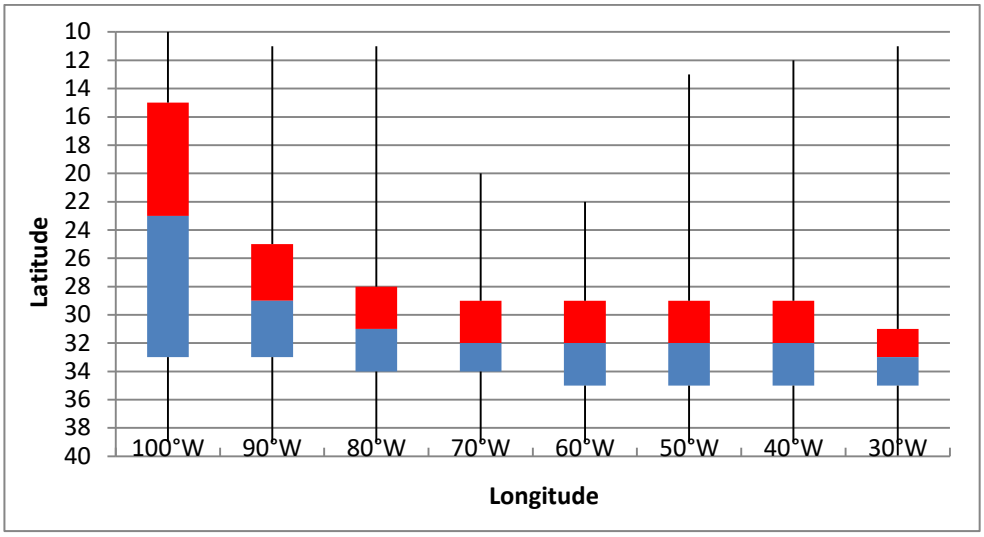


Figure 4.7a - Boxplots corresponding to January, considering the period 1979-2008.

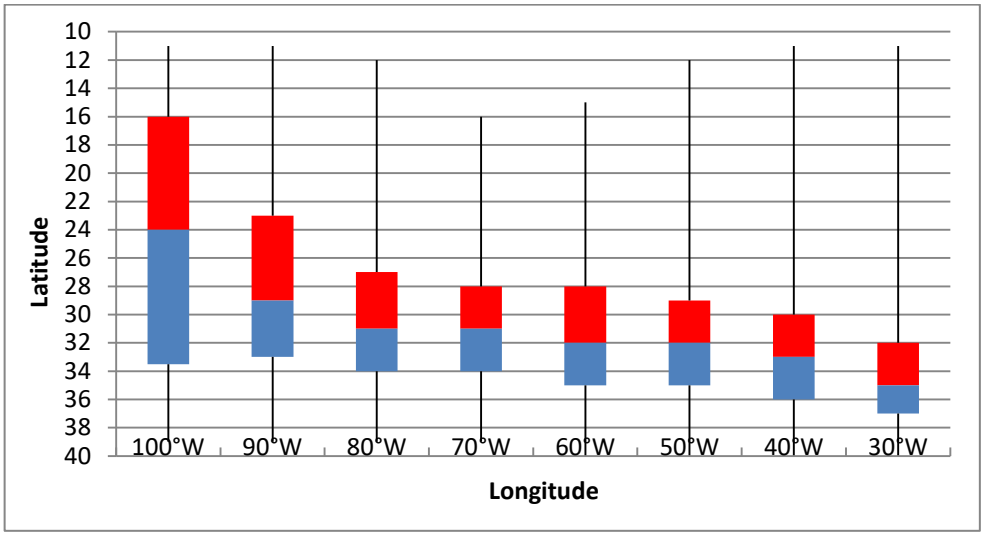


Figure 4.7b Boxplots corresponding to February, considering the period 1979-2008.

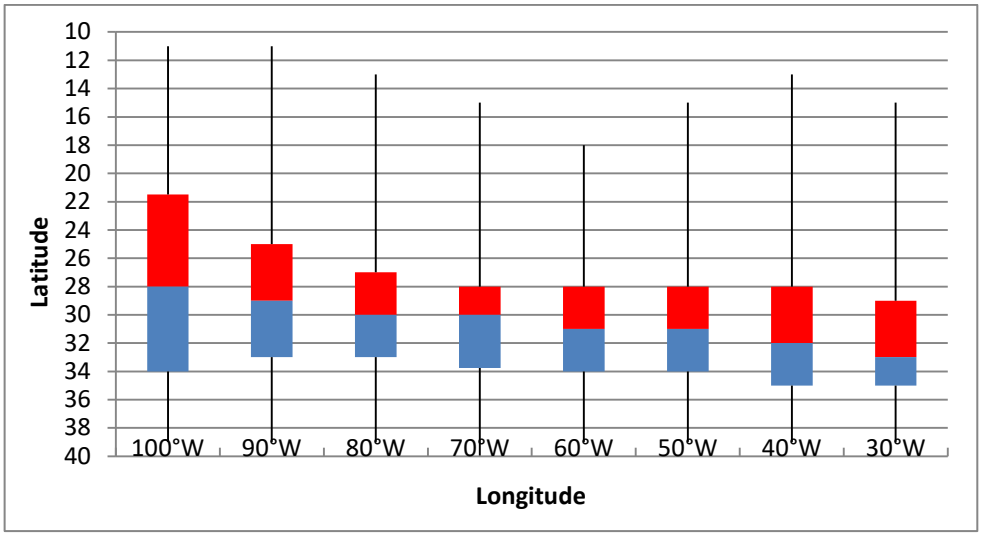


Figure 4.7c Boxplots corresponding to March, considering the period 1979-2008.

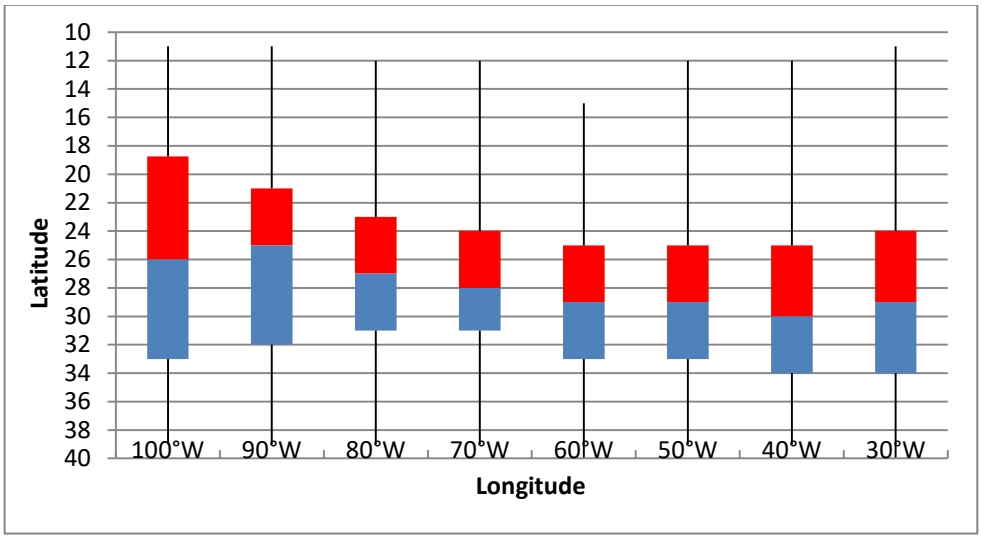


Figure 4.7d Boxplots corresponding to April, considering the period 1979-2008.

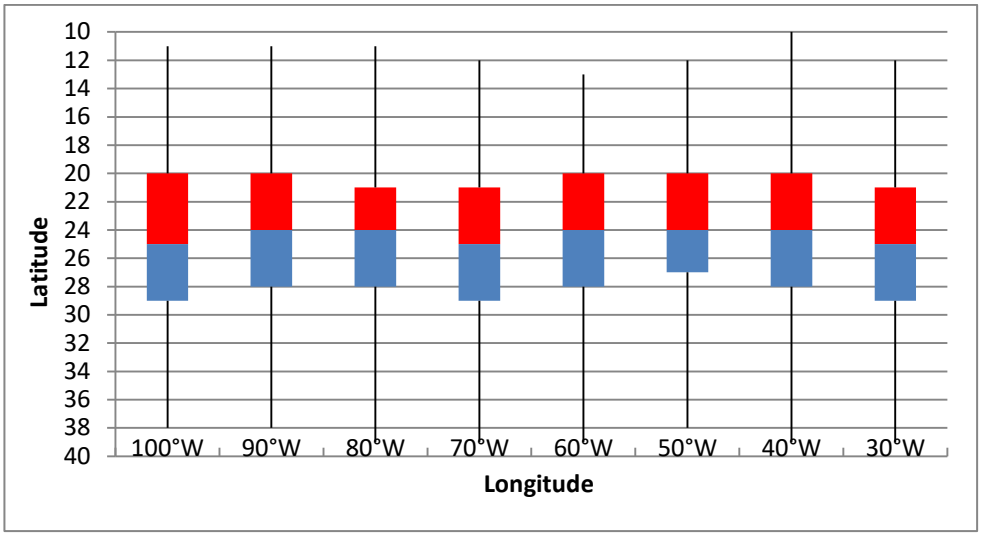


Figure 4.7e Boxplots corresponding to May, considering the period 1979-2008.

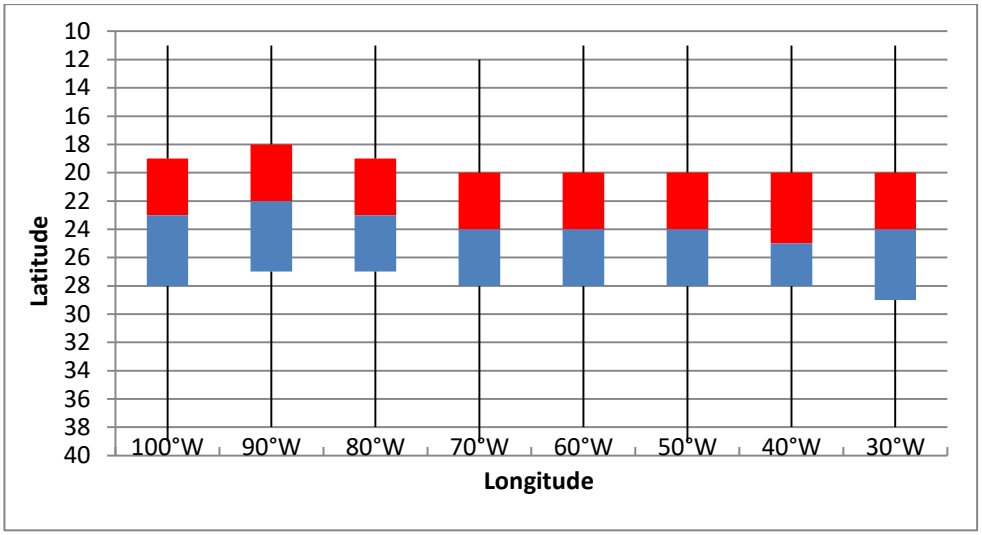


Figure 4.7f Boxplots corresponding to June, considering the period 1979-2008.

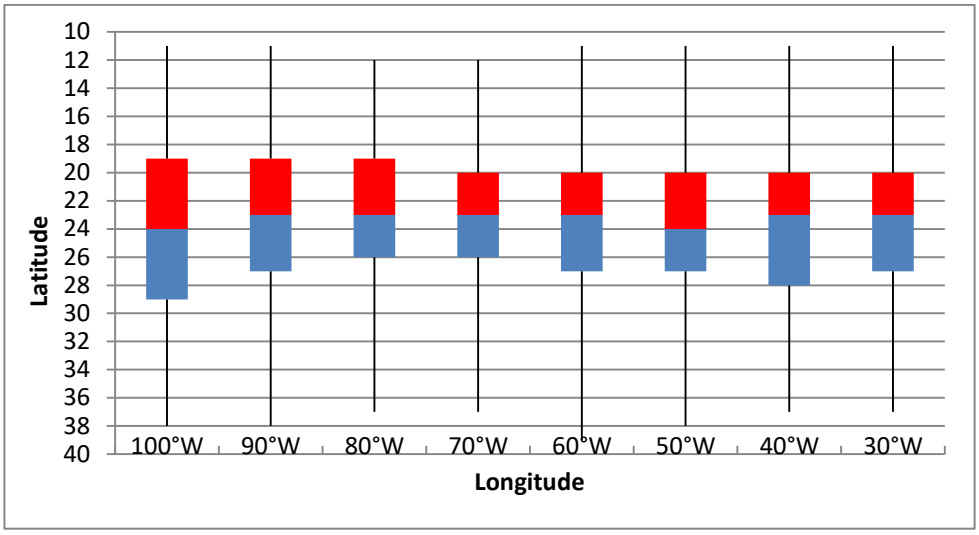


Figure 4.7g Boxplots corresponding to July, considering the period 1979-2008.

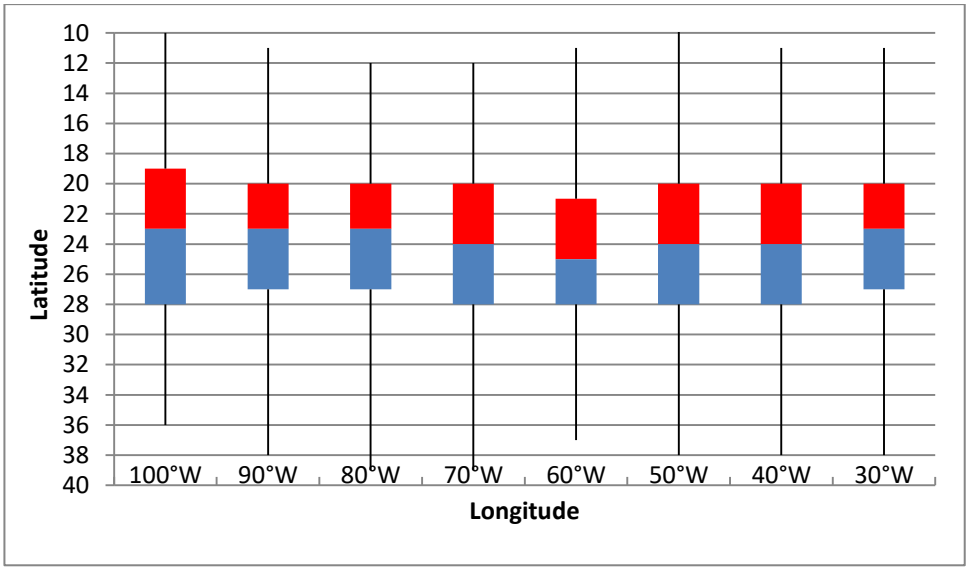


Figure 4.7h Boxplots corresponding to August, considering the period 1979-2008.

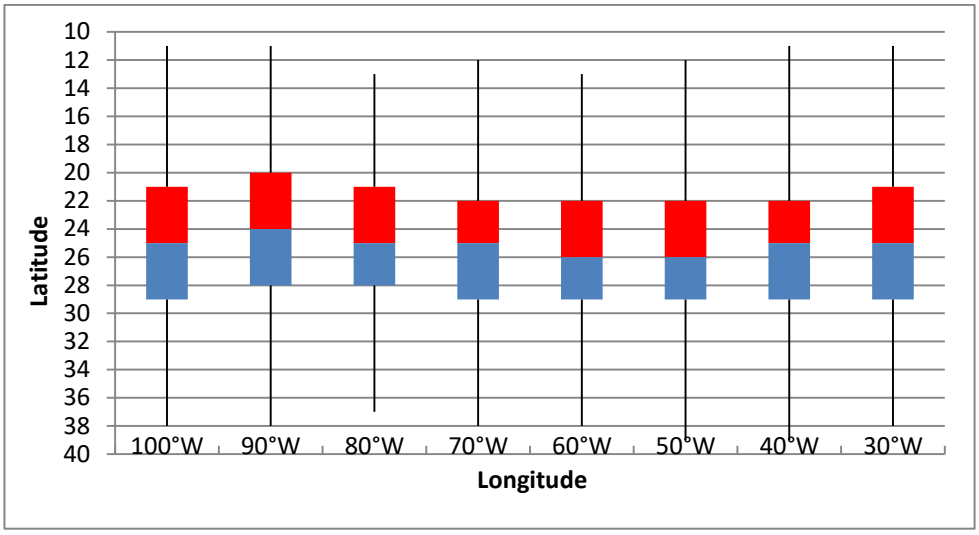


Figure 4.7i Boxplots corresponding to September, considering the period 1979-2008.

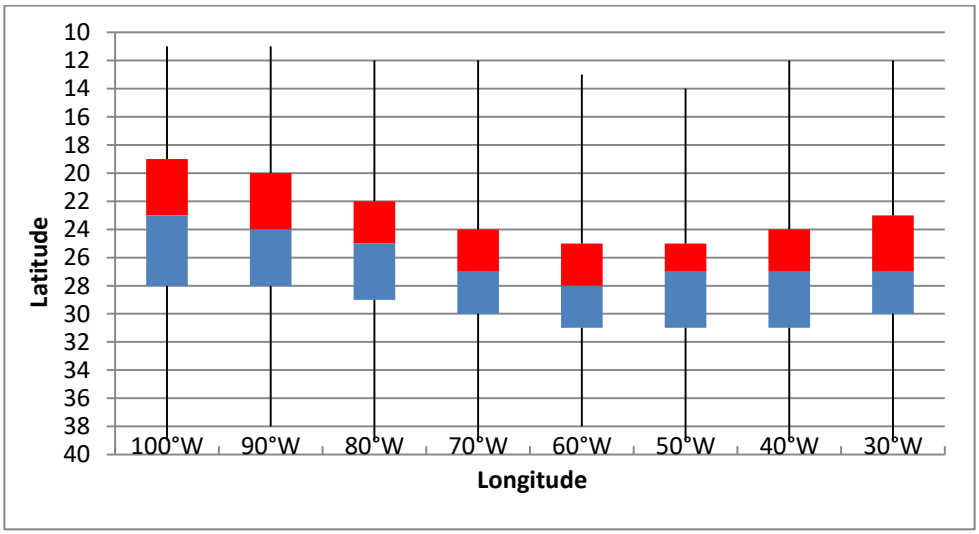


Figure 4.7j Boxplots corresponding to October, considering the period 1979-2008.

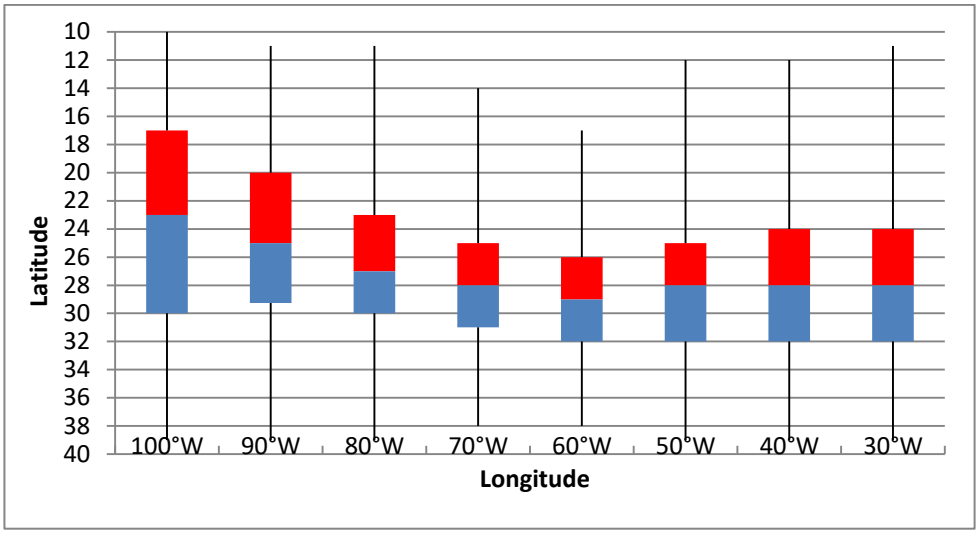


Figure 4.7k Boxplots corresponding to November, considering the period 1979-2008.

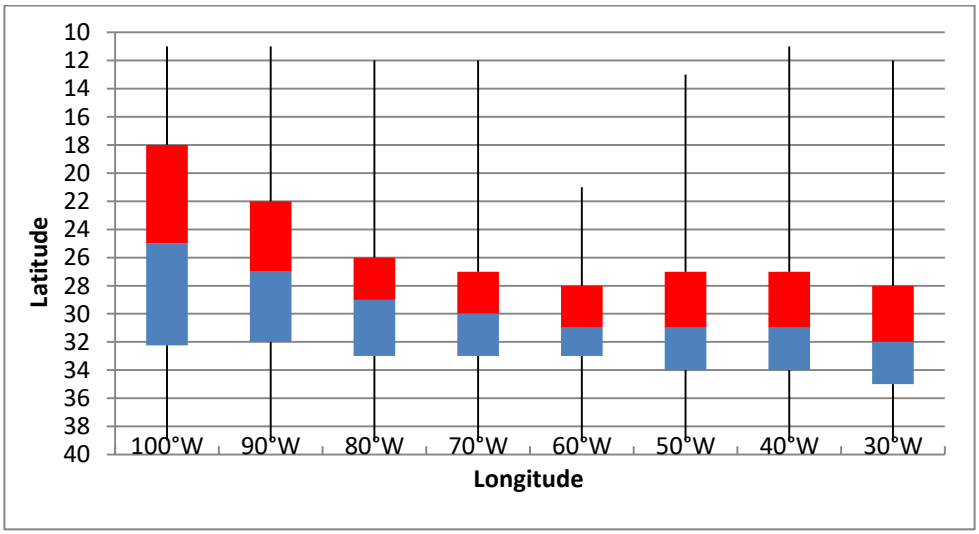


Figure 4.7l Boxplots corresponding to December, considering the period 1979-2008.

### 4.2.2. Subtropical Jet Wind Speed

The SJ wind speed at its core is less intense at the beginning of the year from January through March, summer months in the southern hemisphere, where many authors even argue the SJ does not exist. Then, increases its intensity during the fall, from April to May, and reaches its peek during the winter, from June to September. And finally, its intensity begins to decline through the spring, from October to December. We can see this behavior in more detail in the following **Figures 4.8a** to **4.8d**, where the wind speed frequency is shown for different ranges of intensity, for each longitude and month.

In **Figure 4.8a** we can observe that from January to March the SJ core maintains a rather weak core, with a wind speed of 30 to 39 $ms^{-1}$, 40 to 60% of the days at all longitudes but more frequent over the ocean than over the land. It can also be seen that the SJ gets stronger over land during this period as shown by the percentages of wind speed between 40 to 49 $ms^{-1}$ and 50 to 59 $ms^{-1}$ which represent 35 to 40% and 15 to 20% respectively over land, while only around 30% and 10% over the Atlantic and Pacific oceans respectively.

As seen in **Figure 4.8b** and **Figure 4.8c**, the SJ wind intensity increases from May and maintains a rather stable wind speed during fall and winter, increasing slowly through both seasons reaching speeds above 60 $ms^{-1}$ in 20% of the times during September over both South America and the Pacific Ocean. Also during this period the SJ wind speed becomes very similar over the whole area of study.

Finally in **Figure 4.8d** we can see how the SJ begins again to weaken and recover a similar behavior to that seen from January to March.

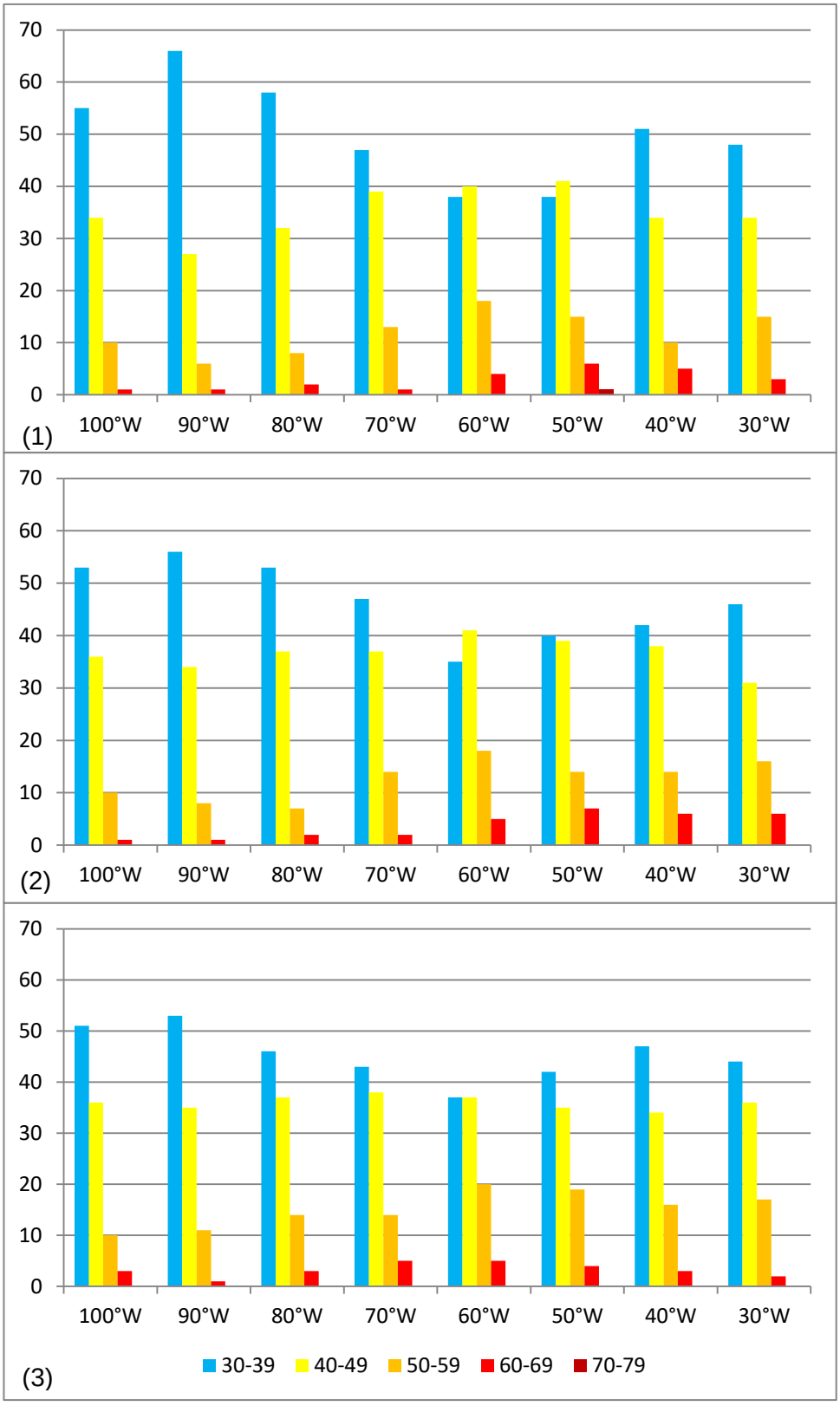


Figure 4.8a – SJ core wind intensity percentage (%) bar graphics within 30 to 79 $ms^{-1}$ (1) January, (2) February and (3) March.

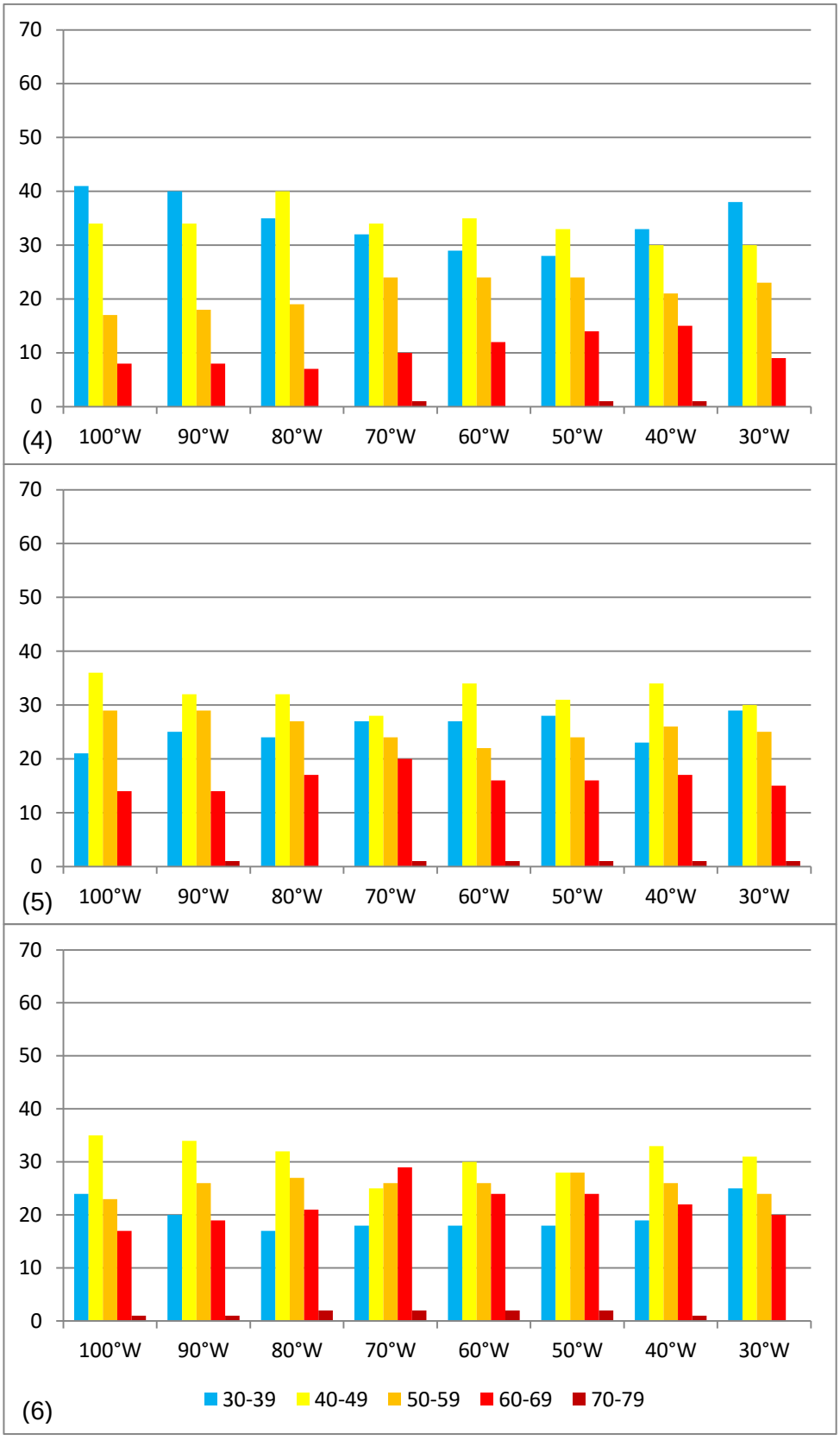


Figure 4.8b SJ core wind intensity percentage (%) bar graphics within 30 to 79 $ms^{-1}$ (4) April, (5) May and (6) June.

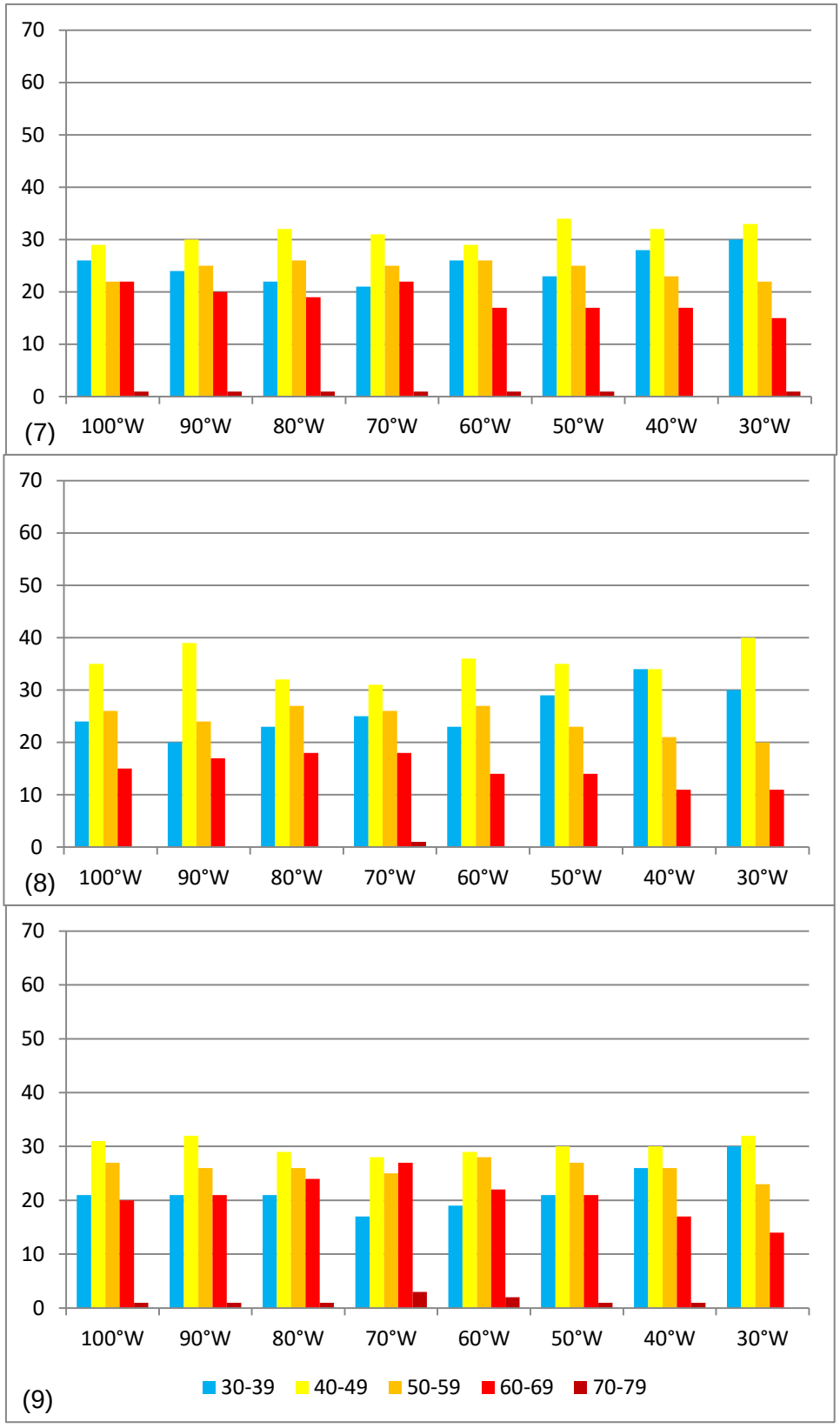


Figure 4.8c SJ core wind intensity percentage (%) bar graphics within 30 to 79 $ms^{-1}$ (7) July, (8) August and (9) September.

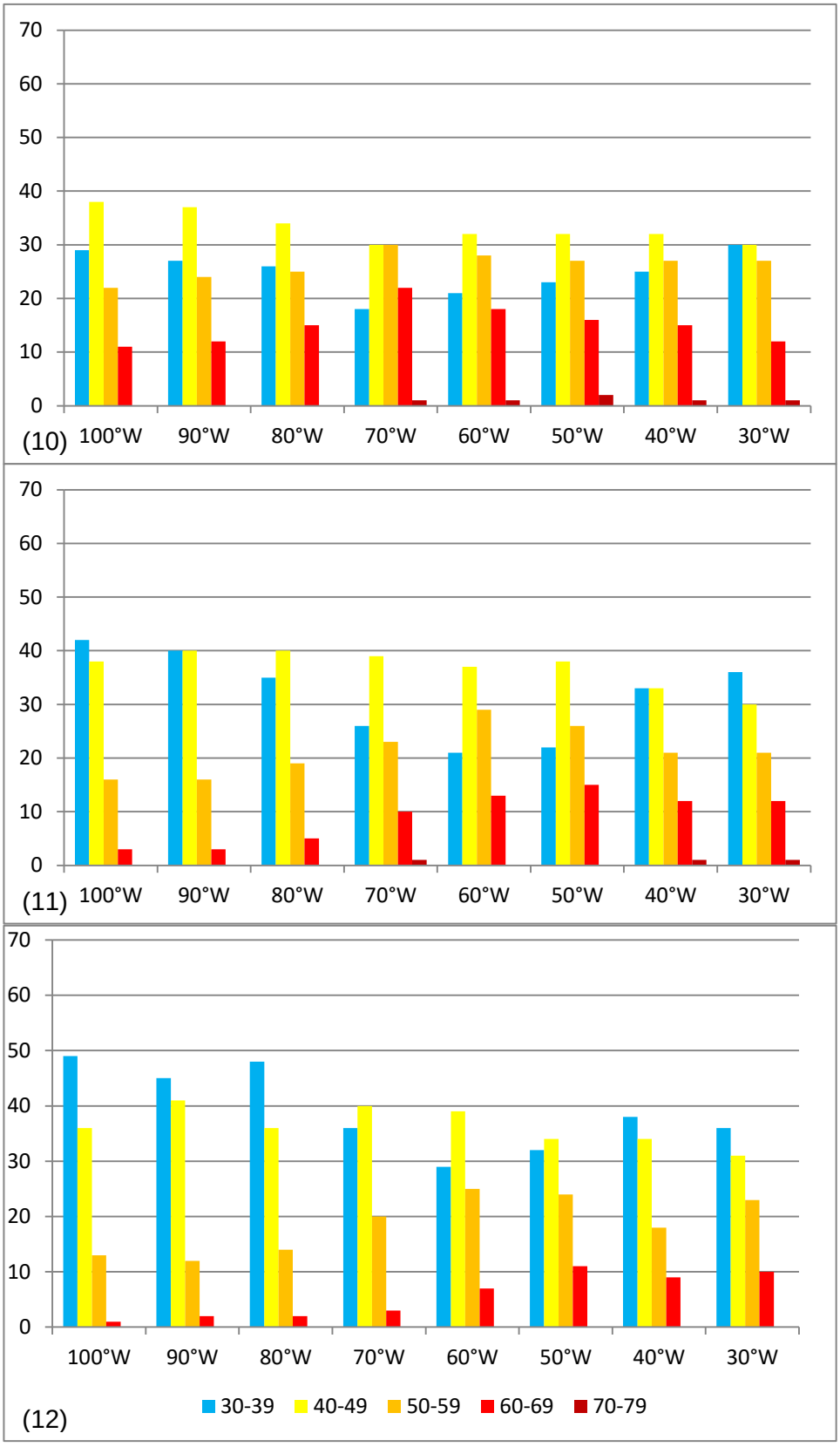


Figure 4.8d SJ core wind intensity percentage (%) bar graphics within 30 to 79 $ms^{-1}$ (10) October, (11) November and (12) December.

### 4.2.3. Subtropical Jet Pressure Level

Although for operational purposes the SJ can be almost always identified at the 250 hPa level, the SJ core level varies.

**Figure 4.9a** and **Figure 4.9b** confirm this, showing that during the period of study the SJ core is located between 201 and 250 hPa above 50% of the time over South America and even over 60% during the trimester of November, December and January. Over the Pacific Ocean this behavior is very similar having the jet core in the same layer between 40 to 50% of the time during all the year; and finally over the Atlantic Ocean we see again the same behavior, this time even reaching over 60% in the month of June.

However, the SJ core could also be frequently identified between 151 to 200 hPa and 251 to 300 hPa. For the layer between 101 and 150; 301 and 350 hPa and 351 to 400 hPa the SJ core is rarely located, being there less than 10% of the time at all longitudes during the year and even less than 5% between April and July at all longitudes and between August and November with the exception of 30°W.

All this shows as that the SJ altitude is very stable, being located most of the time between 201 and 250 hPa at all times and at all longitudes of the area of study.

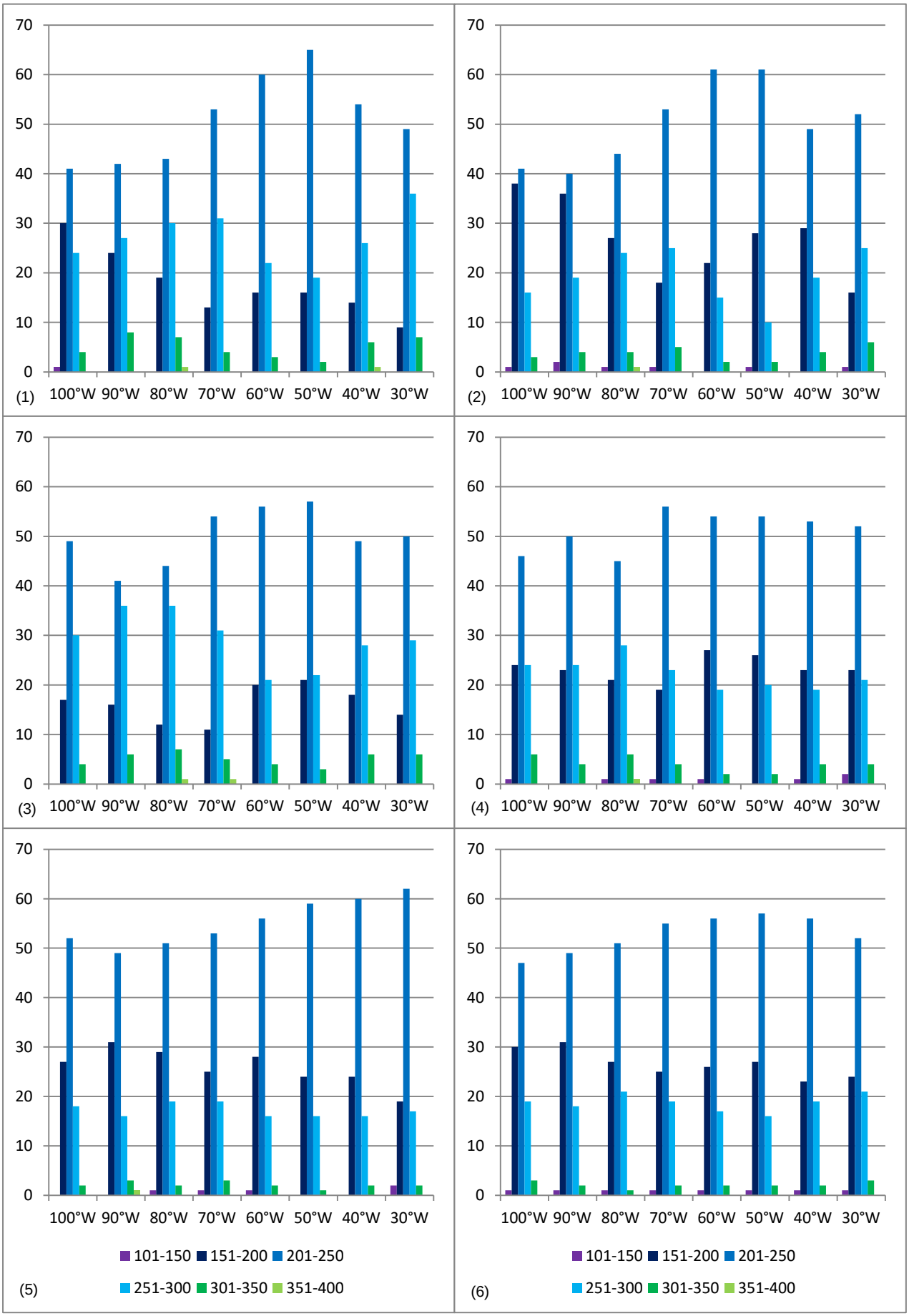


Figure 4.9a - Bar graphics expressing the percentage (%) of the SJ core vertical level (1) January, (2) February, (3) March, (4) April, (5) May and (6) June.

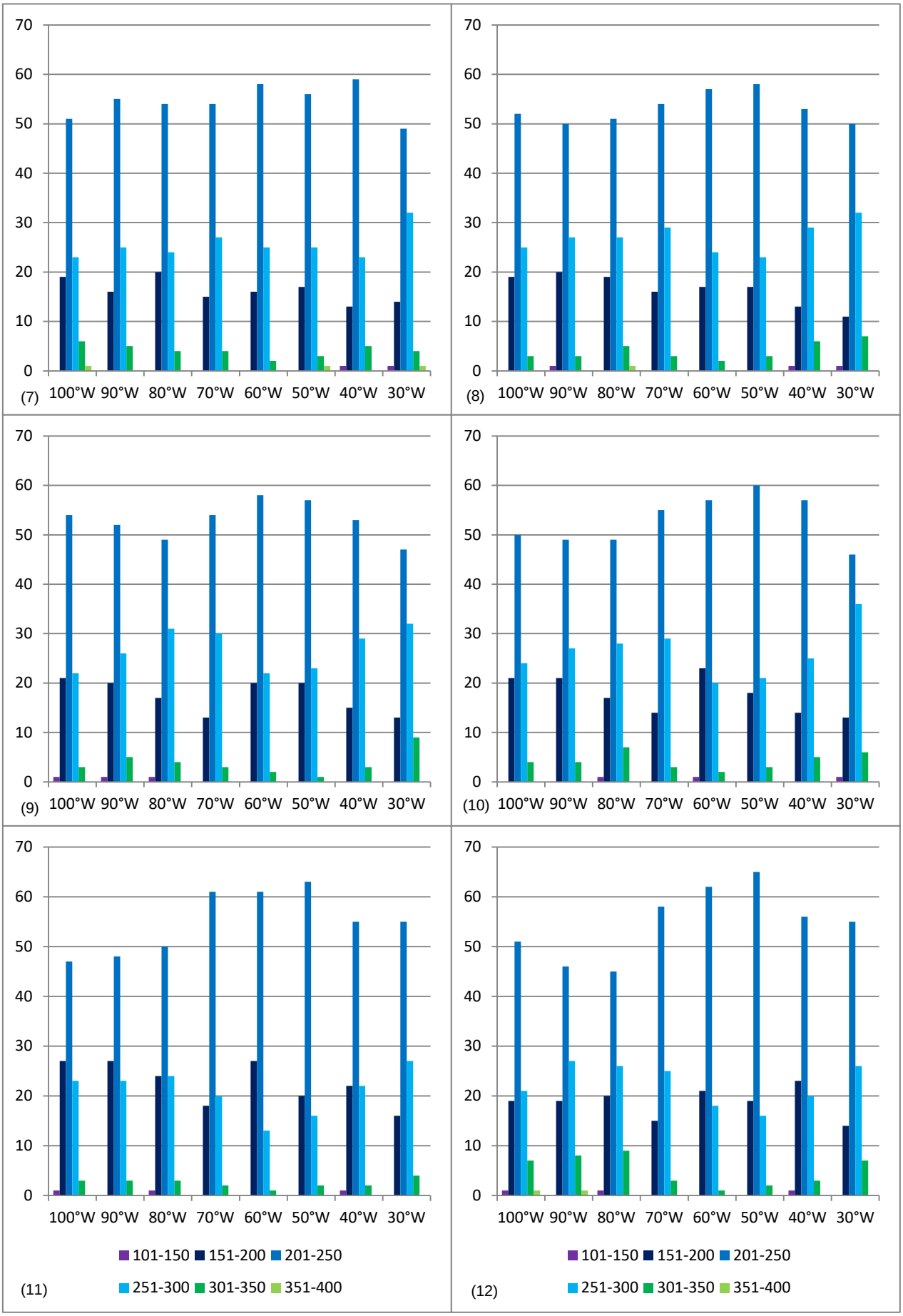


Figure 4.9b Bar graphics expressing the percentage (%) of the SJ core vertical level (7) July, (8) August, (9) September, (10) October, (11) November and (12) December.

### 4.2.4. Subtropical Jet Potential Temperature

In this section we observe the fluctuation of the SJ core potential temperature.

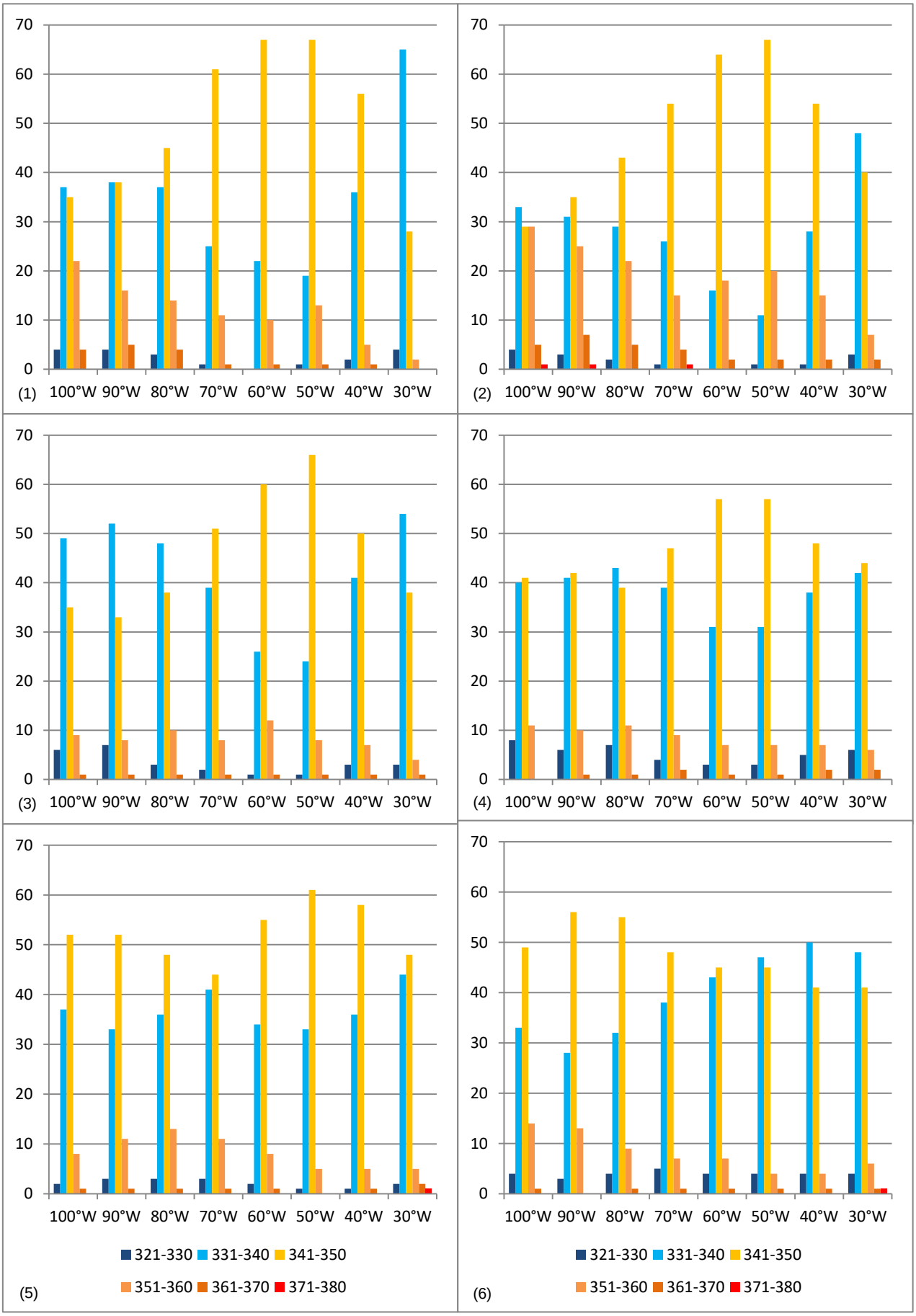

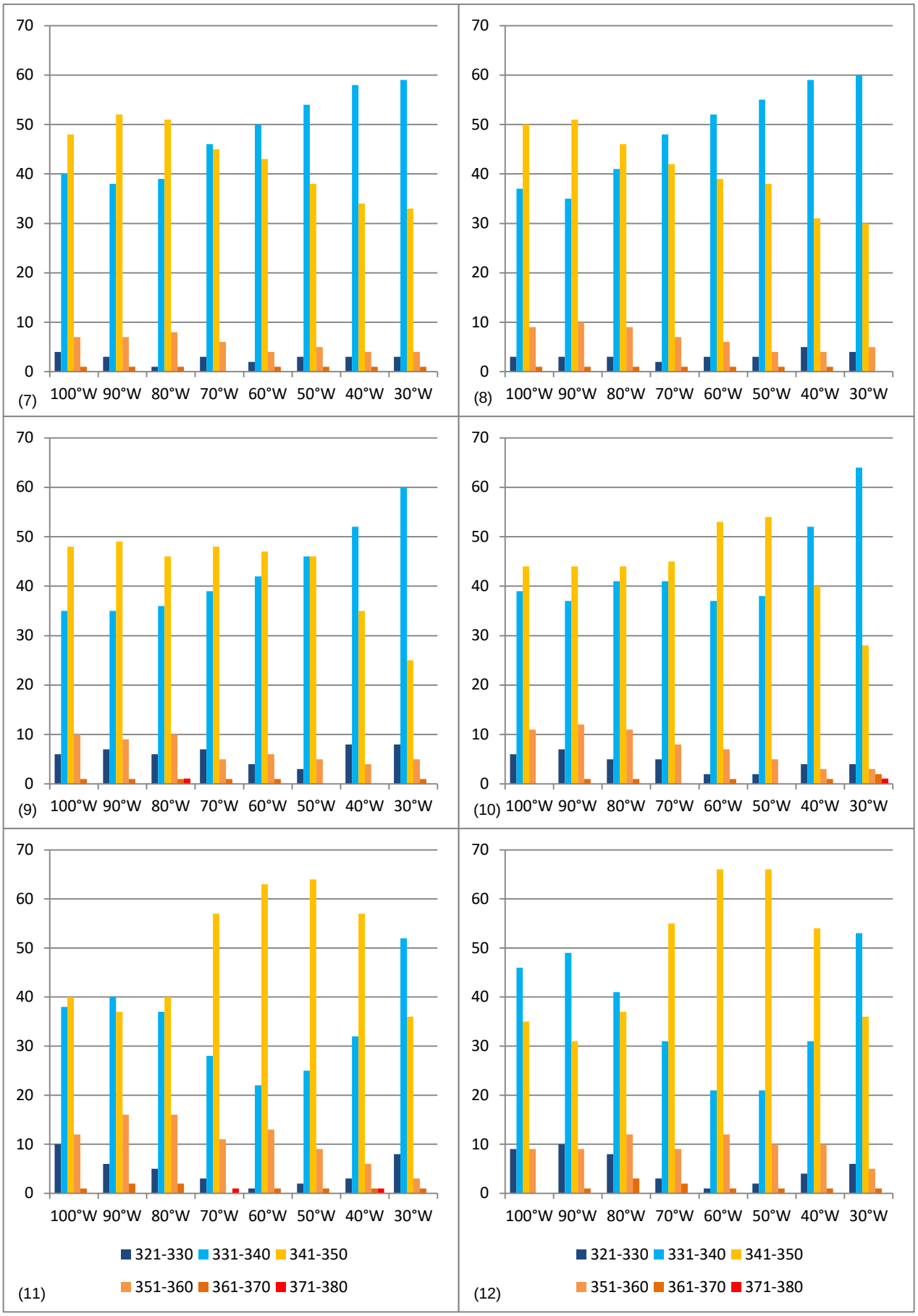


Figure 4.10 - Bar graphics expressing the percentage (%) when SJ core is within a certain potential temperature range (1) January, (2) February, (3) March, (4) April, (5) May, (6) June, (7) July, (8) August, (9) September, (10) October, (11) November and (12) December.

As seen in **Figure 4.10** the SJ core has a Potential Temperature (PT) between 331 and 350K during almost all the entire year and longitudes (almost 90% of the data) which are very similar results to those obtained by Reiter and Whitney in 1969 where they determined that the SJ had an average PT of 340K. We also observe that the PT is distributed in the area of study remains almost the same between January and April with higher temperatures over South America (341-350 K, most of the times) than over the Pacific (a little bit colder, with 30 to 50% of the times with PT of 331-340 K), however from June to August this situation changes with the SJ having a higher PT over the Pacific Ocean. Then in November and December the same behavior as the first four months returns. PT of 351 to 360 K reaches frequencies higher than 10% for almost all the longitudes only on January and February.

### 4.2.5. Subtropical Southern Hemisphere Jet Summary

The SJ is an atmospheric system with the following characteristics: a horizontal wind speed between 30 and 50 $ms^{-1}$ in summer and 40 and 60 $ms^{-1}$ in winter in the majority of cases and stronger over the oceans than over the continent in general during the former; a mean potential temperature of 340K most of the year being between 330 and 340K during winter and 340 to 350 during summer; being located between 200 and 250 hPa more than 50% of the times during the year and having a shift in latitude to the north (south) over the winter (summer) being less fluctuant between May and August.

This latitudinal shifting and change in SJ strength found in this study is in accordance with what had already been stablished, for example by Lachmy and Harnick (2014) and Lee and Kim (2003), but for the southern hemisphere.

## 4.3. The Subtropical jet and the ENSO

The influence of “El Niño” and “La Niña” events were studied only with regard to the SJ position.

### 4.3.1.a The Subtropical jet latitudinal position during “El Niño events”

To identify the “El Niño” events the Southern Oscillation Index (SOI) was used. Considering a threshold of -0.5 for the warm events, **Table 4.6a** shows the months that correspond to the “El Niño” events. It should be noted that in some studies the index is multiplied by 10 in which case the threshold would be considered -5.

Table 4.6a - Months affected by “El Niño” events according to the Southern Oscillation Index during the period (1979-2008)

| Date | SOI | Date | SOI | Date | SOI | Date | SOI | Date | SOI |
|---|---|---|---|---|---|---|---|---|---|
| 198206 | -1 | 198701 | -0.7 | 199202 | -0.9 | 199405 | -0.7 | 199711 | -1.2 |
| 198207 | -1.5 | 198702 | -1.2 | 199203 | -2 | 199407 | -1.3 | 199712 | -1 |
| 198208 | -1.7 | 198703 | -1.3 | 199204 | -1 | 199408 | -1.2 | 199801 | -2.7 |
| 198209 | -1.7 | 198704 | -1.4 | 199206 | -0.6 | 199409 | -1.6 | 199802 | -2 |
| 198210 | -1.7 | 198705 | -1.3 | 199207 | -0.6 | 199410 | -1.1 | 199803 | -2.4 |
| 198211 | -2.6 | 198706 | -1.1 | 199210 | -1.4 | 199411 | -0.6 | 199804 | -1.4 |
| 198212 | -2.2 | 198707 | -1.4 | 199211 | -0.7 | 199412 | -1.2 | 200207 | -0.5 |
| 198301 | -3.5 | 198708 | -0.9 | 199212 | -0.6 | 199704 | -0.6 | 200208 | -1 |
| 198302 | -3.6 | 198709 | -1 | 199301 | -0.9 | 199705 | -1.3 | 200209 | -0.6 |
| 198303 | -2.4 | 199109 | -1.5 | 199302 | -0.7 | 199706 | -1.4 | 200211 | -0.5 |
| 198304 | -0.9 | 199110 | -1 | 199303 | -0.5 | 199707 | -0.8 | 200212 | -1.1 |
| 198609 | -0.5 | 199111 | -0.7 | 199304 | -1.2 | 199708 | -1.4 | 200302 | -0.7 |
| 198611 | -1.2 | 199112 | -1.8 | 199403 | -0.7 | 199709 | -1.4 | | |
| 198612 | -1.4 | 199201 | -2.9 | 199404 | -1.3 | 199710 | -1.5 | | |

**Figures 4.11a** to **Figure 4.11l** show the latitudinal position distribution of the Subtropical Jet from January to December during “El Niño” (EN) events.

In general during the month of January during EN events (**Figure 4.11a**) the behavior of the SJ is pretty similar to the climatology over both oceans; however over the continent it shifts its mean position more to the south. On the other hand, there’s

a bigger quantity of jets that reach lower latitudes as shown in the boxplot (median to 3rd quartile in red). In the period of the study only 5 months of January were accounted.

**Figure 4.11b** shows the distribution of the Subtropical Jet in the month of February during EN events (6 years). The SJ behavior changes drastically, with bigger difference in its position between longitudes over the Pacific and the Atlantic. Its mean position is slightly shifted to the north over the Pacific Ocean, while over the continent and the Atlantic Ocean it shifts further to the south, to higher latitudes. Also, the variance of the SJ position is bigger during these events in general over all longitudes, but with the extreme latitudes being nearer to the mean position.

**Figure 4.11c** shows the distribution of the SJ in the month of March during EN events (6 years). In the month of March the behavior of the SJ over the continent and the Atlantic Ocean is pretty similar, although with a slight shift to the north, most evident over the continent, and a south shift over the Pacific Ocean.

**Figure 4.11d** shows the distribution of the SJ in the month of April during “El Niño” (EN) events (7 years). In the month of April the behavior of the SJ is almost the same as in the climatology but with a smaller variance over the Pacific Ocean.

On May **(Figure 4.11e, 3 years)** the SJ behavior is almost the same over the continent, while over the Atlantic the SJ shifts to the north and over the Pacific shifts slightly to the south. The variance of the SJ position is smaller.

On June **(Figure 4.11f, 4 years)** the SJ position shifts to the north between 2-3 degrees over the whole area of study.

On July **(Figure 4.11g, 6 years)** the SJ shows slight changes in its position of about one degree to the south or to the north in each longitude analyzed.

On August **(Figure 4.11h, 5 years)** the behavior of the SJ changes over the Pacific Ocean moving to the south significantly and causing a bigger difference of the SJ position between the ocean and the continent. Over South America and the Atlantic Ocean the SJ shifts slightly to the north.

**Figure 4.8i** shows the distribution of the Subtropical Jet in the month of September during EN events (7 years). In the month of September the SJ behavior

changes between South America and the Atlantic Ocean having a much sharper slope with the shift in position to the north over the ocean and to the south over the continent. Over the Pacific the SJ only shifts slightly to the south.

On October **(Figure 4.8j, 5 years)** the SJ behaves almost the same as in the climatology with no significant difference but with a smaller variance over all the area.

**Figure 4.11k** shows the distribution of the Subtropical Jet in the month of November during EN event (7 years). The behavior of the SJ is pretty similar to the climatology, however it shifts slightly to the south (between 1-2 degrees mostly) over South America and the Atlantic Ocean.

Finally, on December **(Figure 4.11l, 7 years)** the SJ behavior is the same as in the climatology but with a slight change in position of 1 degree at most to the south except over 100°W where it shifts to the north.

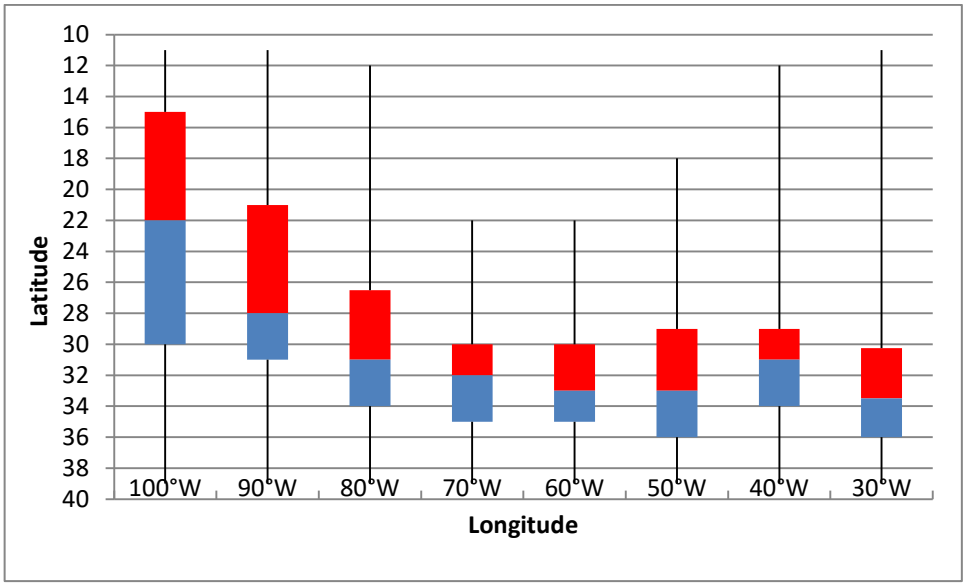


Figure 4.11a - Boxplots corresponding to January, considering the period of El Niño events

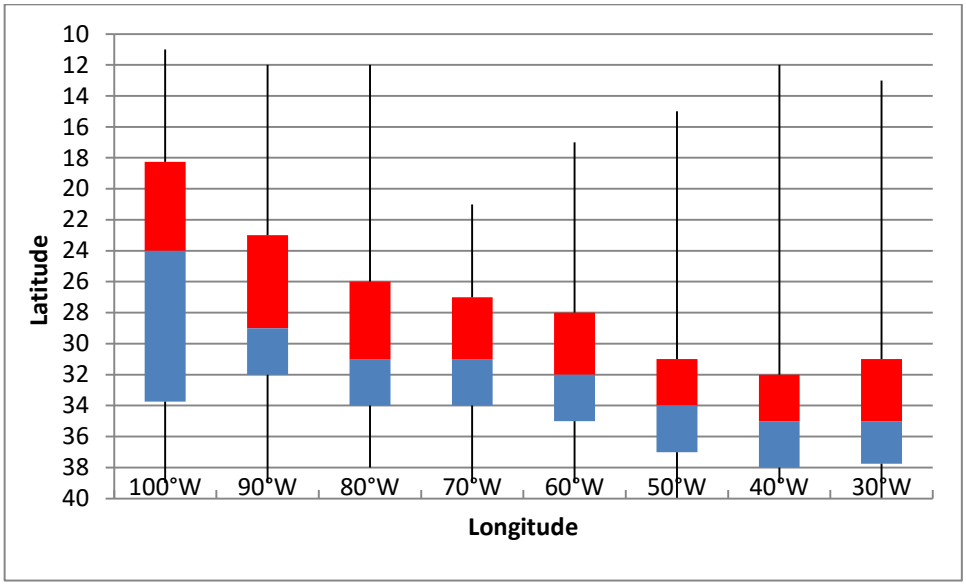


Figure 4.11b Boxplots corresponding to February, considering the period of El Niño events.

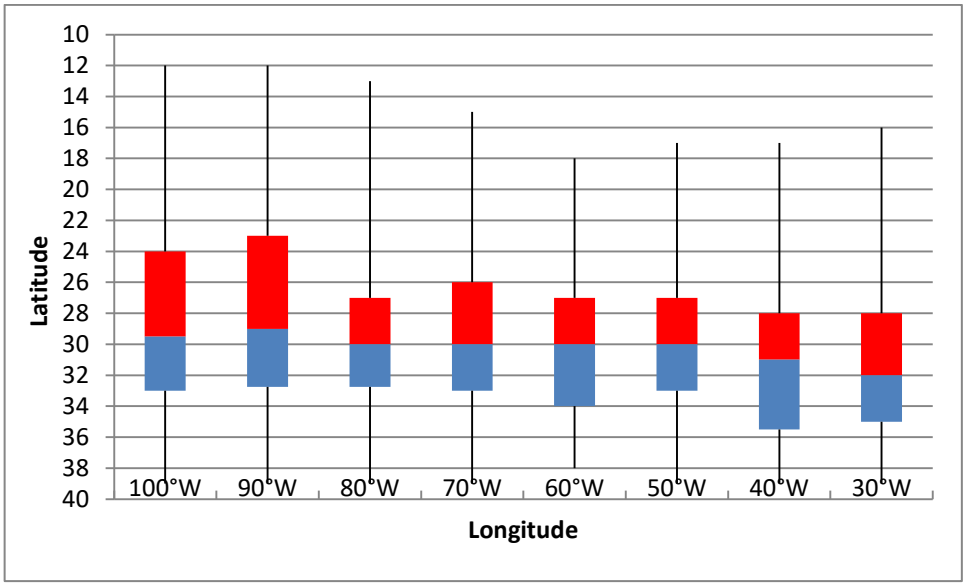


Figure 4.11c Boxplots corresponding to March, considering the period of El Niño events.

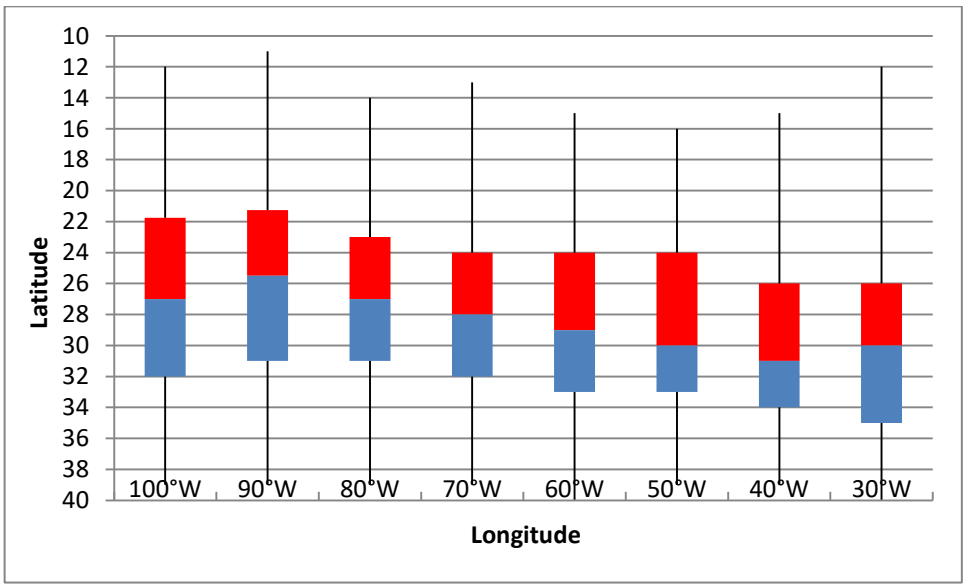


Figure 4.11d Boxplots corresponding to April, considering the period of El Niño events.

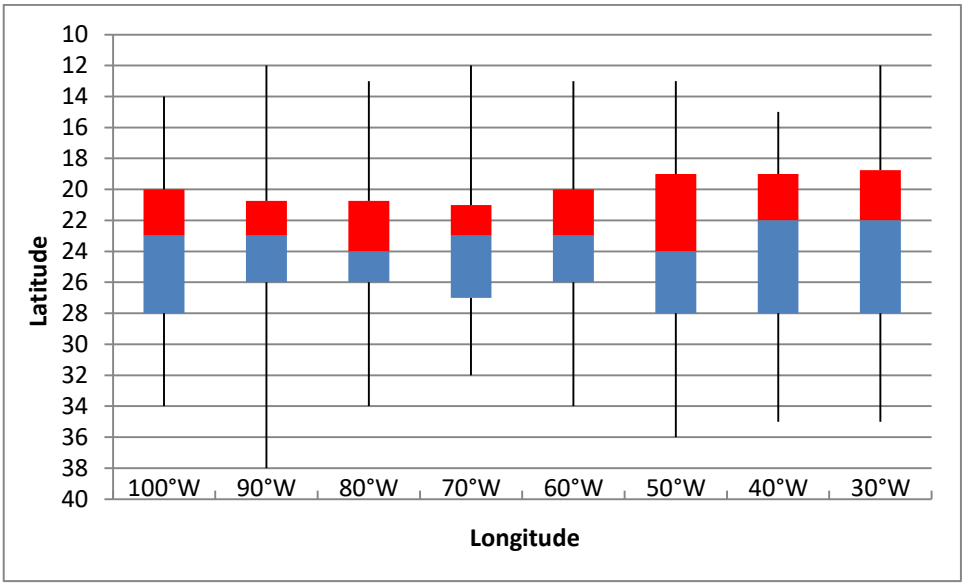


Figure 4.11e Boxplots corresponding to May, considering the period of El Niño events.

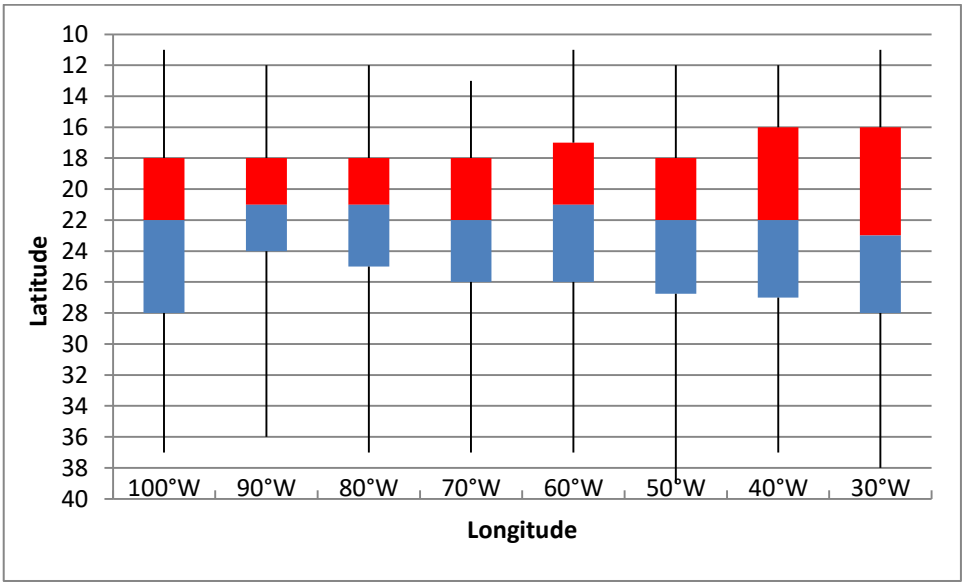


Figure 4.11f Boxplots corresponding to June, considering the period of El Niño events.

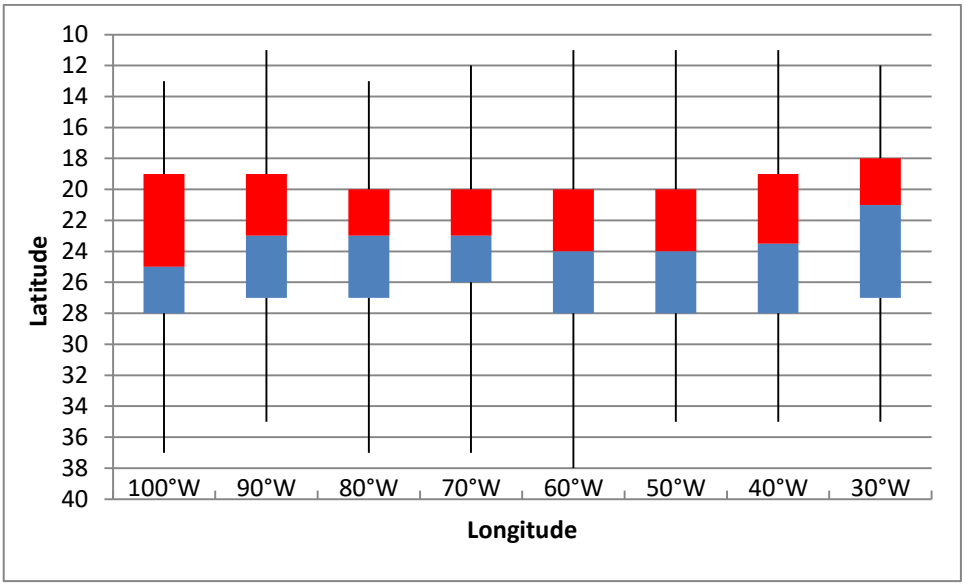


Figure 4.11g Boxplots corresponding to July, considering the period of El Niño events.

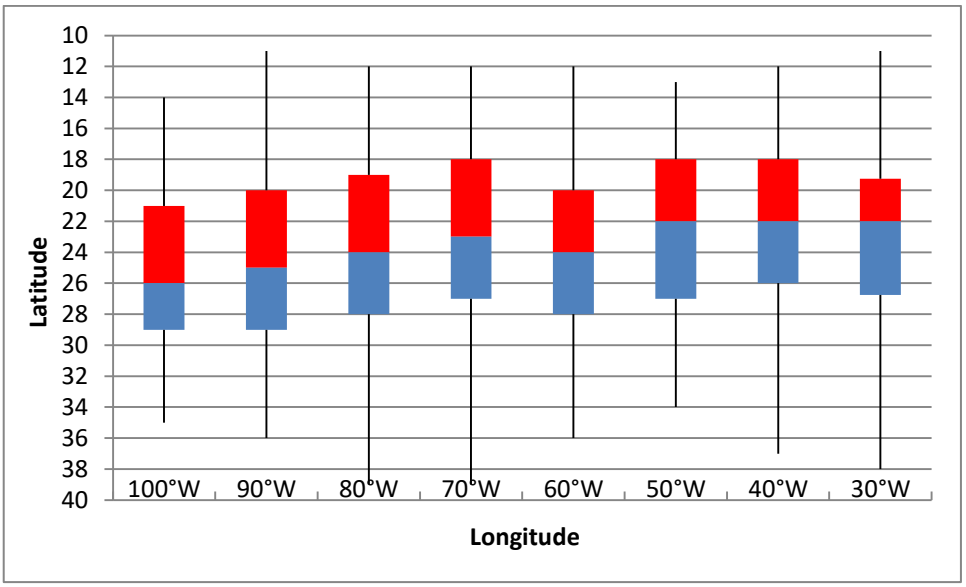


Figure 4.11h Boxplots corresponding to August, considering the period of El Niño events.

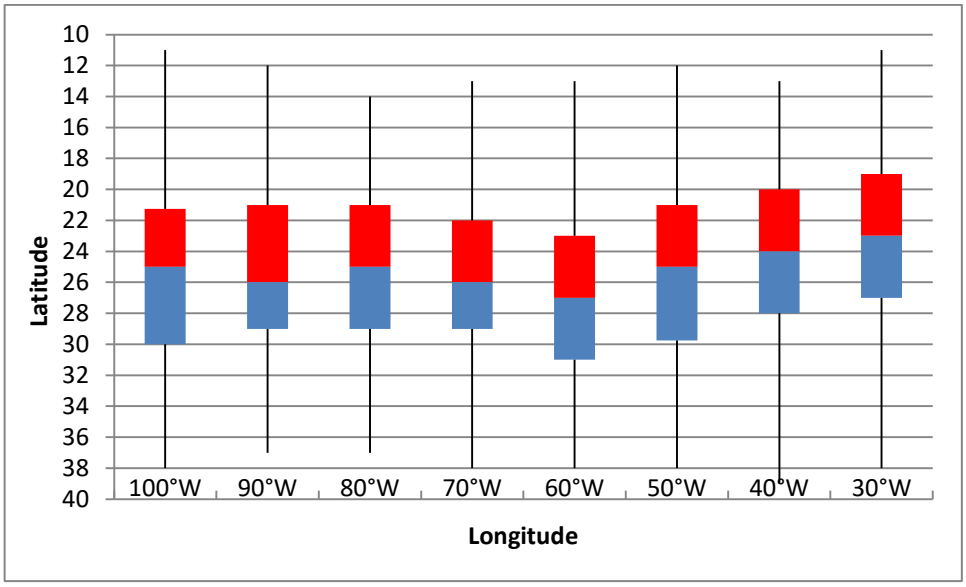


Figure 4.11i Boxplots corresponding to September, considering the period of El Niño events.

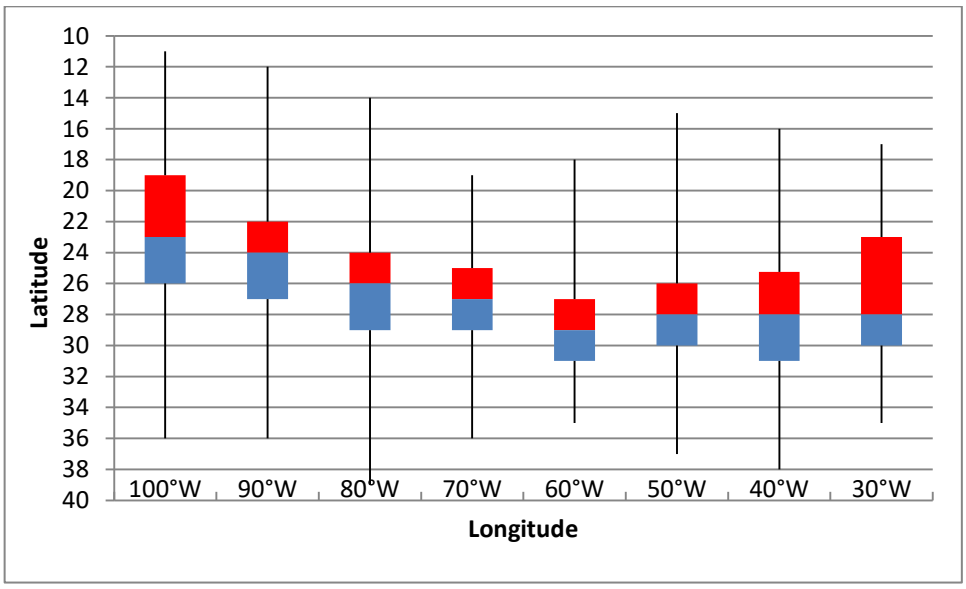


Figure 4.11j Boxplots corresponding to October, considering the period of El Niño events.

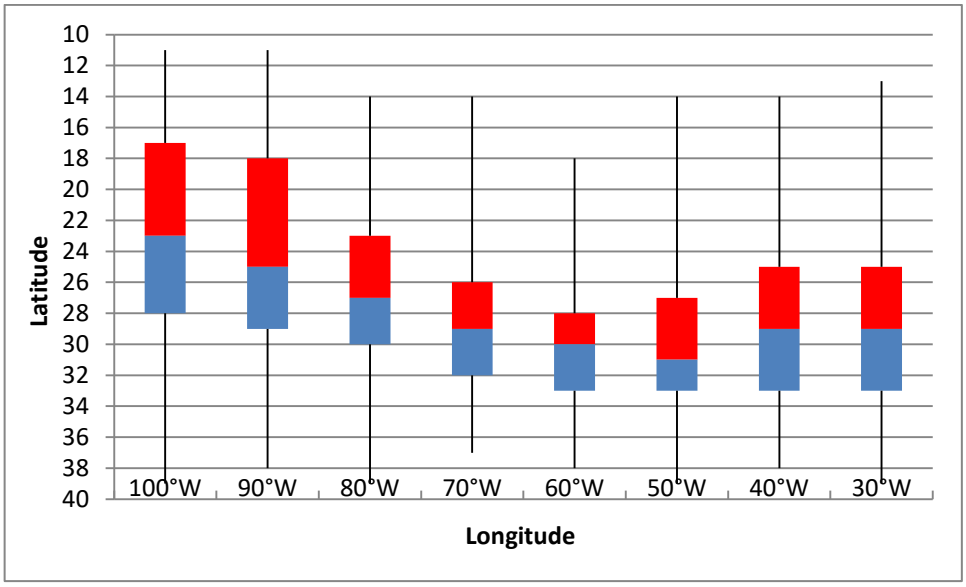


Figure 4.11k Boxplots corresponding to November, considering the period of El Niño events.

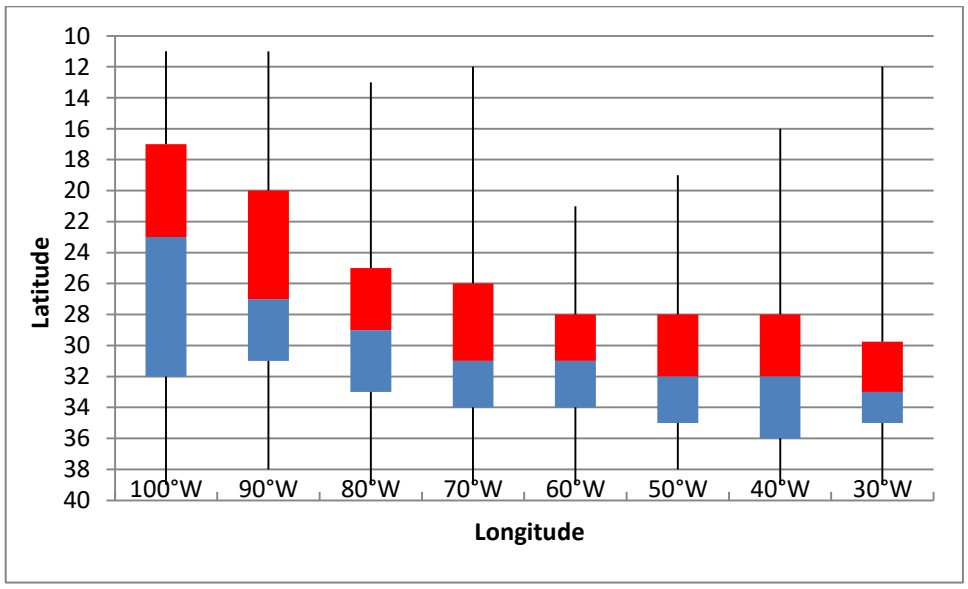


Figure 4.11l Boxplots corresponding to December, considering the period of El Niño events.

Overall, during El Niño events, the behavior of the SJ stays the same during mostly all the months of summer and autumn but changes slightly during winter and spring, especially between June and November (except for July). Also the SJ position shifts significantly in these seasons over both South America and the Atlantic, but not over the Pacific.

### 4.3.1. b The Subtropical jet wind speed during “El Niño events”

As discussed by Kousky and Cavalcanti (1984) the El Niño Southern Oscillation has an important influence in many atmospheric systems, altering the temperature gradient over the Southern hemisphere and as a result, in general ENSO is associated with intensified SJ. **Figures 4.12a** and **b** shows this is true, except for the winter (June to September) when the SJ close to climatology.

It should also be noted that the same pattern, intensification of the SJ during EN events, is not replicated when analyzing the maximum wind speeds, so we can conclude that while in general the SJ is intensified by EN events, the maximum speed diminishes.

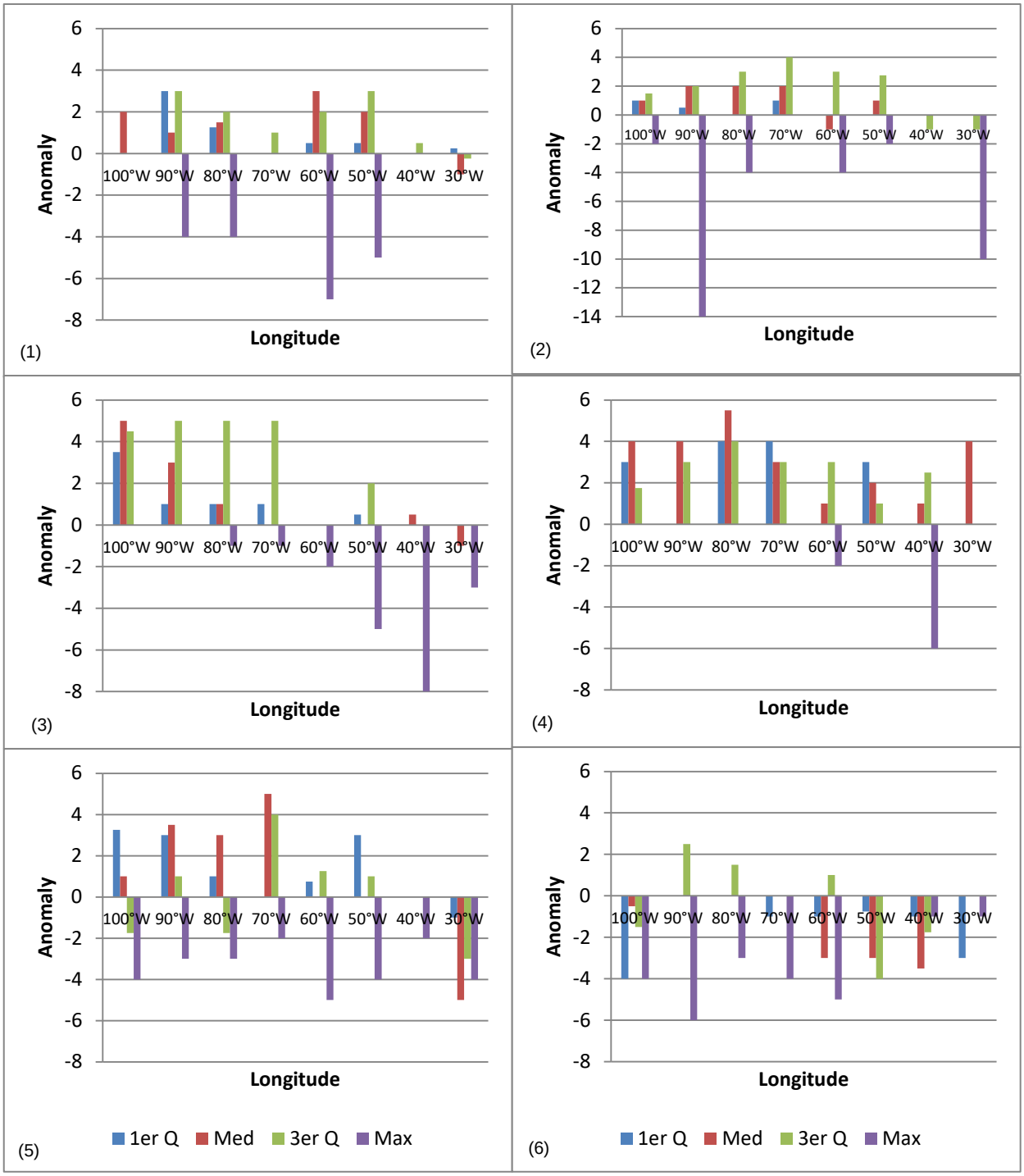


Figure 4.12a - Bar graphics expressing the SJ wind speed anomaly in “El Niño” events: (1) January, (2) February, (3) March, (4) April, (5) May and (6) June.

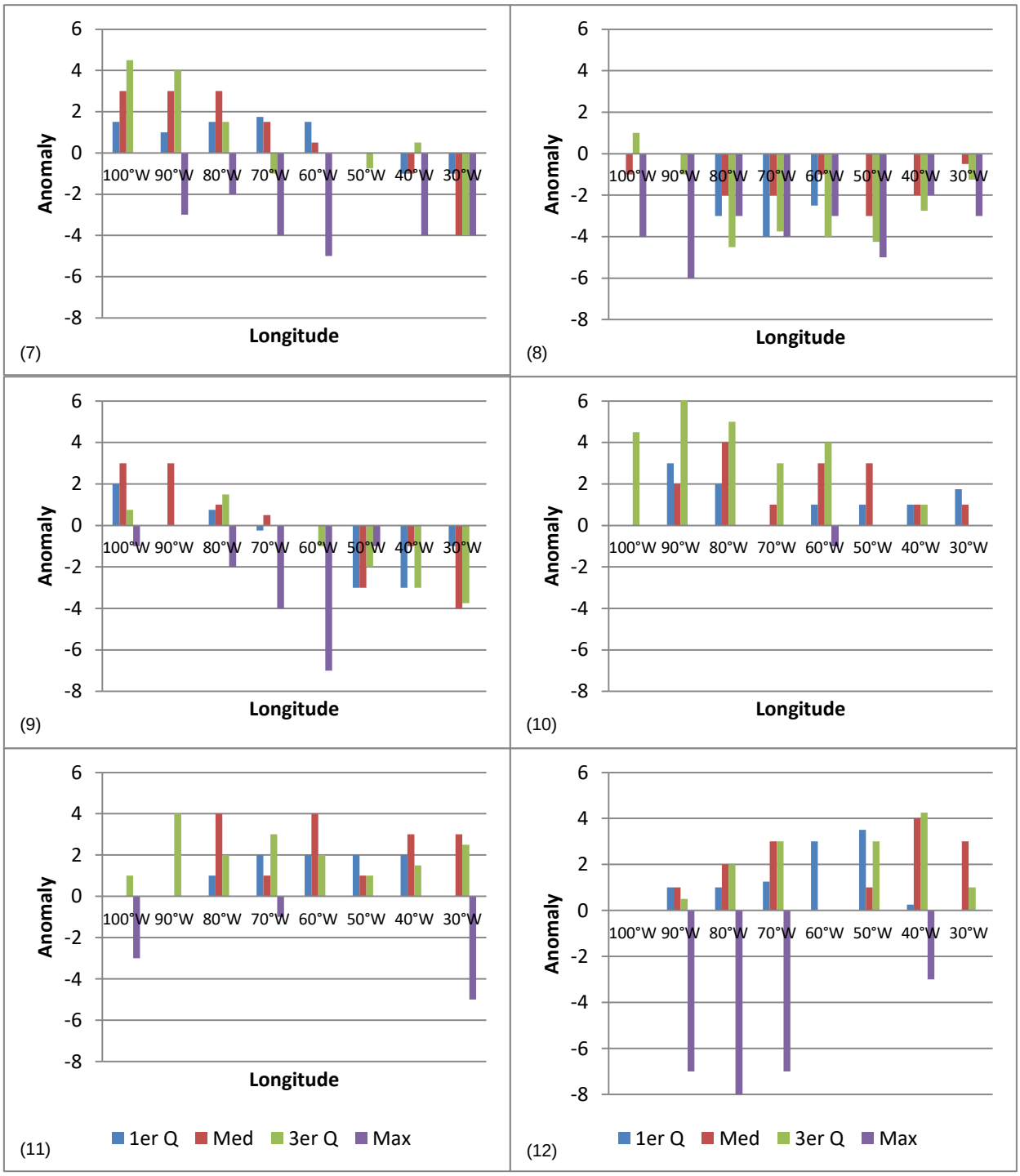


Figure 4.12b Bar graphics expressing the SJ wind speed anomaly in “El Niño” events: (7) July, (8) August, (9) September, (10) October, (11) November and (12) December.

### 4.3.2.a The Subtropical jet latitudinal position during "La Niña events"

To identify the "La Niña" (LN) events the Southern Oscillation Index (SOI) was used. Considering a threshold of 0.5 for the cold events, **Table 4.6b** shows the months that correspond to the LN events. It should be noted that in some studies the index is multiplied by 10 in which case the threshold would be considered 5.

Table 4.6b Months affected by "La Niña" events according to the Southern Oscillation Index during the period of study (1979-2008)

| Date | SOI | Date | SOI | Date | SOI | Date | SOI | Date | SOI |
|---|---|---|---|---|---|---|---|---|---|
| 198807 | 1 | 198910 | 0.8 | 199808 | 1.2 | 200003 | 1.3 | 200802 | 2.6 |
| 198808 | 1.5 | 199601 | 1 | 199809 | 1 | 200004 | 1.2 | 200803 | 1.4 |
| 198809 | 1.8 | 199603 | 1.1 | 199810 | 1.1 | 200008 | 0.7 | 200804 | 0.7 |
| 198810 | 1.4 | 199604 | 0.8 | 199811 | 1 | 200009 | 0.9 | 200806 | 0.6 |
| 198811 | 1.7 | 199606 | 1.2 | 199812 | 1.4 | 200010 | 1.1 | 200808 | 1 |
| 198812 | 1.2 | 199607 | 0.7 | 199901 | 1.8 | 200011 | 1.8 | 200809 | 1.2 |
| 198901 | 1.5 | 199608 | 0.7 | 199902 | 1 | 200012 | 0.8 | 200810 | 1.3 |
| 198902 | 1.2 | 199609 | 0.6 | 199903 | 1.3 | 200101 | 1 | 200811 | 1.3 |
| 198903 | 1.1 | 199610 | 0.6 | 199904 | 1.4 | 200102 | 1.7 | 200812 | 1.4 |
| 198904 | 1.6 | 199612 | 0.9 | 199910 | 1 | 200103 | 0.9 | | |
| 198905 | 1.2 | 199701 | 0.5 | 199911 | 1 | 200710 | 0.7 | | |
| 198906 | 0.7 | 199702 | 1.7 | 199912 | 1.4 | 200711 | 0.9 | | |
| 198907 | 0.9 | 199806 | 1 | 200001 | 0.7 | 200712 | 1.7 | | |
| 198909 | 0.5 | 199807 | 1.2 | 200002 | 1.7 | 200801 | 1.8 | | |

**Figure 4.13a** shows the distribution of the Subtropical Jet in the month of January during LN events (7 years). In this month, over the Pacific, the position of the SJ shifts drastically to the south, while over both South America and the Atlantic stays mostly the same.

**Figure 4.13b** shows the distribution of the Subtropical Jet in the month of February during LN events (6 years). In this month the SJ shifts completely to the south and changes its behavior slightly as it moves more to the south over the Pacific than the rest of the area.

**Figure 4.13c** shows the distribution of the Subtropical Jet in the month of March during LN events (6 years). In this month the SJ shifts to the south over the Pacific Ocean while shifting slightly to the north over South America and staying near the same position over the Atlantic resulting in a mayor change in its behavior.

**Figure 4.13d** shows the distribution of the Subtropical Jet in the month of April during LN events (5 years). In this month both behavior and position of the subtropical jet are extremely similar to the climatology with no significant difference.

**Figure 4.13e** shows the distribution of the Subtropical Jet in the month of May during LN events (1 year). Only one event occurred during the period of study for this month, as such this detail should be considered when reviewing conclusions for this particular month.

In the month of May the SJ behaves completely different changing its relative position between each area, shifting to the south over 100°W but changing to the north in the next point, then being displaced to the south again over South America and then again to the north over the Atlantic Ocean.

On June **(Figure 4.13f, 4 years)** the behavior of the SJ changes in a way similar to May with the only difference in position being over 40°W (Shifting now to the south) and a much smaller variance.

On July **(Figure 4.13f, 4 years)** the SJ stays almost the same over the continent but changes its behavior over the ocean, shifting to the north both over the Pacific and Atlantic Ocean.

On August **(Figure 4.13h, 5 years)** the SJ behavior does not change much but shifts its position to the south at all longitudes, albeit moving just between 1-2 degrees over the oceans and over 2-3 degrees over South America.

**Figure 4.13i** shows the distribution of the Subtropical Jet in the month of September during LN events (6 years). During this month the changes in the SJ behavior are minimal and inconsistent, with and irregular shift in position of about one degree either to the north or south over all the area resulting in a jet similar to what is normally expected.

**Figure 4.13j** shows the distribution of the Subtropical Jet in the month of October during LN events (8 years). During this month the SJ has a behavior and general position very similar to the climatology with no significant change.

On November **(Figure 4.13k, 6 years)** the SJ behaves pretty differently over South America shifting to the south significantly comparing it to its climatology, while over the Pacific moves to lower latitudes accentuating the change of behavior over the continent, over the Atlantic it shifts slightly to the north.

**Figure 4.13l** shows the distribution of the Subtropical Jet in the month of December during LN events (7 years). During this month the SJ stays pretty much the same and it's very similar to its climatology with no particular change in latitudinal position or behavior.

As seen in the graphics, during LN events the season where more changes of the behavior of the Subtropical jet are noted is the summer, specifically between January and March, for the rest of the year, with the exception of November, the SJ behaves similar to its climatology, albeit shifting either to the south or to the north but maintaining its general structure over the area of study.

We can also see that the changes in the variance of the position of the jet are much smaller than in EN events, meaning that the SJ is probably more stable during these events, as it is known to be weakened and thus it becomes less likely to shift its position more radically.

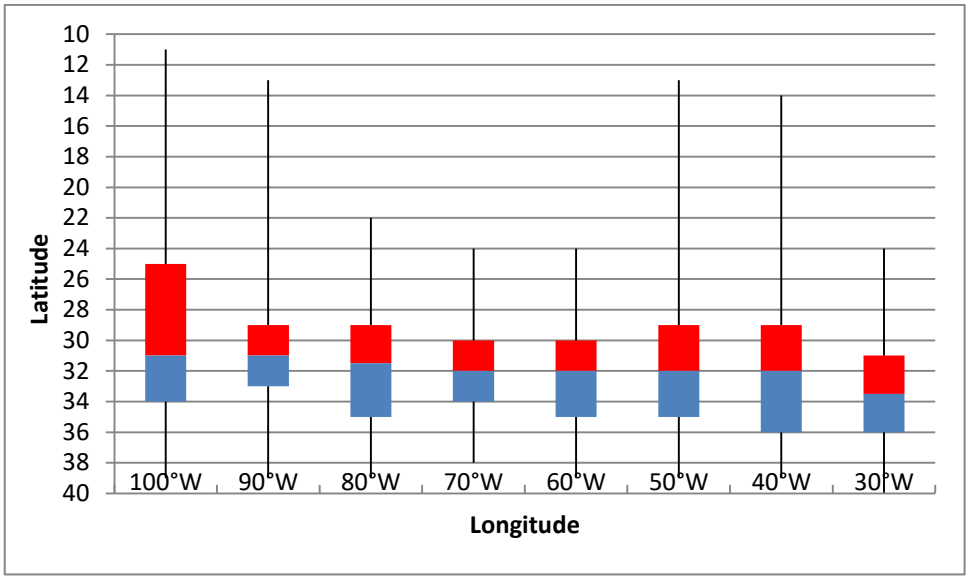


Figure 4.13a Boxplots corresponding to January, considering the period of La Niña events.

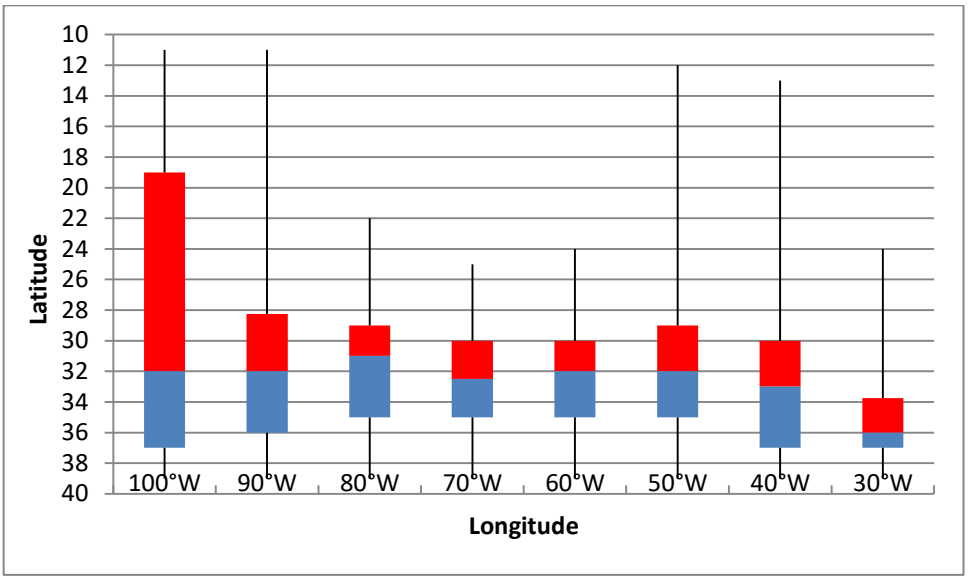


Figure 4.13b Boxplots corresponding to February, considering the period of La Niña events.

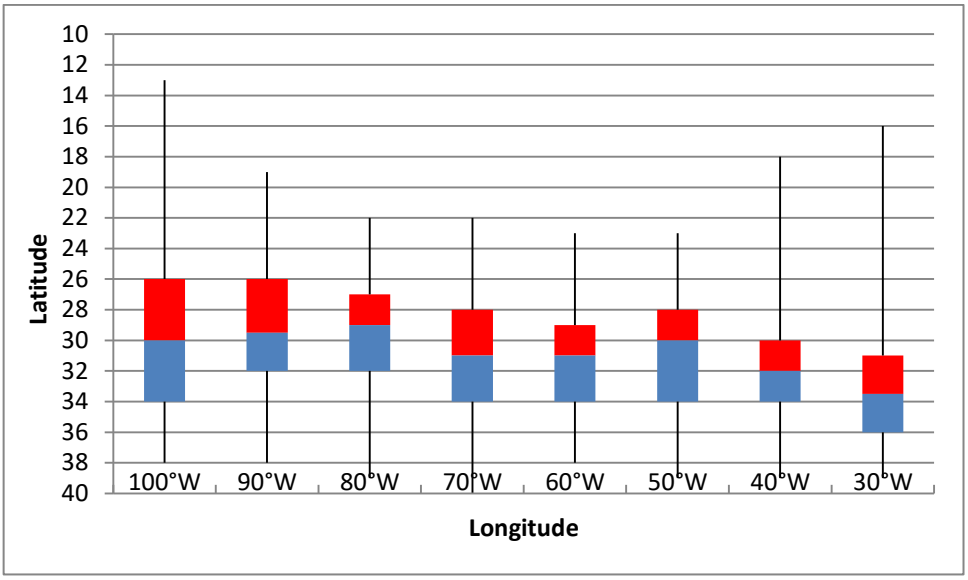


Figure 4.13c Boxplots corresponding to March, considering the period of La Niña events.

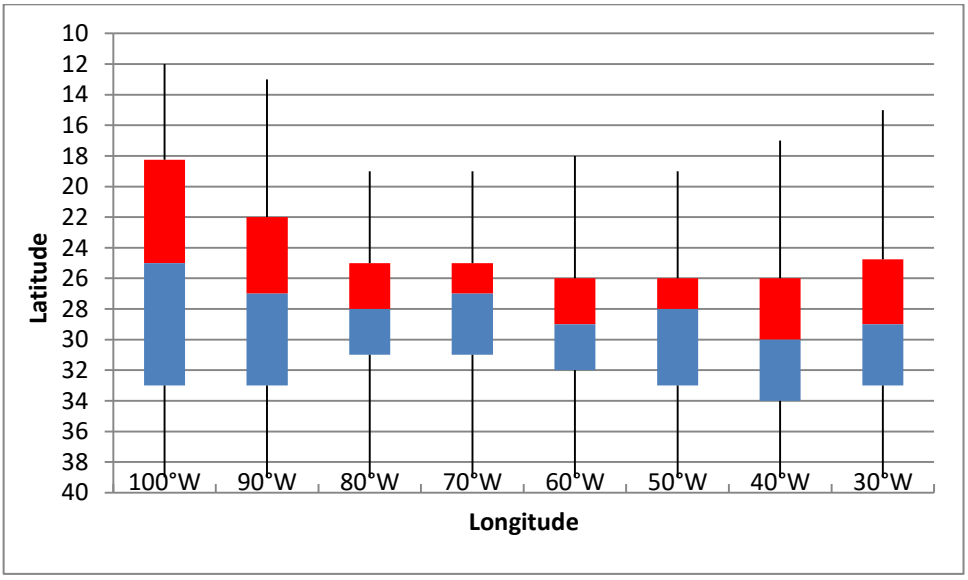


Figure 4.13d Boxplots corresponding to April, considering the period of La Niña events.

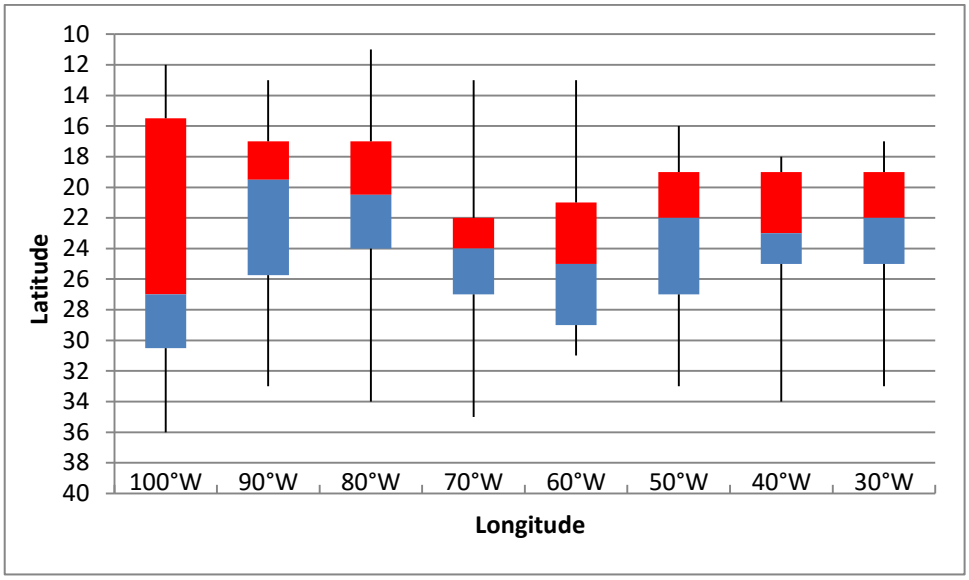


Figure 4.13e Boxplots corresponding to May, considering the period of La Niña events.

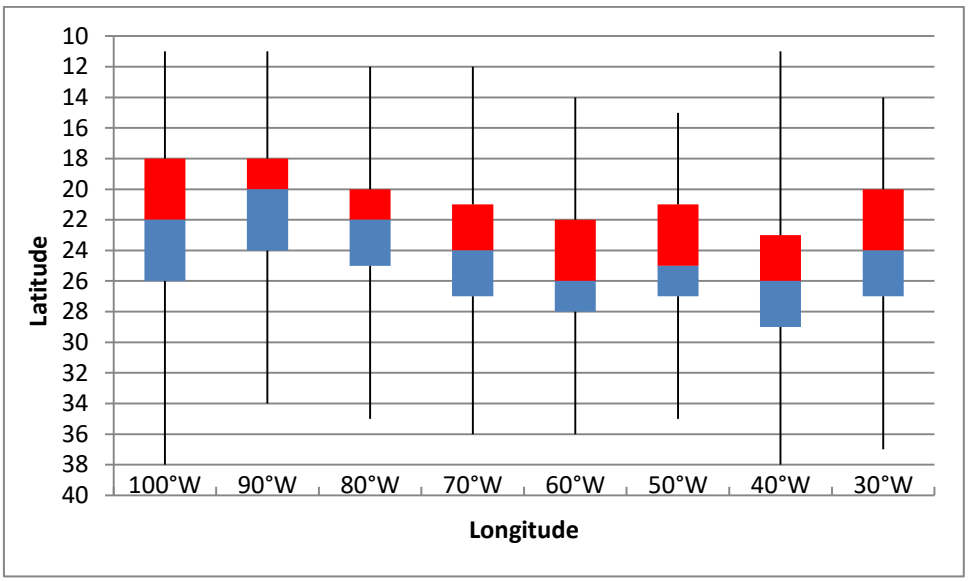


Figure 4.13f Boxplots corresponding to June, considering the period of La Niña events.

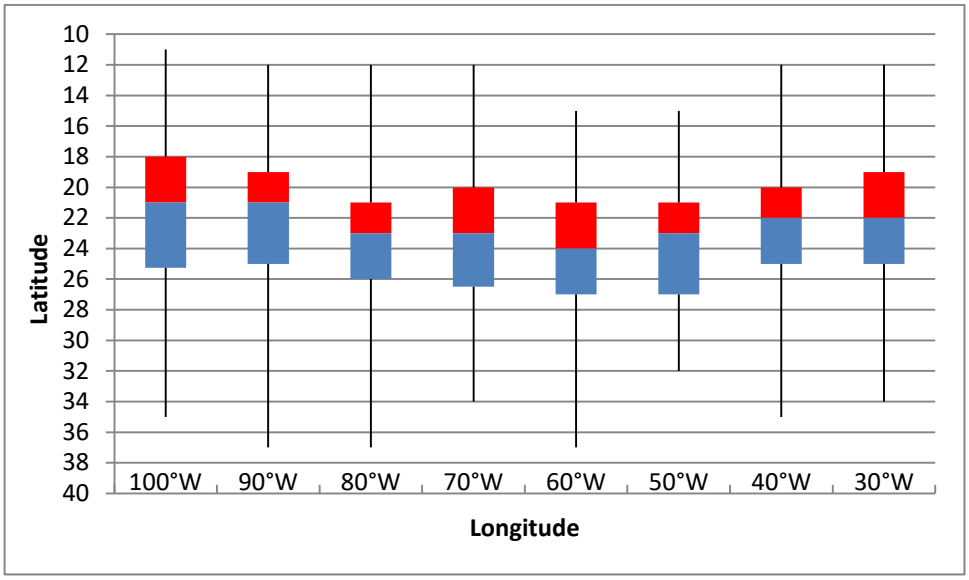


Figure 4.13g Boxplots corresponding to July, considering the period of La Niña events.

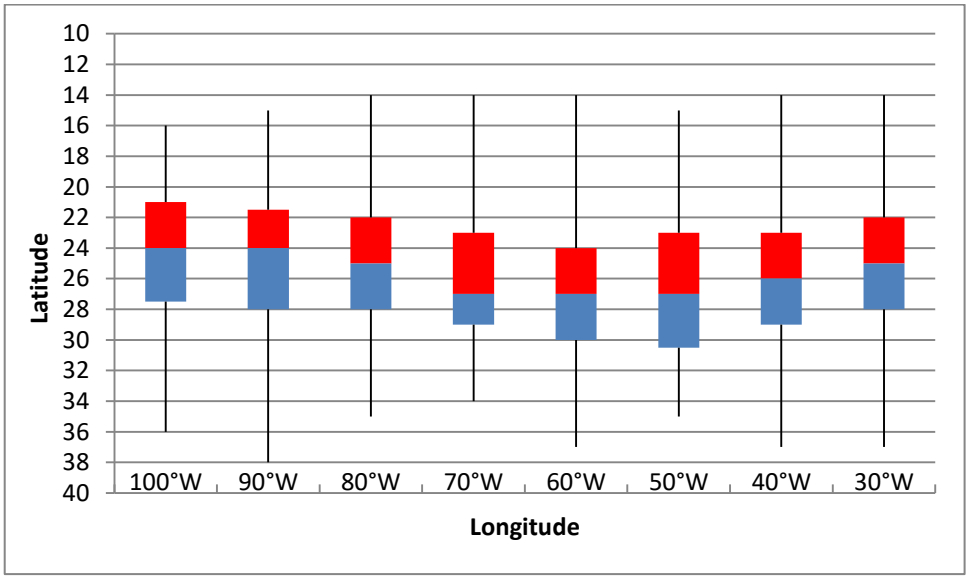


Figure 4.13h Boxplots corresponding to August, considering the period of La Niña events.

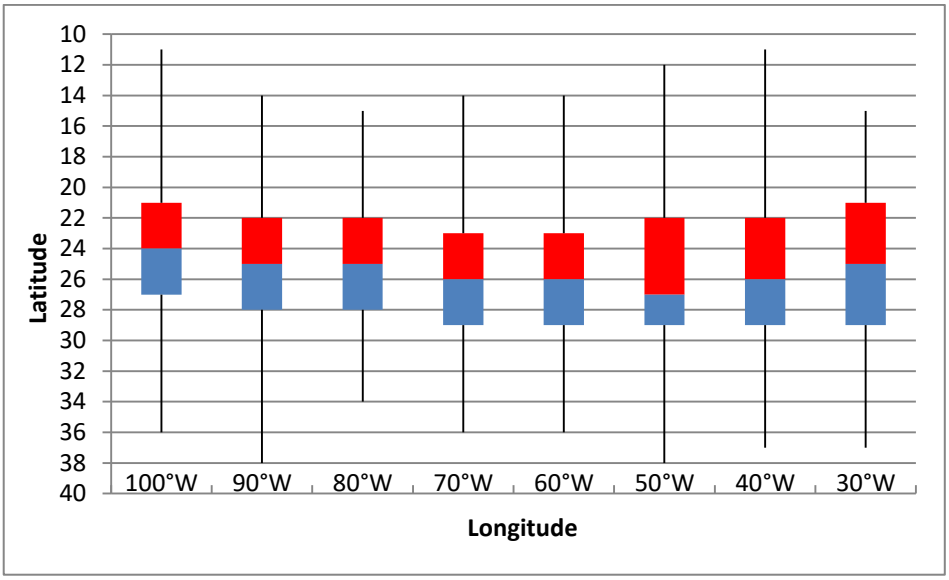


Figure 4.13i Boxplots corresponding to September, considering the period of La Niña events.

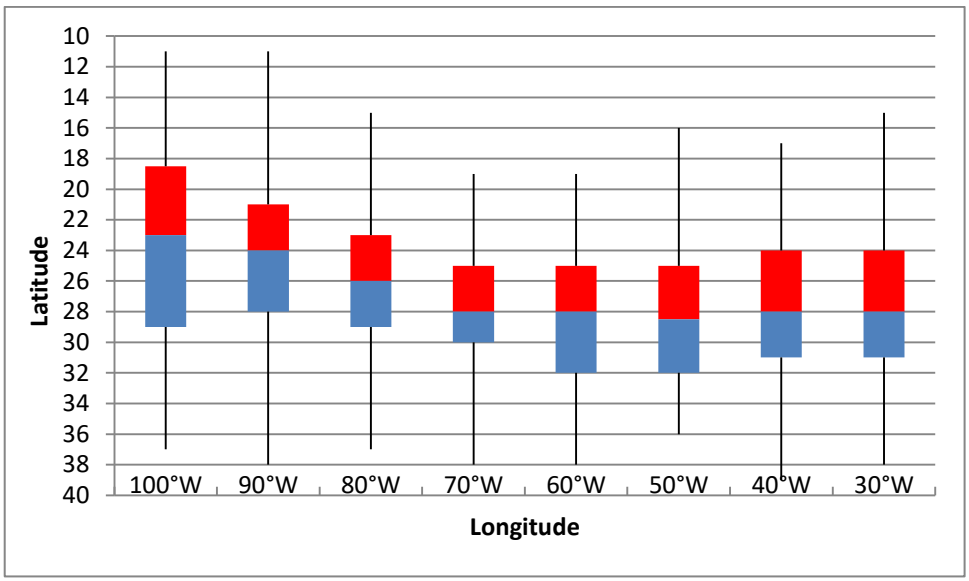


Figure 4.13j Boxplots corresponding to October, considering the period of La Niña events.

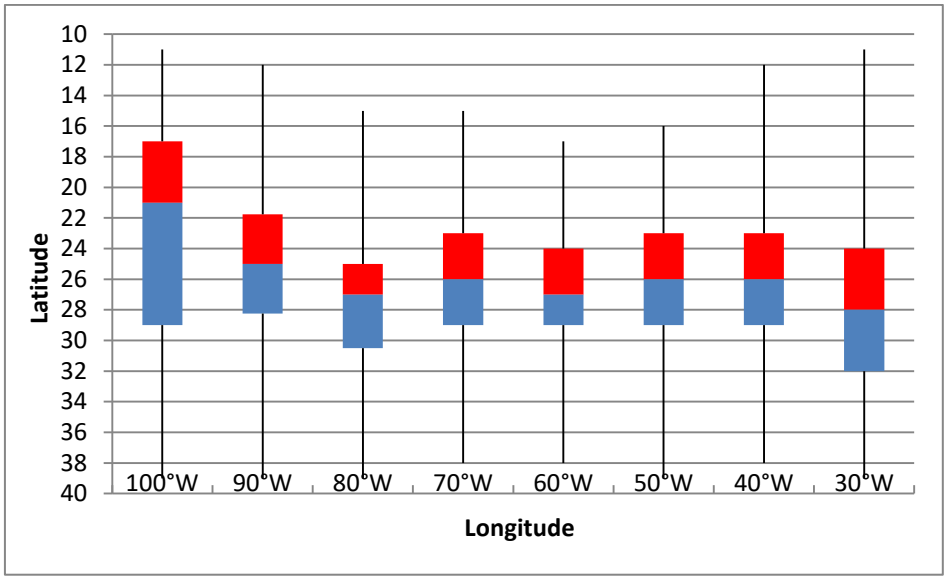


Figure 4.13k Boxplots corresponding to November, considering the period of La Niña events.

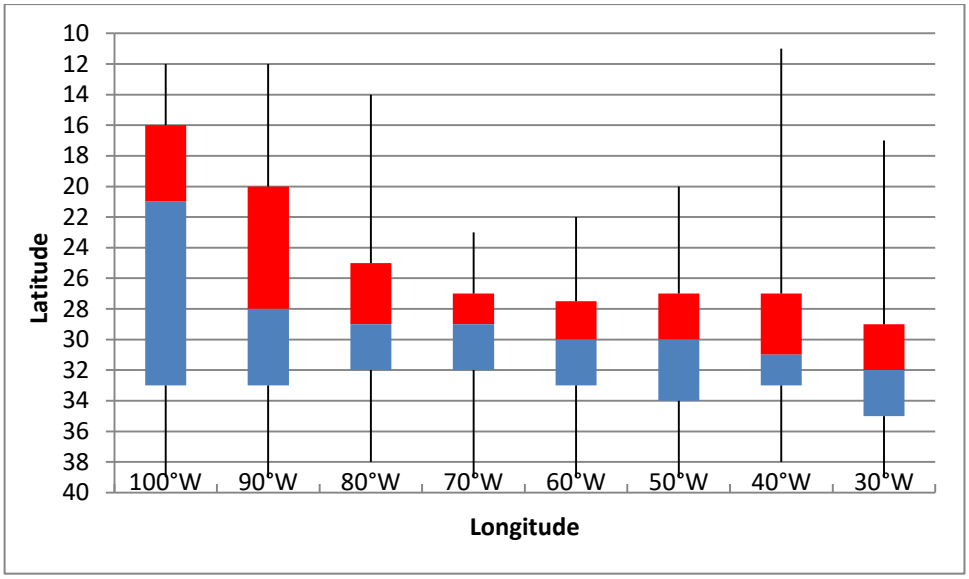


Figure 4.13l Boxplots corresponding to December, considering the period of La Niña events.

### 4.3.2.b The Subtropical jet wind speed during “La Niña events”

When observing **Figure 4.14a** and **Figure 4.14b** it can be easily appreciated that during these cold events the immediate effect results in the weakening of the Subtropical jet almost all the year, with the exception of the months of August and September where the SJ is greatly intensified. This can be considered an important contrast with the behavior we have seen in the same period of time during El Niño events and could be attributed to the fact that this period coincides with the southern hemisphere winter, which while during El Niño events mitigates its influence, as it is a warm phase in a cold season, during La Niña events the pattern might be reinforced, a cold event in a cold season, and increasing the horizontal temperature gradient resulting in an stronger jet.

It can also be observed that the greater impact occurs during transition months between the autumn and winter and between spring and summer, having in these periods a major drop in the SJ wind speed.

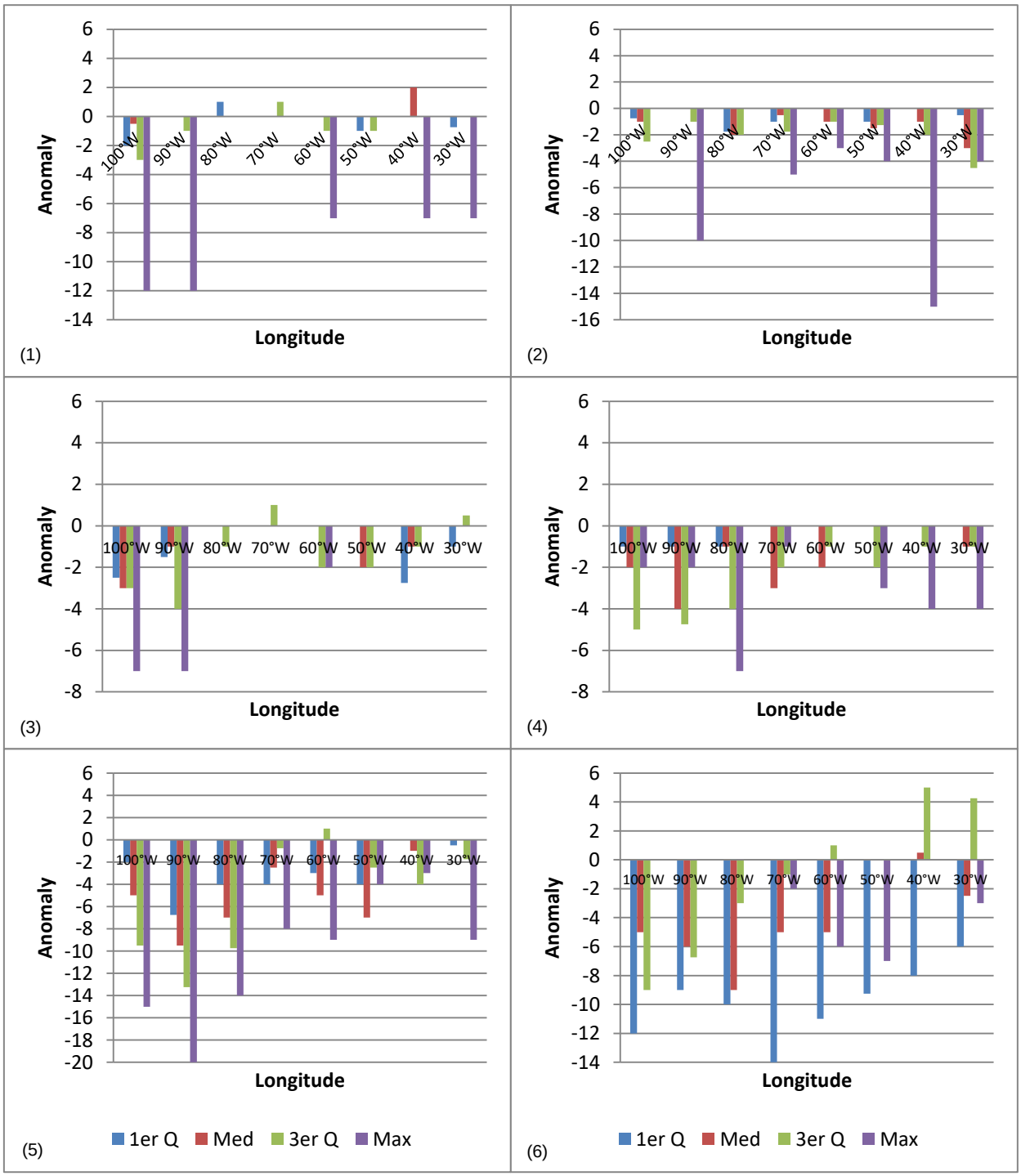


Figure 4.14a - Bar graphics expressing the SJ wind speed anomaly in “La Niña” events: (1) January, (2) February, (3) March, (4) April, (5) May and (6) June.

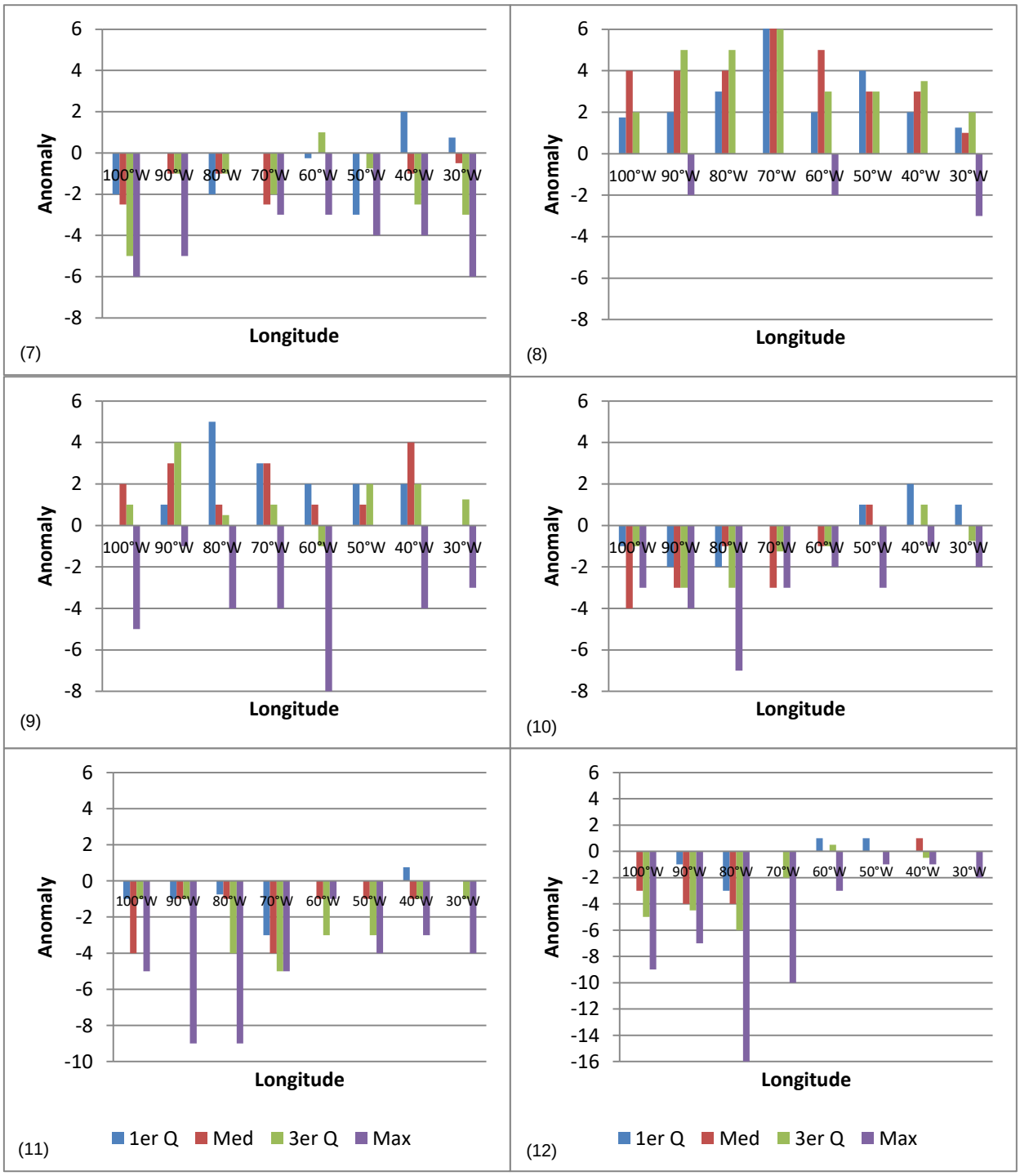


Figure 4.14b Bar graphics expressing the SJ wind speed anomaly in La Niña" events: June, (7) July, (8) August, (9) September, (10) October, (11) November and (12) December.

### 4.4. Comparison between normal, El Niño and La Niña conditions

As we see in Figures 4.15a and 4.15b the shift of the SJ during the ENSO events is most prominent in the winter, while during the rest of the year the difference between all three conditions (EN, LN and normal) are not so evident. However during

the winter, a latitudinal difference of even 5° can be seen; in these cases the SJ tends to shift to the north (south) during EN (LN) events. This correlates well with the description provided by Seagar (2005).

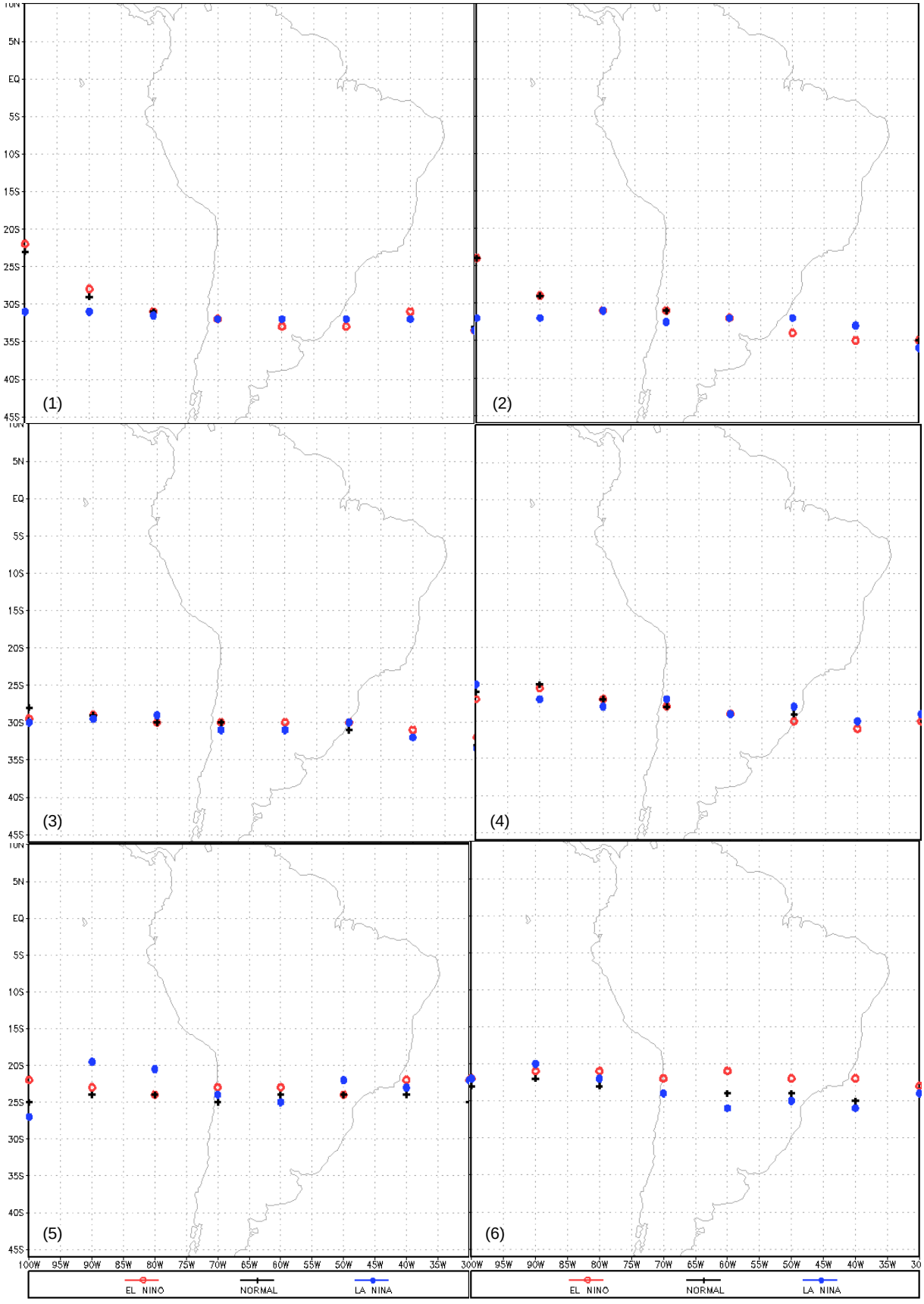


Figure 4.15a - Subtropical jet climatology (black marks), El Niño JS (red marks) and La Niña (blue Marks). (1) January, (2) February, (3) March, (4) April, (5) May and (6) June.

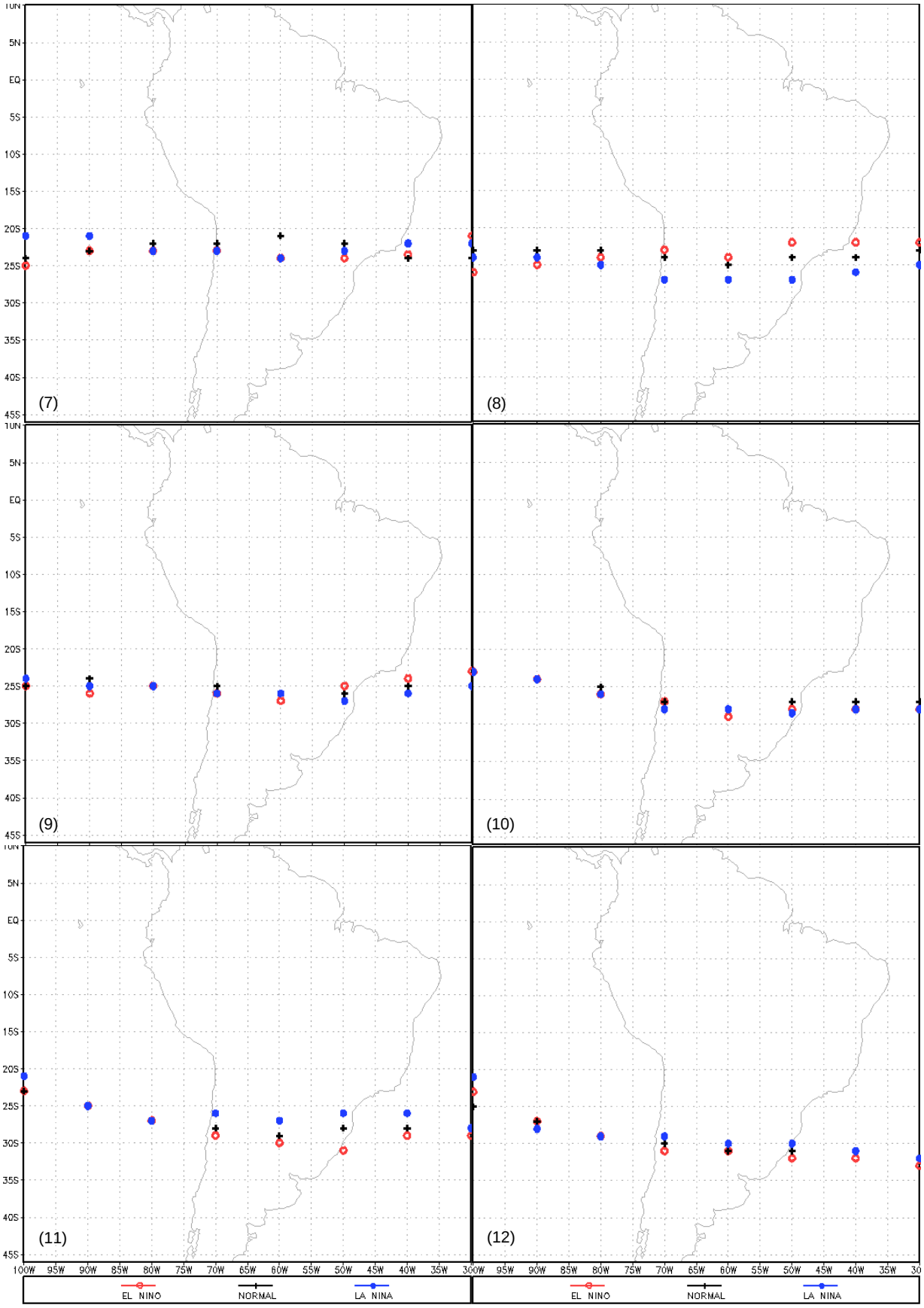


Figure 4.15b Subtropical jet climatology (black marks), El Niño JS (red marks) and La Niña (blue Marks). (7) July, (8) August, (9) September, (10) October, (11) November and (12) December.

# 5. CHAPTER V: CONCLUSIONS

This work analyzed the subtropical jet (SJ) characteristics in the Southern Hemisphere over South America and vicinities, between 10° and 40°S and every 10° degrees between 100° and 30°W. In order to stablish a climatological pattern, an objective methodology would be desirable, however, the SJ could not be identified with a limit of constraints and thus, a subjective approach – visual inspection – was used. Identification criteria were tested and validated for January and June of 2014, with CPTEC analyses and water vapor images. The climatology was done for the period of January 1979 to December 2008 with ERA-Interim reanalysis.

CPTEC criteria of determining the SJ latitude by wind speed and potential temperature at 250 hPa were the first test made. It resulted in a similar SJ as that obtained in the CPTEC, however when confronting it with water vapor imagery it was evident that determining the SJ position in only one level resulted in an incomplete SJ structure: it was mixed with the Polar Jet when both were merged, and failed at some points to represent its structure over the area of study, mainly due to the interference of other atmospheric systems such as cyclones.

Visual determination of the SJ core was made for daily (12 UTC) vertical profiles of horizontal wind velocity and potential temperature from 100 hPa to 400 hPa for each 10° degrees from 100 to 30°W, between 10° and 40°S. In order to be considered an SJ core, almost all of it should be observable inside the study area, more specifically, the southern speed gradient. Also, the core should be in the troposphere, stratospheric cores were not considered. The SJ obtained were better collocated with the SJ observed in water vapor images and its overall characteristics were in agreement to literature references. The SJ core has a horizontal wind speed between 30 and 50 $ms^{-1}$, in summer, and between 40 and 60 $ms^{-1}$, in winter, usually stronger over the oceans than over the continent. Its mean potential temperature is 340K most of the year being, but frequently reached values within 330 and 340 K during winter and 340 to 350K during summer. Almost all the times it is found between 200 and 250 hPa, and between the latitudes of 18° - 29°S during the winter, and 16° - 35°S during the summer.

When analyzing the influence of ENSO events in the SJ it can be concluded that “La Niña” (LN) weakens the SJ, more pronouncedly during the winter, and “El Niño” (EN) intensifies the SJ, especially during the summer.

# 6. CHAPTER VI: SUGESTIONS FOR FUTURE STUDIES

In this study the Subtropical jet behavior and position were analyzed in great extent however there are suggestions for future studies. Climate change impact on the SJ, for example, including the evolution of the SJ during the years; a more detailed characterization of the SJ analyzing days when it was merged with the PJ; and also the impact of the SJ on the precipitation.

Although this study could not use a completely objective method to identify the SJ, it might prove useful to study the Hadley and Ferrel cells with a numeric model, as both cells are deeply related to the SJ position and intensity reproducing the research made by Webster (2004) to the southern hemisphere.

# 7. CHAPTER 7: REFERENCES


- Abish, B., Joseph, P.V., e Johannessen, O.M., 2015: Climate Change in the Subtropical Jetstream during 1950–2009. Advances in atmospheric sciences, vol. 32, pp 140-148.

- Arkin, P.A., 1982: The relationship between interannual variability in the 200-mb tropical wind field and the Southern Oscillation, Monthly Weather Review, Vol 110, 1393-1404.

- Barton, N. e Ellis, A., 2009: Variability in wintertime position and strength of the North Pacific jet stream as represented by re-analysis. International Journal of Climatology, vol. 29, pp 851-862.

- Browing, K. A., 1985. Conceptual Models of Precipitation Systems. Meteorological Magazine, Bracknell. Eng. 114(1359):293-319.

- Eichelberger, S.J., and Hartmann, D.L., 2007: Zonal Jet Structure and the Leading Mode of Variability, American Meteorological Society, vol. 20, pp 5149-5163.

- Galvin, 2007: The weather and climate of the tropics. Weather, 62, 295–299.

- Krishnamurti, T. N., 1961: The subtropical Jetstream of winter. J. Meteor., 18, 172–191.

- Kousky, V., e Cavalcanti, I. F. A., 1984. Eventos Oscilação Sul - El Niño: Características, evolução e anomalias de precipitação. Ciência e Cultura 36(11), 1888-1899.

- Koch, P., Wernli, H. e Davies, H.C., 2006: An Event-Based Jet-Stream Climatology and Typology. International, Journal of Climatology, vol. 26, pp 283-301.

- Lachmy, O., e Harnick, N., 2014: The Transition to a Subtropical Jet Regime and Its Maintenance, American Meteorological Society, vol. 71, pp 1389-1409.

- Lee, S., e Kim, H.K., 2003: The Dynamical Relationship between Subtropical and Eddy-Driven Jets, Journal of the Atmospheric Sciences, vol. 60, pp 1490-1503.

- Manney, G.L., Hegglin, M.I., Daffer, W.H., Schwartz, M.J., Santee, M.L. e Pawson, S., 2013: Climatology of Upper Tropospheric–Lower Stratospheric (UTLS) Jets and Tropopauses in MERRA, Journal of Climate, vol. 27, pp 3248-3271.

- Mitas, C. M., and A. Clement, 2005: Has the Hadley cell been strengthening in recent decades? Geophys. Res. Lett., 32, L03809, doi: 10.1029/2004GL021765.

- Oort, A.H. 1996: Observed Interannual Variability I the Hadley Circulation and its connection to ENSO, Journal of Climate Vol 9, 2751-2767

- Ramaswamy, C., 1956: On the Subtropical Jet Stream and its Role in the Development of Large-scale Convection. Tellus VIII, 1, 26-60.

- Reiter, E.R. 1963. Jet-stream Meteorology. The University of Chicago Press: Chicago; 515.

- Reiter, E.R., e Whitney, L.F., 1969: Interaction between Subtropical and Polar-front Jet Stream, Monthly Weather Review, vol. 97, No. 6, pp 432-438.

- Reiter, E. R., 1969. Tropopause Circulations and Jet Streams. World Survey of Climatology, v (4). Climate of Free Atmosphere, 85-204.

- Riehl, H., 1969. Jet Streams of the Atmosphere. Medical Opinion & Review (September), 33-50.

- Seager, R., Harnik, N., Robinson, W.A., Kushnir, Y., Ting, M., Huang, H.P. e Velez, J., 2005: Mechanisms of ENSO-forcing of hemispherically symmetric precipitation variability, Q. J. R. Meteorological Society, 131, pp 1501-1527.

- Santurette, P. and Gergiev, C., G.: Weather analysis and forecasting Appying Water Vapor Imagery and Potential Vorticity Analysis, Elsevier Academic Press; 2009. Chap 3, Significant Water Vapor Imagery Features I, 30-34.

- Webster, P. J., 2004: The elementary Hadley circulation. The Hadley Circulation: Past, Present and Future. H. Diaz, and R. Bradley, Eds., Cambridge University Press, 9–60.